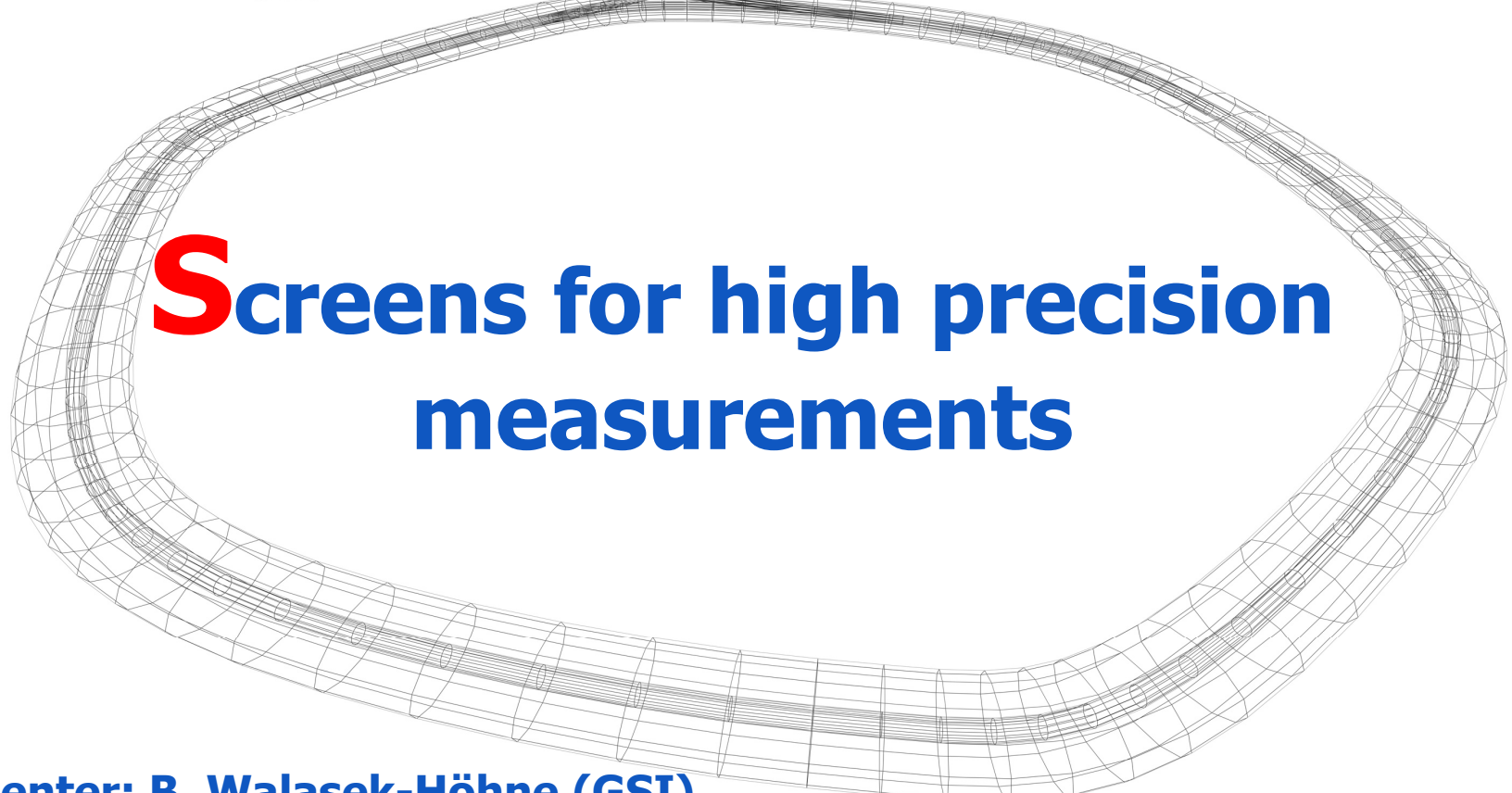


Screens for high precision measurements



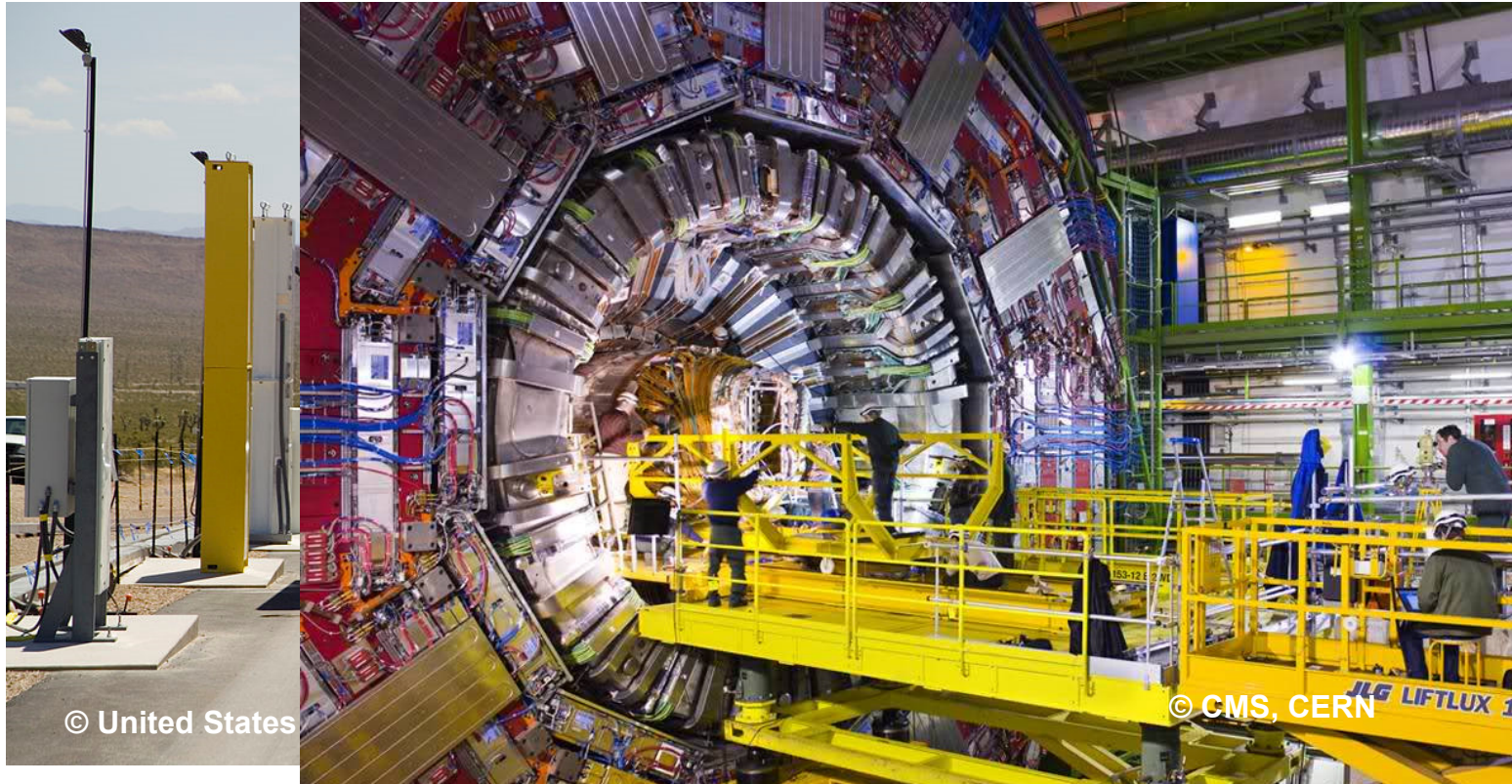
Presenter: B. Walasek-Höhne (GSI)

There is a long history of scintillator applications in particle detection. Traditionally used in physics, scintillators today serve many purposes in science and engineering (e.g. medicine, geophysics, homeland security)

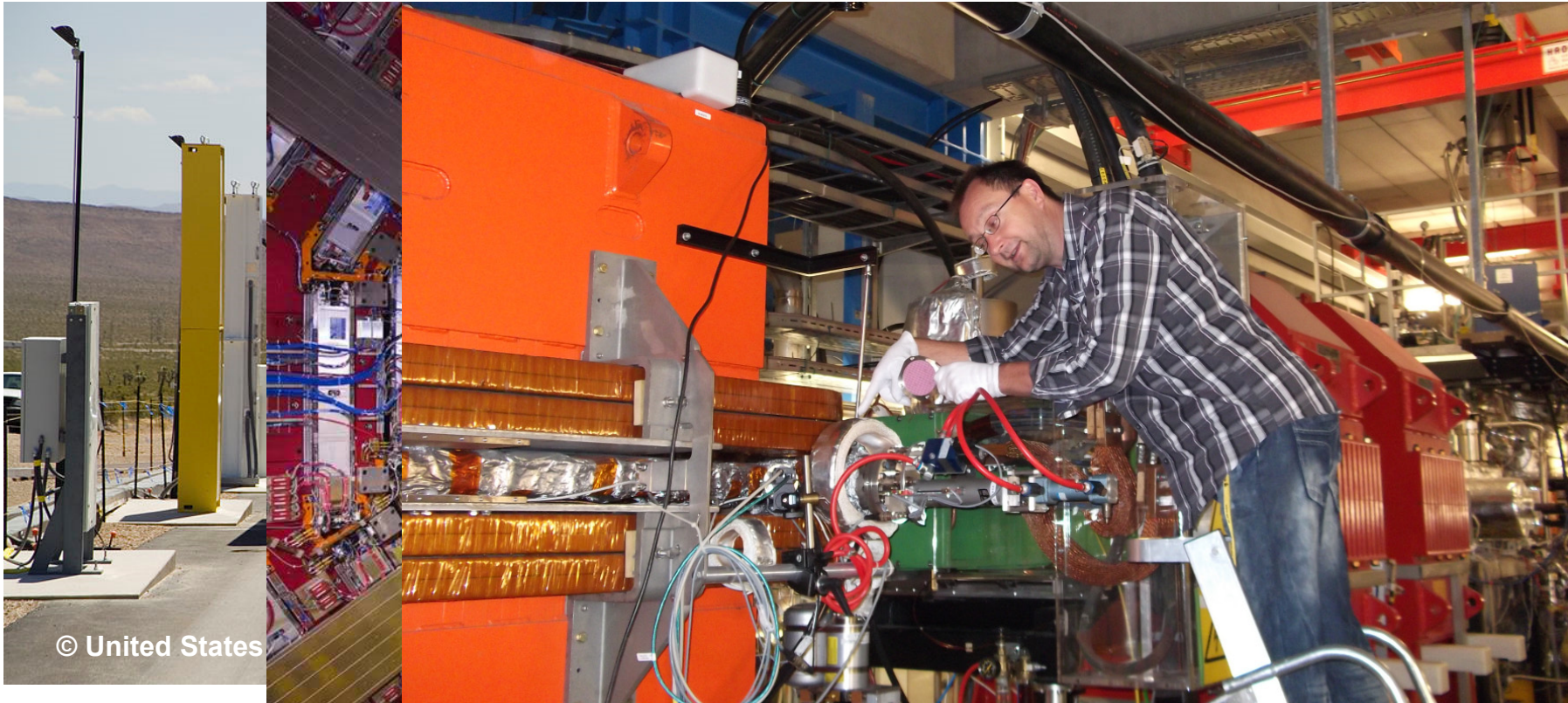


© United States Department of Energy

There is a long history of scintillator applications in particle detection. Traditionally used in physics, scintillators today serve many purposes in science and engineering (e.g. medicine, geophysics, homeland security, particle detection)



There is a long history of scintillator applications in particle detection. Traditionally used in physics, scintillators today serve many purposes in science and engineering (e.g. medicine, geophysics, homeland security, particle detection ... and beam diagnostics).



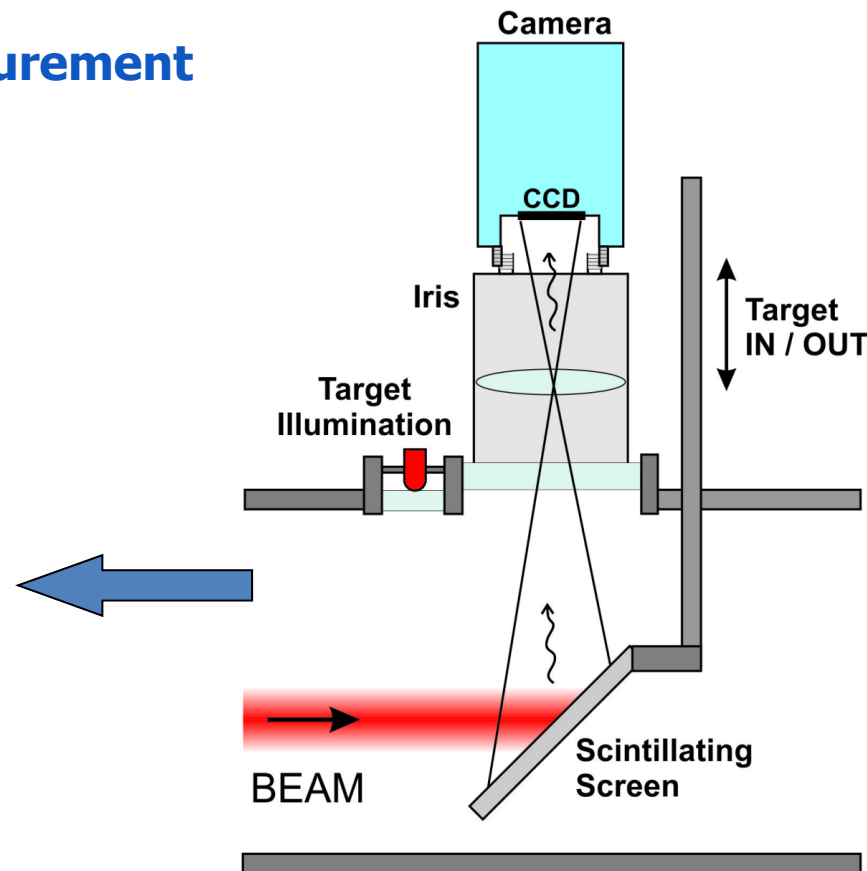
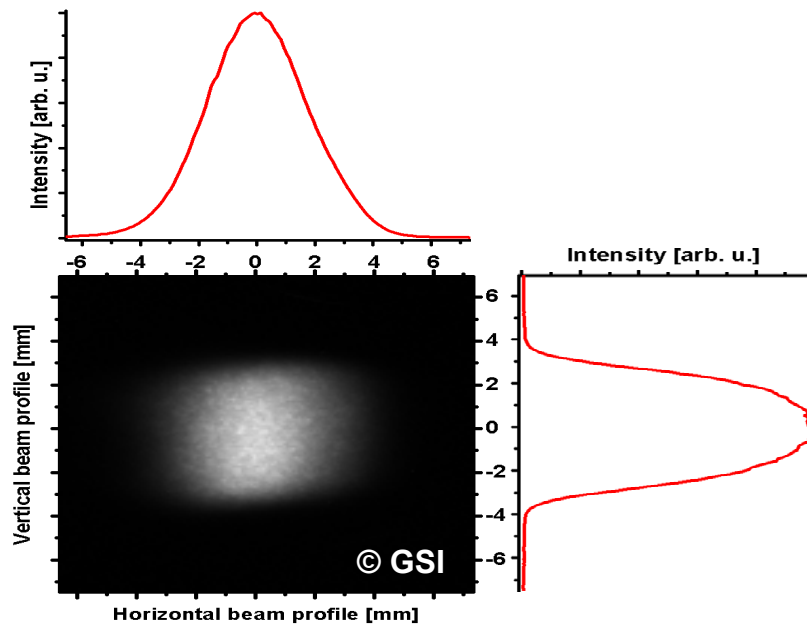
Scintillators are used for beam diagnostics in all accelerator laboratories

- ❖ Since many years in hadron and low energy electron machines.
- ❖ In modern LINAC-based light sources the interest in scintillators was revived when coherent effects were discovered that spoil the standard OTR measurements.

Applications in beam diagnostics

Scintillating screens are widely used in accelerator facilities for transversal beam profile and precise single shot emittance measurements

- ❖ simple, reliable profile measurement system
- ❖ used for beam alignment

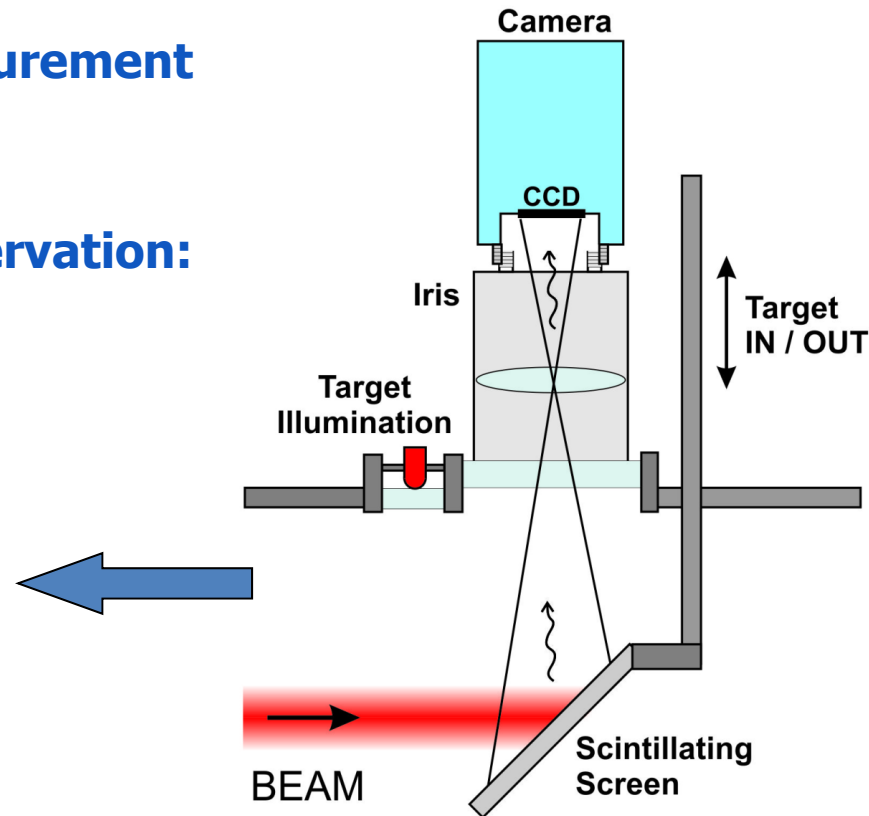
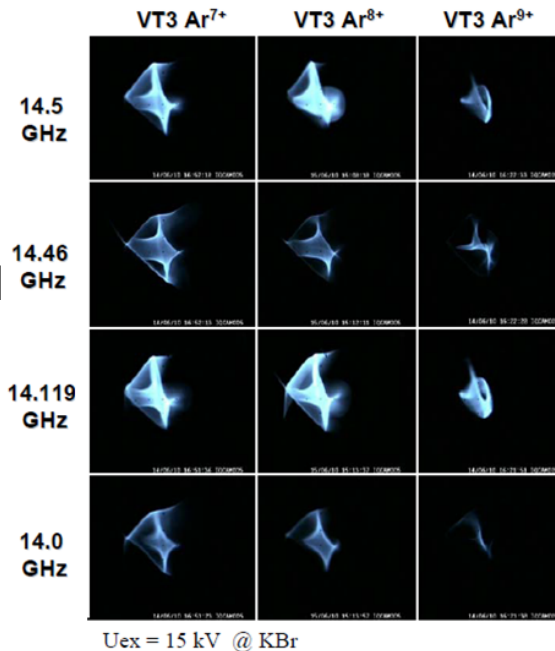


From the projection: light output (integral), centre of projection, beam width, asymmetry

Applications in beam diagnostics

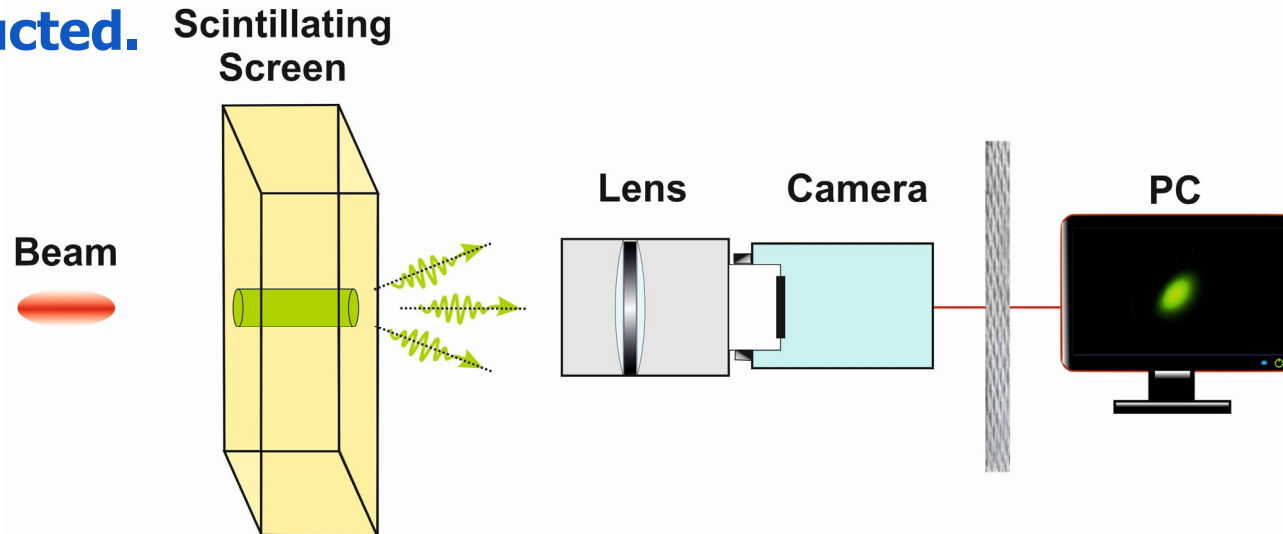
Scintillating screens are widely used in accelerator facilities for transversal beam profile and precise single shot emittance measurements

- ❖ simple, reliable profile measurement system
- ❖ used for beam alignment
- ❖ most direct way of beam observation: complete 2D information

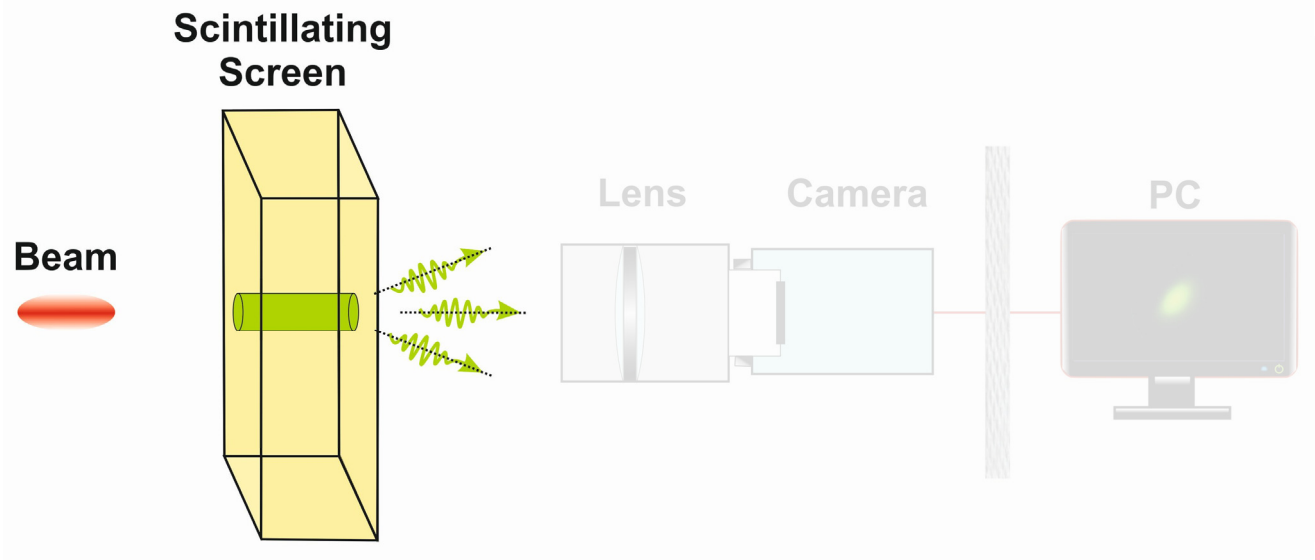


Precise measurements of the size, profile and position of a particle beam striking a scintillator screen requires

- ❖ theoretical and practical understanding of scintillating materials and their interactions with charged beams.
- ❖ a carefully designed optical system to transfer the scintillation light to the camera, so that the true particle distribution can be reconstructed.



Scintillation is the process, in which energy deposited in a material, e.g. by charged particles, is converted into photons



Physical state:

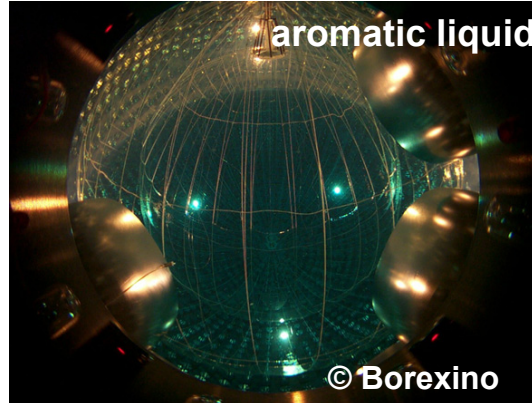
- ❖ solid



Scintillating materials

Physical state:

- ❖ solid
- ❖ liquid



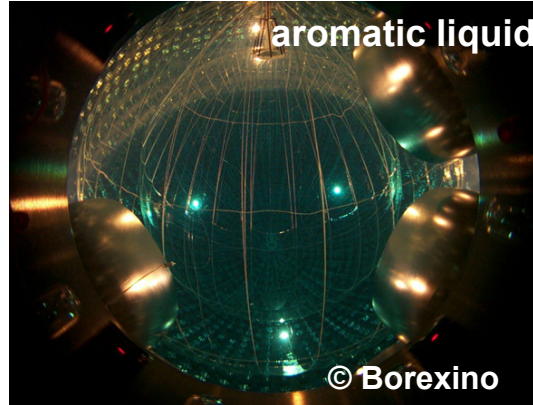
Scintillating materials

Physical state:

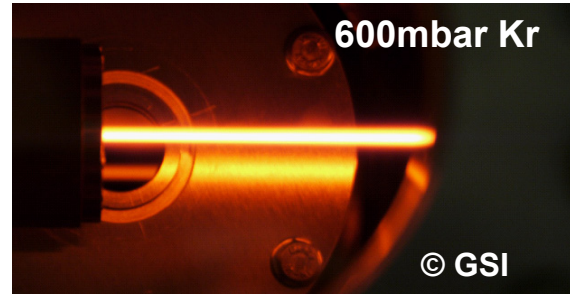
- ❖ solid
- ❖ liquid
- ❖ gas



© crytur



© Borexino

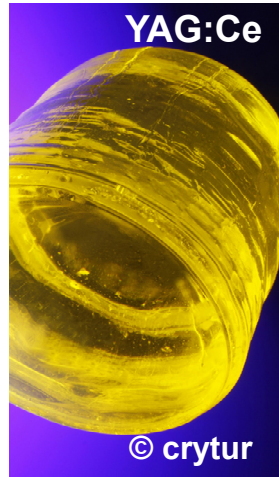


© GSI

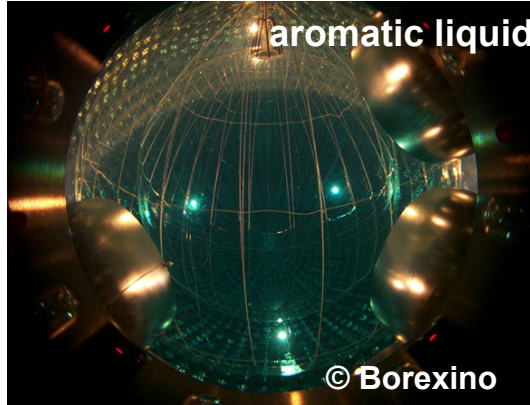
Scintillating materials

Physical state:

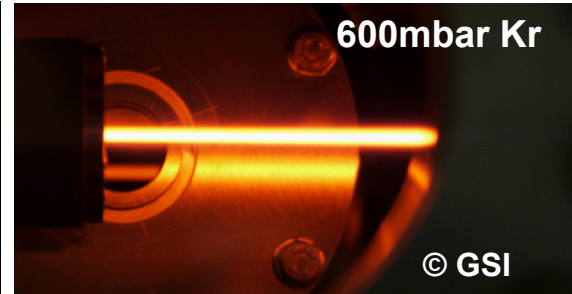
- ❖ solid
- ❖ liquid
- ❖ gas



© crytur



© Borexino



© GSI

Composition:

- ❖ organic

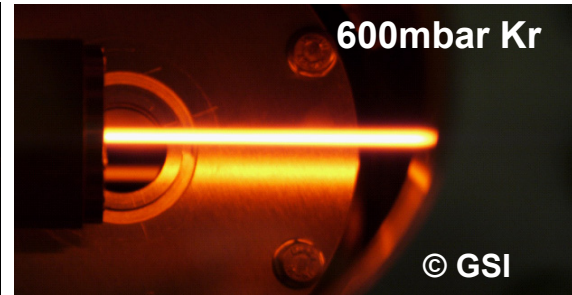
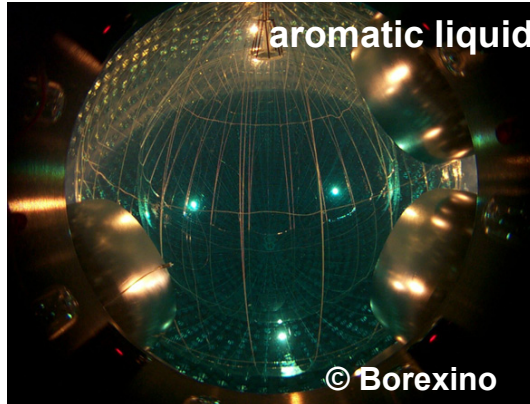


plastic

© GSI

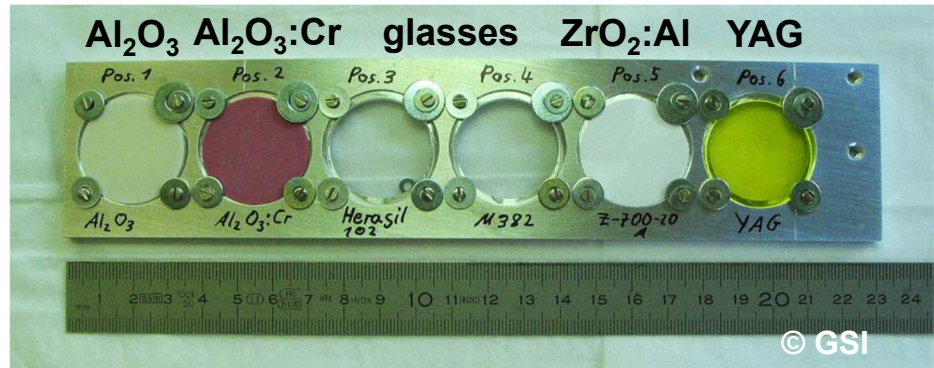
Physical state:

- ❖ solid
- ❖ liquid
- ❖ gas

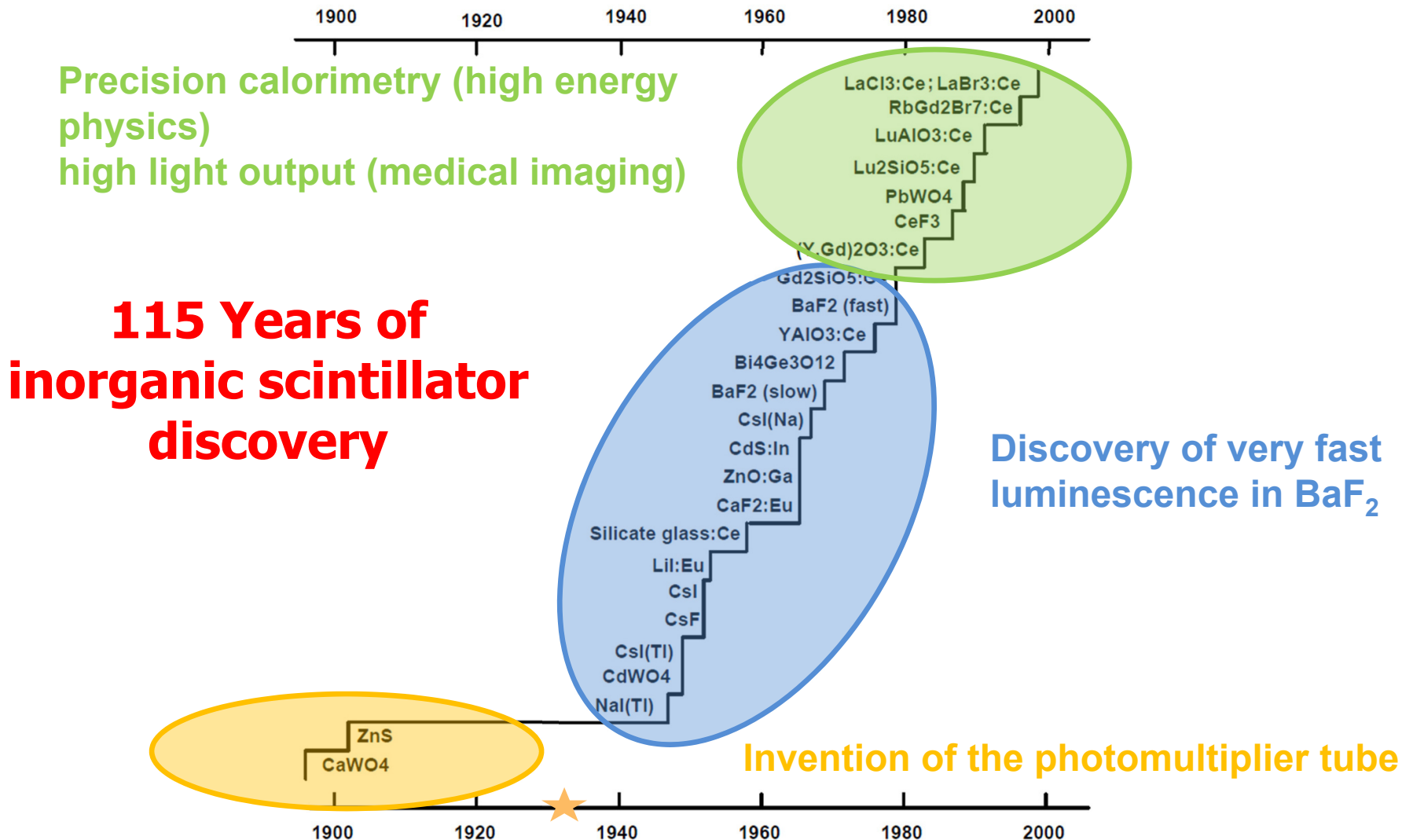


Composition:

- ❖ organic
- ❖ inorganic

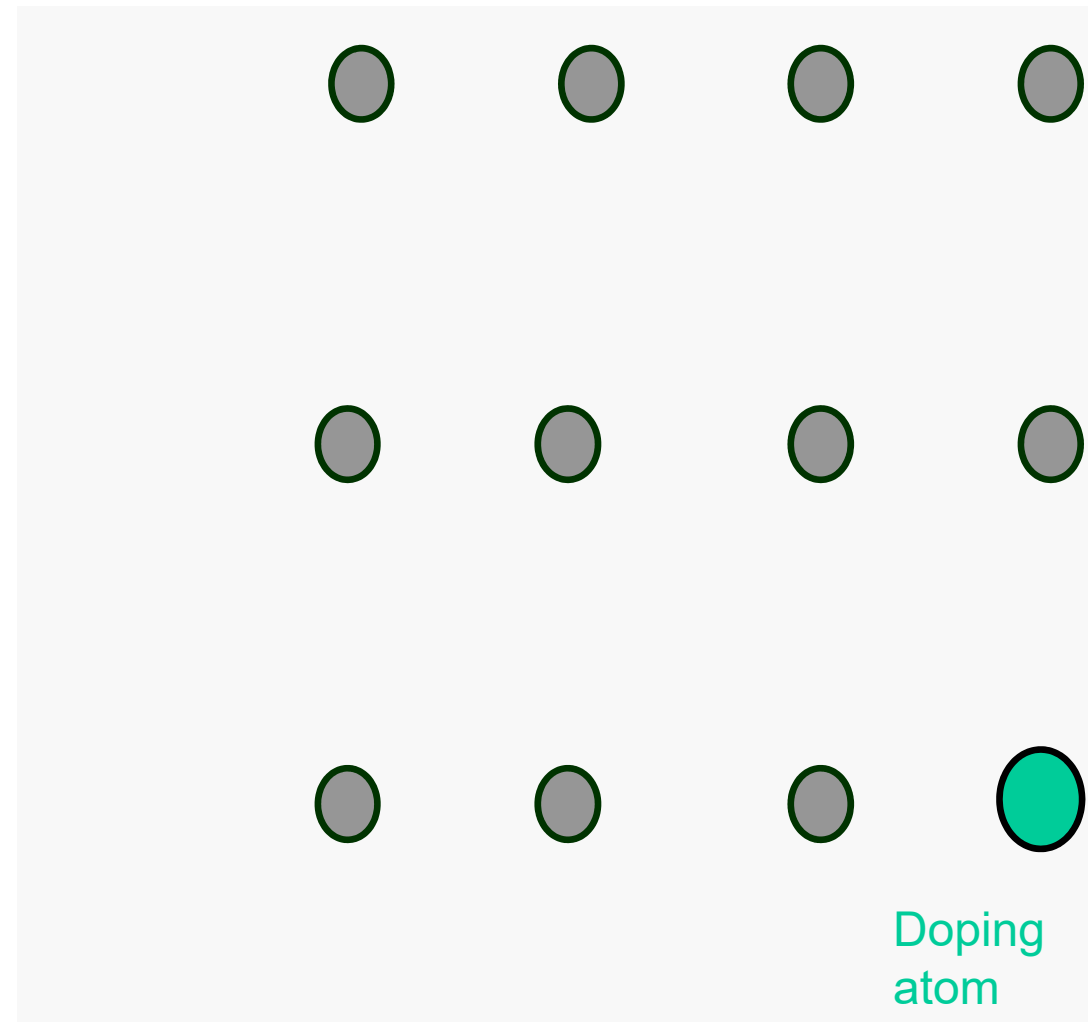


History of scintillator discovery



Scintillating process

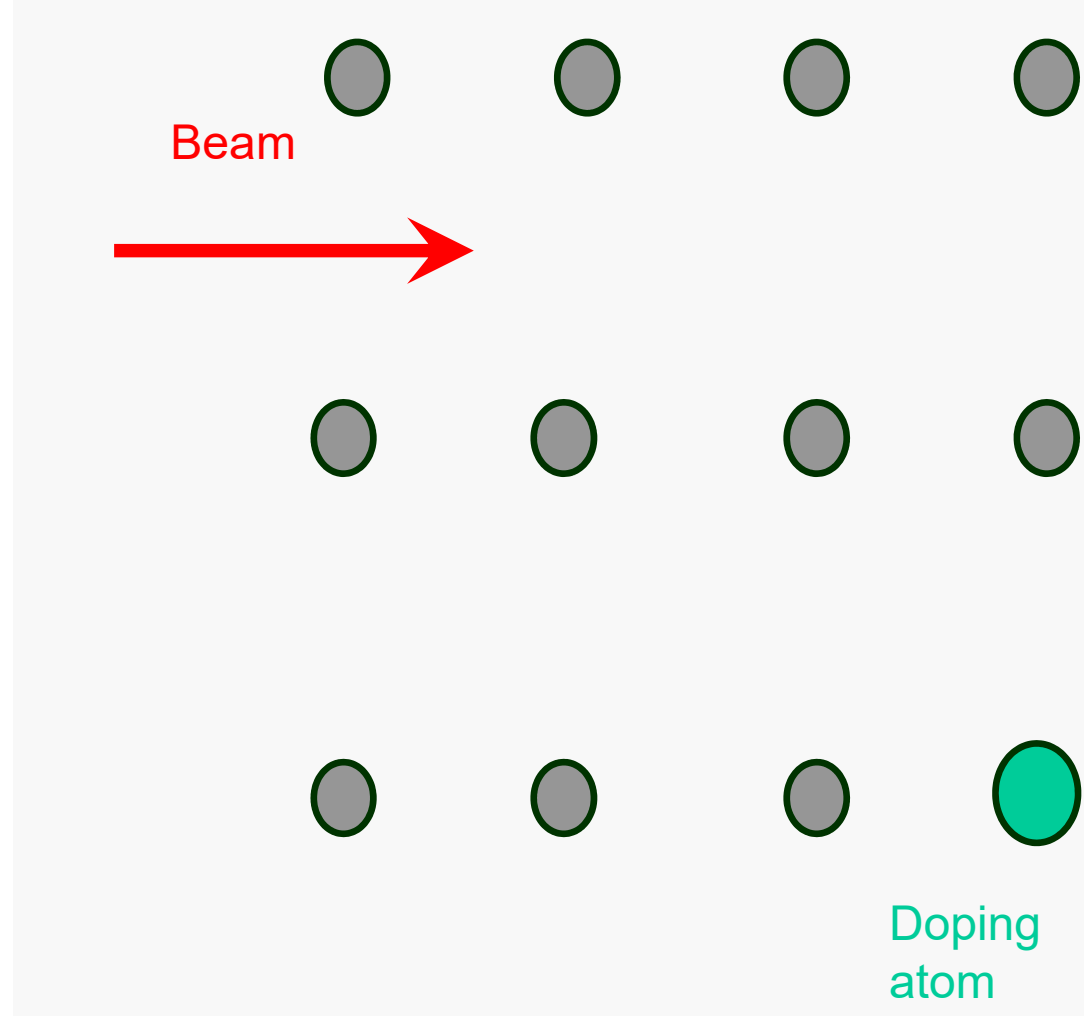
Interaction steps within the scintillation process



Scintillating process

Interaction steps within the scintillation process

- beam (electron, ions)

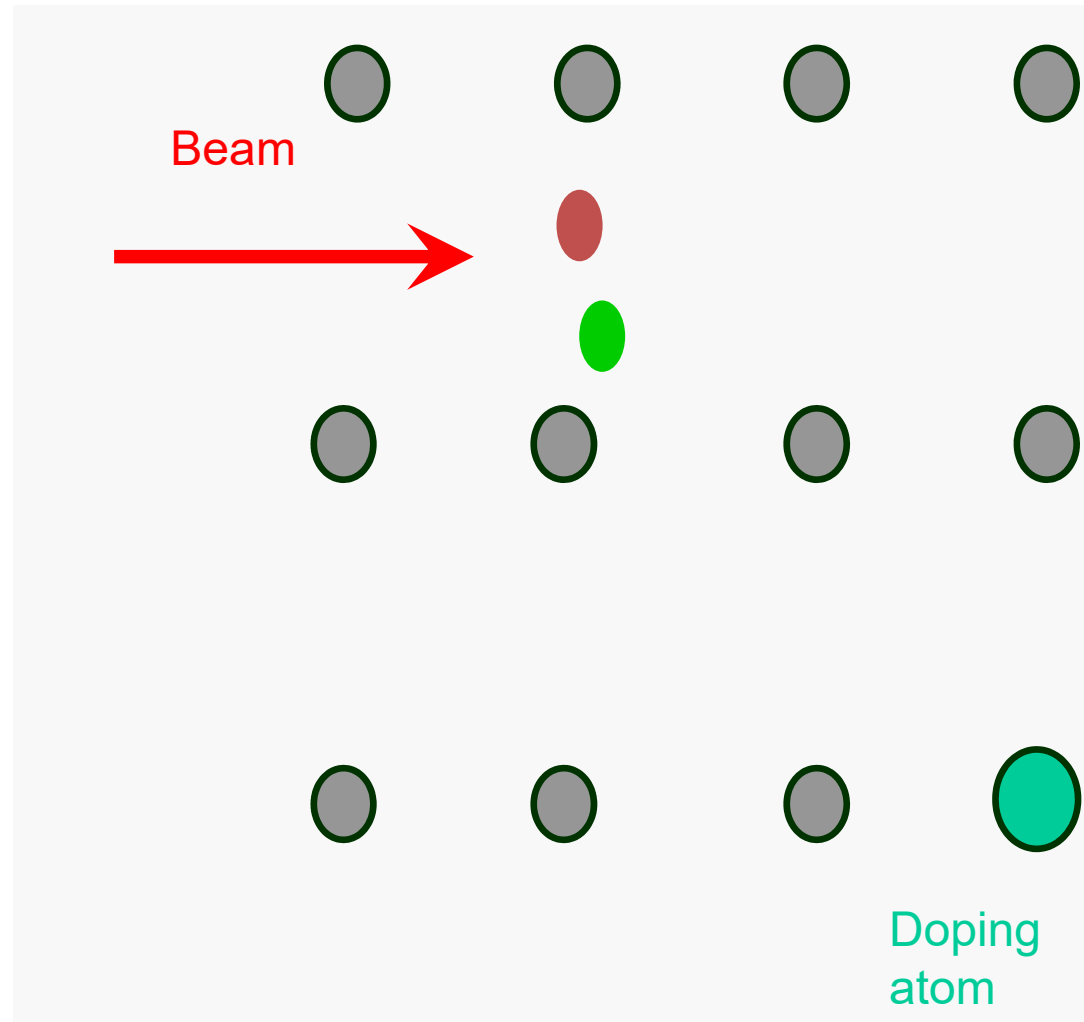


Scintillating process

Interaction steps within the scintillation process

- beam (electron, ions)

1. Primary excitations:
creation of hot electrons +
deep holes



Scintillating process

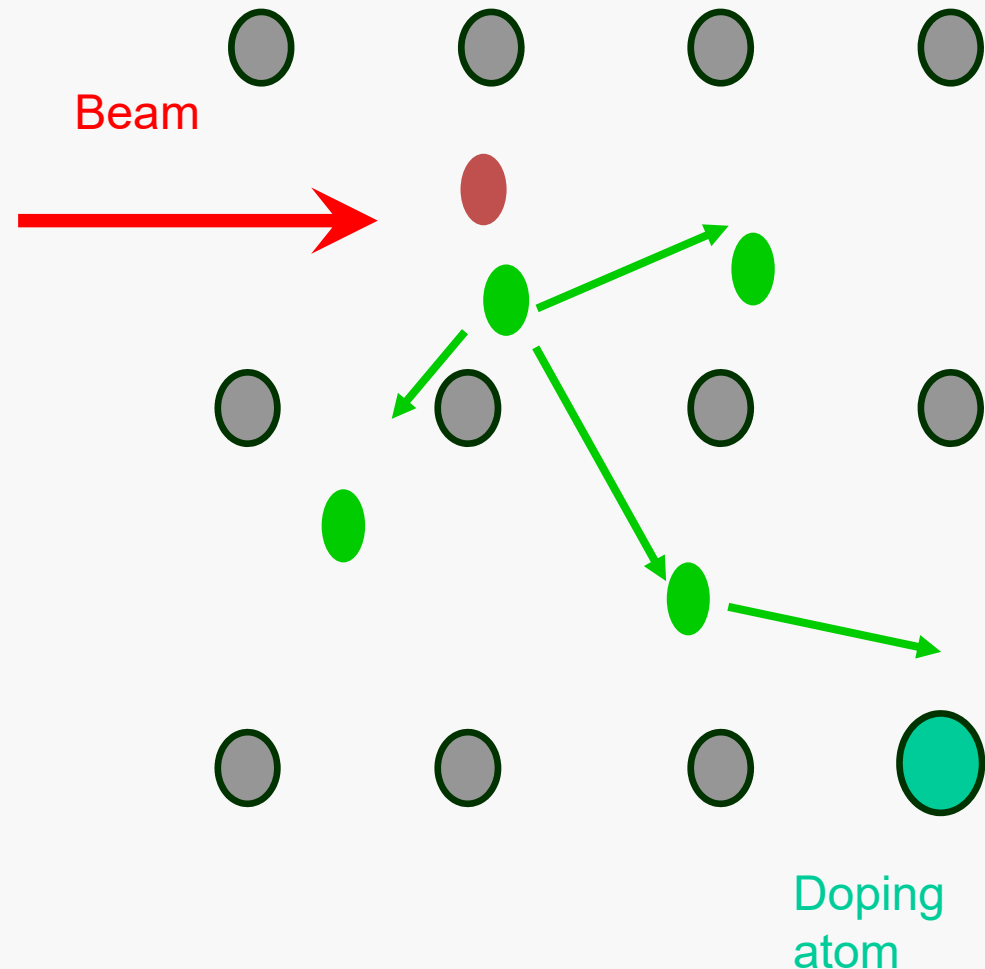
Interaction steps within the scintillation process

- beam (electron, ions)

1. Primary excitations:

creation of hot electrons +
deep holes

2. Multiplication (10^{-16} - 10^{-14} s): electron – electron scattering and Auger process



Scintillating process

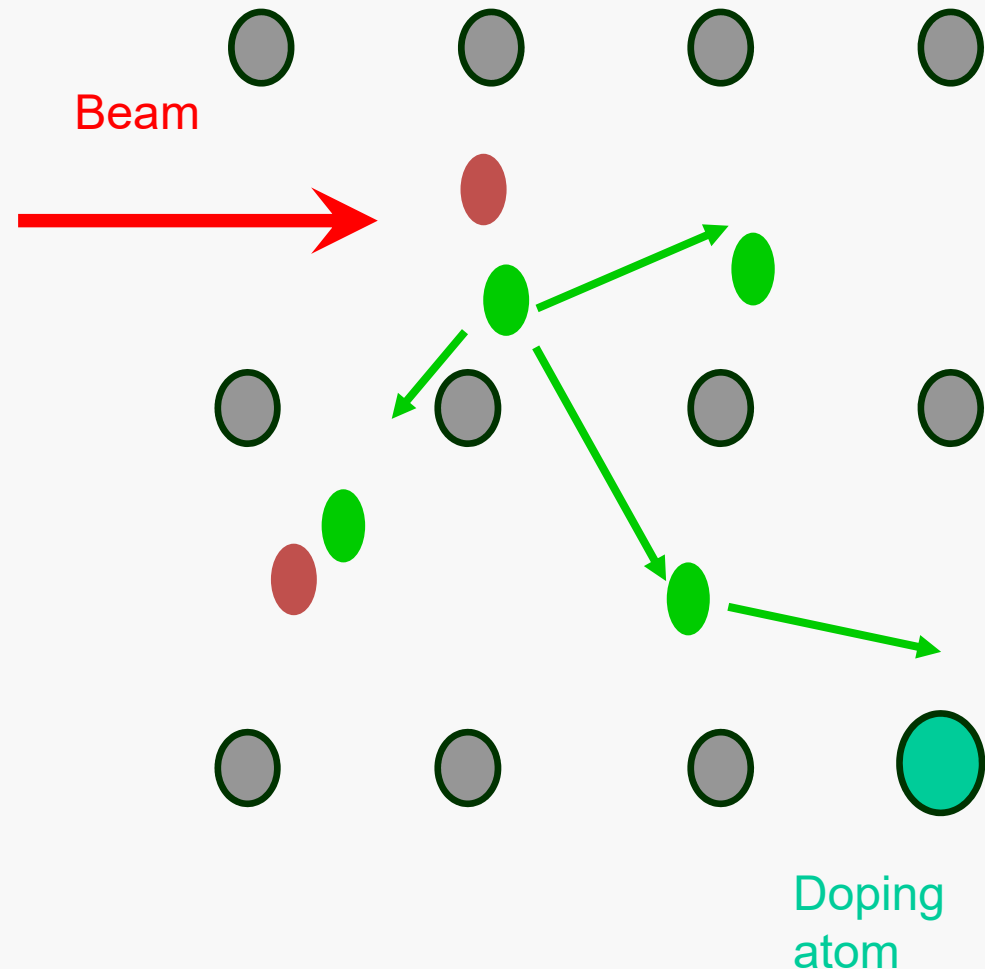
Interaction steps within the scintillation process

- beam (electron, ions)

1. Primary excitations:
creation of hot electrons +
deep holes

2. Multiplication:
electron – electron scattering
and Auger process

3. Thermalization (10^{-14} - 10^{-12} s):
electron – phonon coupling



Scintillating process

Interaction steps within the scintillation process

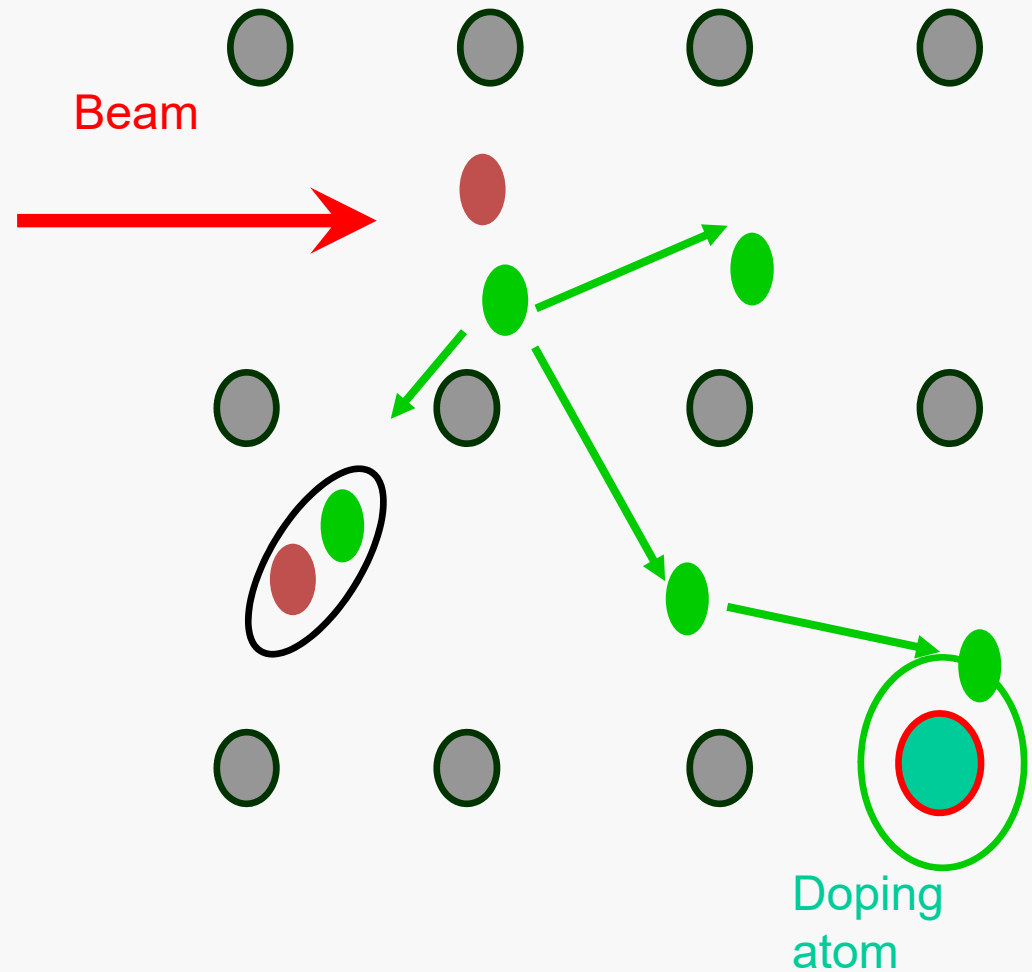
- beam (electron, ions)

1. Primary excitations:
creation of hot electrons +
deep holes

2. Multiplication:
electron – electron scattering
and Auger process

3. Thermalization:
electron – phonon coupling

4. Localisation (10^{-12} - 10^{-8} s):
capture at **doped atom** and/or
electron - hole pair creation



Scintillating process

Interaction steps within the scintillation process

- beam (electron, ions)

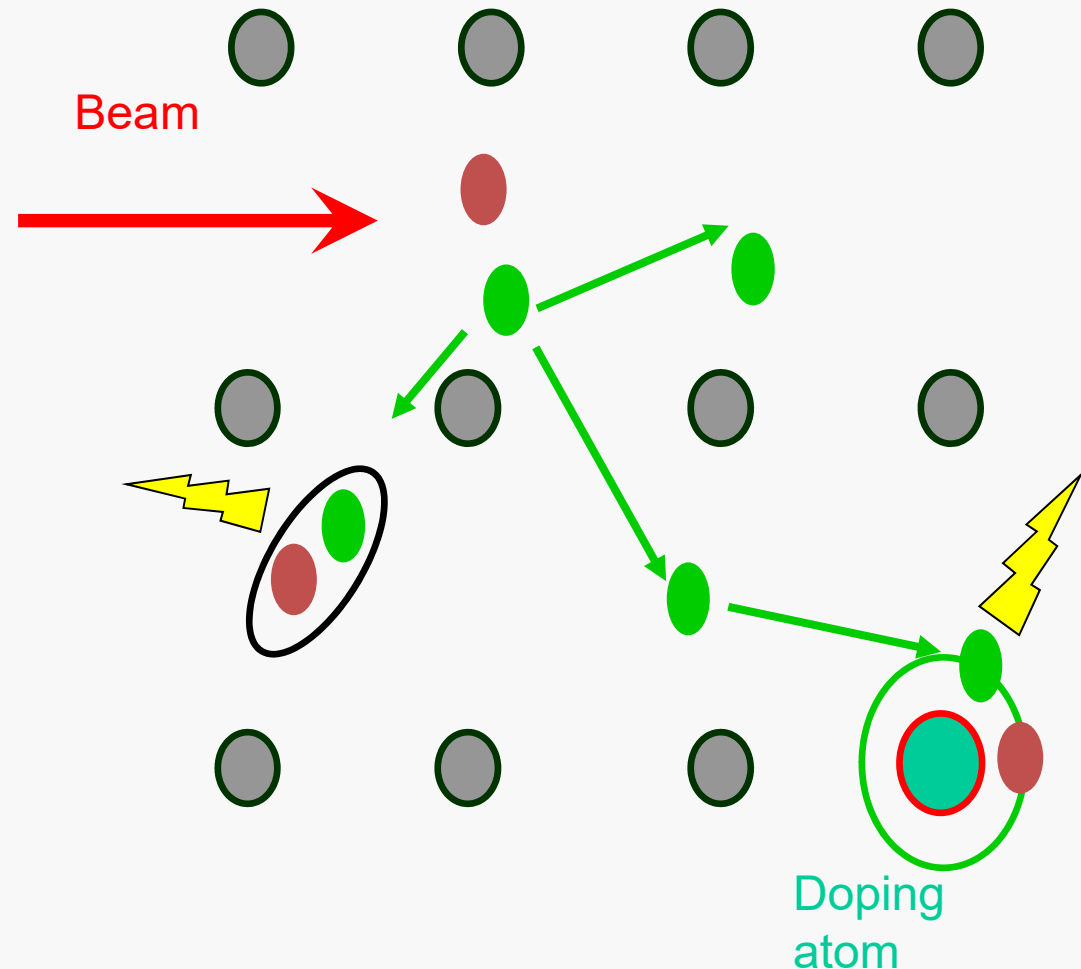
1. Primary excitations:
creation of hot electrons +
deep holes

2. Multiplication:
electron – electron scattering
and Auger process

3. Thermalization:
electron – phonon coupling

4. Localisation:
capture at **doped atom** and/or
electron - hole pair creation

5. Recombination (10^{-8} s -...):
emission of photons



Scintillation process can be influenced by many factors:

- ❖ Temperature: thermal quenching is related to electron-phonon interactions and non-radiative processes.

Scintillation process can be influenced by many factors:

- ❖ **Temperature**: thermal quenching is related to electron-phonon interactions and non-radiative processes.
- ❖ **Concentration**: interaction between luminescence centers increases with their concentration in the material. Energy migration through non-radiative energy transfer can take place if concentration is high enough.

Scintillation process can be influenced by many factors:

- ❖ **Temperature**: thermal quenching is related to electron-phonon interactions and non-radiative processes.
- ❖ **Concentration**: interaction between luminescence centers increases with their concentration in the material. Energy migration through non-radiative energy transfer can take place if concentration is high enough.
- ❖ **Impurities**: e.g. killer ions can compete with active ions and limit the scintillation efficiency.

Scintillation process can be influenced by many factors:

- ❖ **Temperature**: thermal quenching is related to electron-phonon interactions and non-radiative processes.
- ❖ **Concentration**: interaction between luminescence centers increases with their concentration in the material. Energy migration through non-radiative energy transfer can take place if concentration is high enough.
- ❖ **Impurities**: e.g. killer ions can compete with active ions and limit the scintillation efficiency.
- ❖ **Local density-induced quenching**: relaxation of electronic excitation can lead to the formation of nano-scale regions containing several electronic excitation separated by short distance.

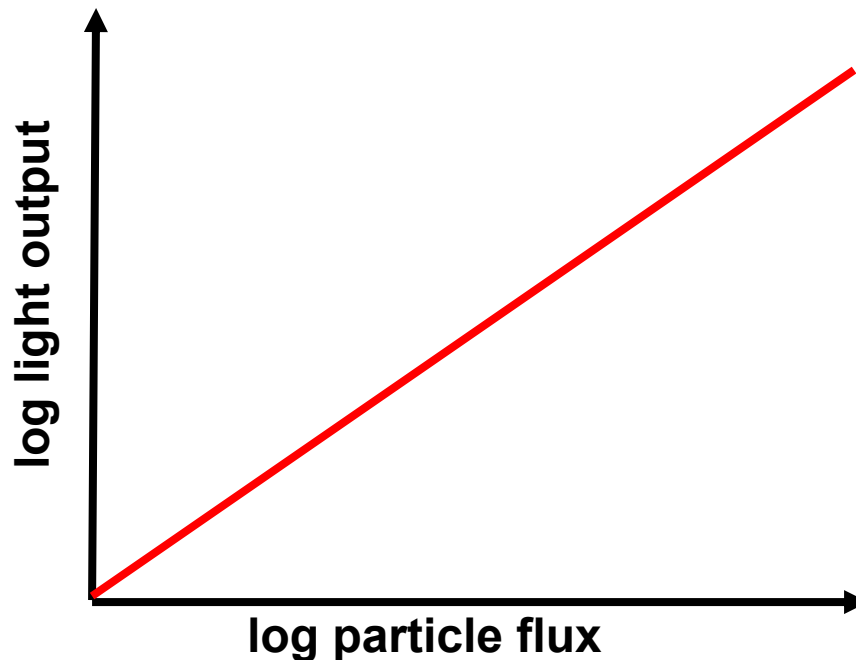
Scintillator characteristics of interest

- ❖ matched efficiency for energy conversion

Material	Photons/ MeV	Wavelength [nm]	Efficiency [%]
<i>Intrinsic</i>			
CsI	2000	315	0.8
<i>Self-activated</i>			
CdWO ₄	15000	480	3.6
Bi ₄ GeO ₁₂	8200	480	2.1
<i>Activated</i>			
NaI:Tl	38000	415	11.3
CsI:Tl	65000	540	13.7
LYSO:Ce	25000	420	7.4
YAG:Ce	16000	512	3.9

Scintillator characteristics of interest

- ❖ matched efficiency for energy conversion
- ❖ **high dynamic range and “good linearity” (power law) between the incident particle flux and the light output**



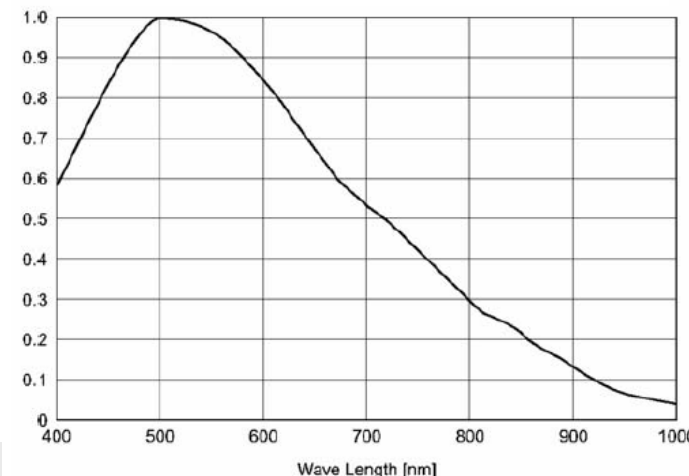
Scintillator characteristics of interest

- ❖ matched efficiency for energy conversion
- ❖ high dynamic range and “good linearity” (power law) between the incident particle flux and the light output
- ❖ emission spectrum matches the transmission spectrum of the optical system and the spectral sensitivity of the light detector

Material	Photons/ MeV	Wavelength [nm]	Efficiency [%]
<i>Intrinsic</i>			
CsI	2000	315	0.8
<i>Self-activated</i>			
CdWO ₄	15000	480	3.6
Bi ₄ GeO ₁₂	8200	480	2.1
<i>Activated</i>			
NaI:TI	38000	415	11.3
CsI:TI	65000	540	13.7
LYSO:Ce	25000	420	7.4
YAG:Ce	16000	512	3.9



Spectral sensitivity of typical CCD Camera



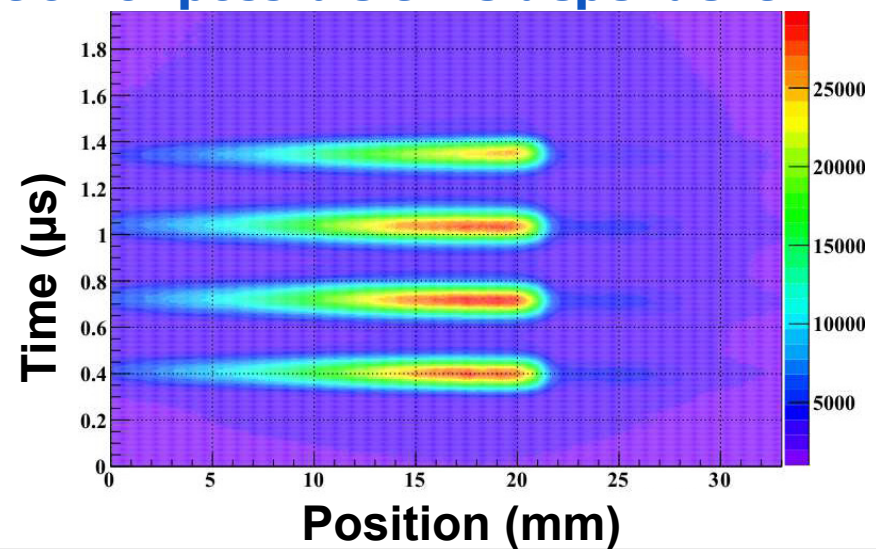
Scintillator characteristics of interest



- ❖ matched efficiency for energy conversion
- ❖ high dynamic range and “good linearity” (power law) between the incident particle flux and the light output
- ❖ emission spectrum matches the transmission spectrum of the optical system and the spectral sensitivity of the light detector
- ❖ no absorption or reemission of the emitted light to prevent artificial broadening by stray light inside the material

Scintillator characteristics of interest

- ❖ matched efficiency for energy conversion
- ❖ high dynamic range and “good linearity” (power law) between the incident particle flux and the light output
- ❖ emission spectrum matches the transmission spectrum of the optical system and the spectral sensitivity of the light detector
- ❖ no absorption or reemission of the emitted light to prevent artificial broadening by stray light inside the material
- ❖ **fast decay time, to enable observation of possible time dependent beam size variations**



Scintillator characteristics of interest

- ❖ matched efficiency for energy conversion

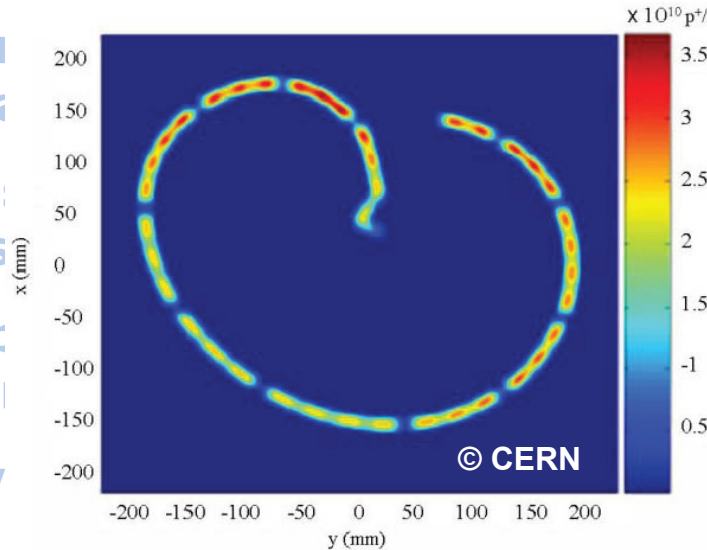
- ❖ high dynamic range for incident particles

- ❖ emission intensity matched to optical system

- ❖ no absorption by artificial backgrounds

- ❖ fast decay length matched to beam size

- ❖ good mechanical and thermal properties



(power law) between the

emission spectrum of the

incident particle and the

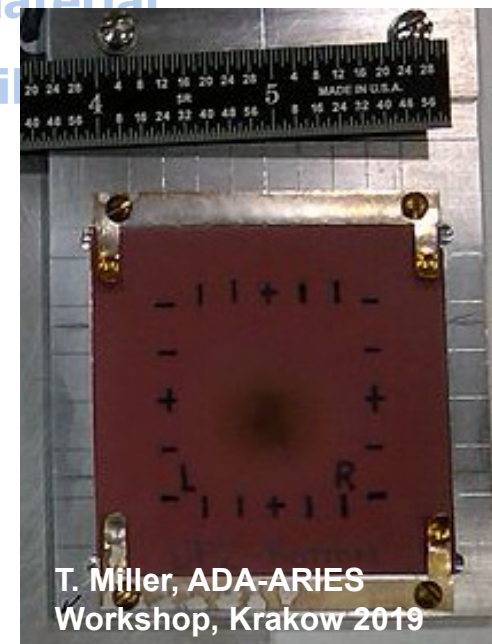
beam size

and the position of the



Scintillator characteristics of interest

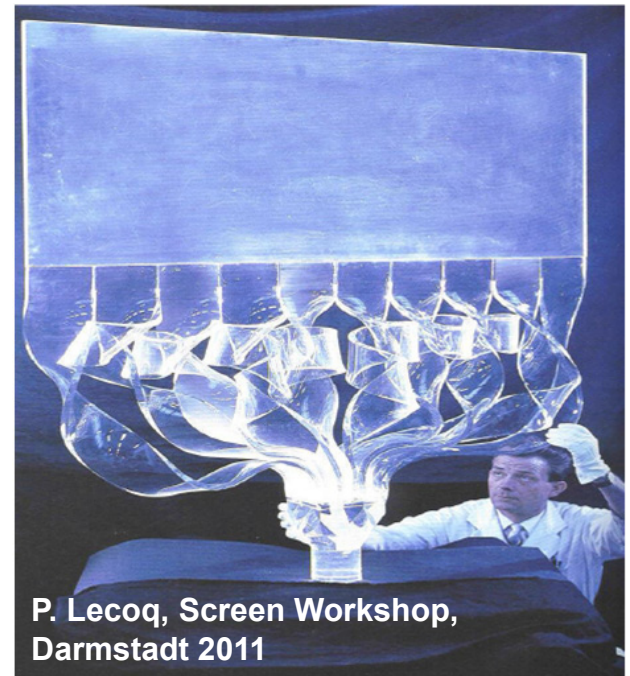
- ❖ matched efficiency for energy conversion
- ❖ high dynamic range and “good linearity” (power law) between the incident particle flux and the light output
- ❖ emission spectrum matches the transmission spectrum of the optical system and the spectral sensitivity of the light detector
- ❖ no absorption or reemission of the emitted light to prevent artificial broadening by stray light inside the material
- ❖ fast decay time, to enable observation of possible beam size variations
- ❖ good thermal and mechanical properties
- ❖ **high radiation hardness to prevent damages**



Typical screen materials

Plastic organic scintillators

- + high light output
- + very fast
- + cheap
- + easy cast in big sizes and flexible shapes
- not radiation hard



P. Lecoq, Screen Workshop,
Darmstadt 2011

Typical screen materials

Plastic organic scintillators

- + high light output
- + very fast
- + cheap
- + easy cast in big sizes and flexible shapes
- not radiation hard

Crystals e.g. ZnS, YAG:Ce ($\text{Y}_3\text{Al}_5\text{O}_{12}:\text{Ce}$), BGO ($\text{Bi}_4\text{Ge}_3\text{O}_{12}$), LYSO ($\text{Lu}_{1.8}\text{Y}_{0.2}\text{SiO}_5:\text{Ce}$), CWO (CdWO_4)

- + high light output
- + scintillation in narrow spectral range: reduced chromatic aberration
- high costs for single crystal samples
- degradation effects for high current beams



Typical screen materials

Plastic organic scintillators

- + high light output
- + very fast
- + cheap
- + easy cast in big sizes and flexible shapes
- not radiation hard

Crystals e.g. ZnS, YAG:Ce ($\text{Y}_3\text{Al}_5\text{O}_{12}:\text{Ce}$), BGO ($\text{Bi}_4\text{Ge}_3\text{O}_{12}$), LYSO

- + high light output
- + scintillation in narrow spectral range: reduced chromatic aberration
- high costs for single crystal samples
- degradation effects for high current beams



Powder crystals e.g. P43 ($\text{Gd}_2\text{O}_2\text{S}:\text{Tb}$), P46 ($\text{Y}_3\text{Al}_5\text{O}_{12}:\text{Ce}$), P47 ($\text{Y}_2\text{Si}_5\text{O}_5:\text{Tb}$)

- + high light output
- + resolution limited by grain size
- + flexible sizes and shapes
- mechanical degradation effects for high current beams

Typical screen materials

Plastic organic scintillators

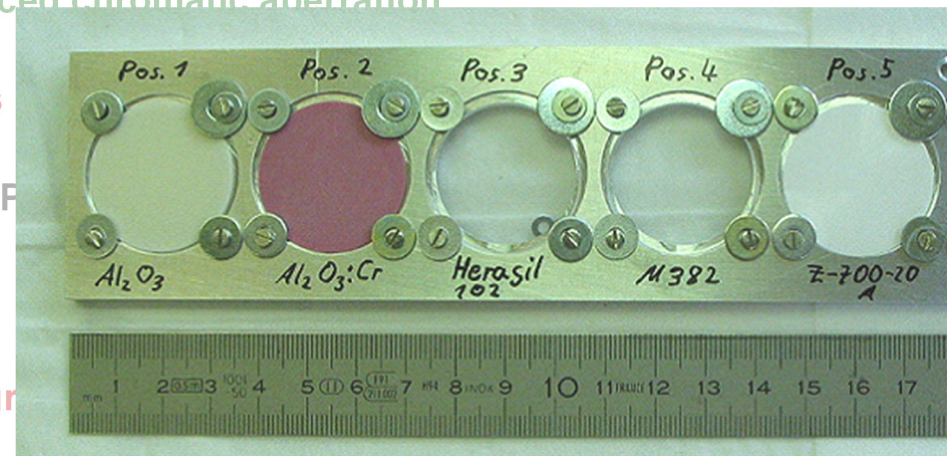
- + high light output
- + very fast
- + cheap
- + easy cast in big sizes and flexible shapes
- not radiation hard

Crystals e.g. ZnS, YAG:Ce ($\text{Y}_3\text{Al}_5\text{O}_{12}:\text{Ce}$), BGO ($\text{Bi}_4\text{Ge}_3\text{O}_{12}$), LYSO ($\text{Lu}_{1.8}\text{Y}_{0.2}\text{SiO}_5:\text{Ce}$), CWO (CdWO_4)

- + high light output
- + scintillation in narrow spectral range: reduced chromatic aberration
- high costs for single crystal samples
- degradation effects for high current beams

Powder crystals e.g. P43 ($\text{Gd}_2\text{O}_2\text{S}:\text{Tb}$), P

- + high light output
- + resolution limited by grain size
- + flexible sizes and shapes
- mechanical degradation effects for high cur



Ceramics e.g. $\text{ZrO}_2:\text{Al}$, $\text{ZrO}_2:\text{Mg}$, $\text{ZrO}_2:\text{Y}$, Al_2O_3 , Chromox ($\text{Al}_2\text{O}_3:\text{Cr}$), **AlN**, **BN**

- low and moderate light output
- + high resistance against high current beams
- + flexible sizes and shapes

Energy loss in material

$$-\left(\frac{dE}{dx}\right) = 2\pi N_A r_e^2 m_e c^2 \rho \cdot \frac{Z}{A} \cdot \frac{z^2}{\beta^2} \left[\ln \left(\frac{2m_e \beta^2 \vartheta^2 W_{max}}{I^2} \right) - 2\beta^2 \right]$$

N_A Avogadro number

m_e and r_e electron mass and classical radius

c velocity of light

ρ density of the target with

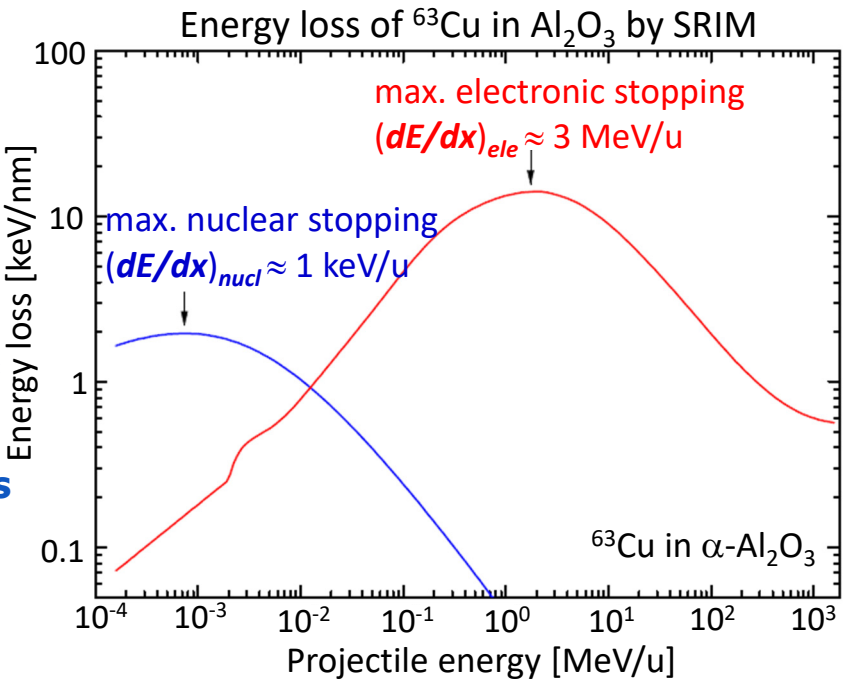
nuclear mass A and nuclear charge Z

I mean ionization potential for the target

z nuclear charge of the ion with velocity β and $\gamma =$

$$(1 - \beta^2)^{-\frac{1}{2}}$$

$W_{max} = 2m_e(c \cdot \beta)^2 \gamma^2$ max. kin. energy of electrons



Nuclear stopping: Binary collision of ion with one target nucleus

Electronic stopping: Collision of ion with many target electrons

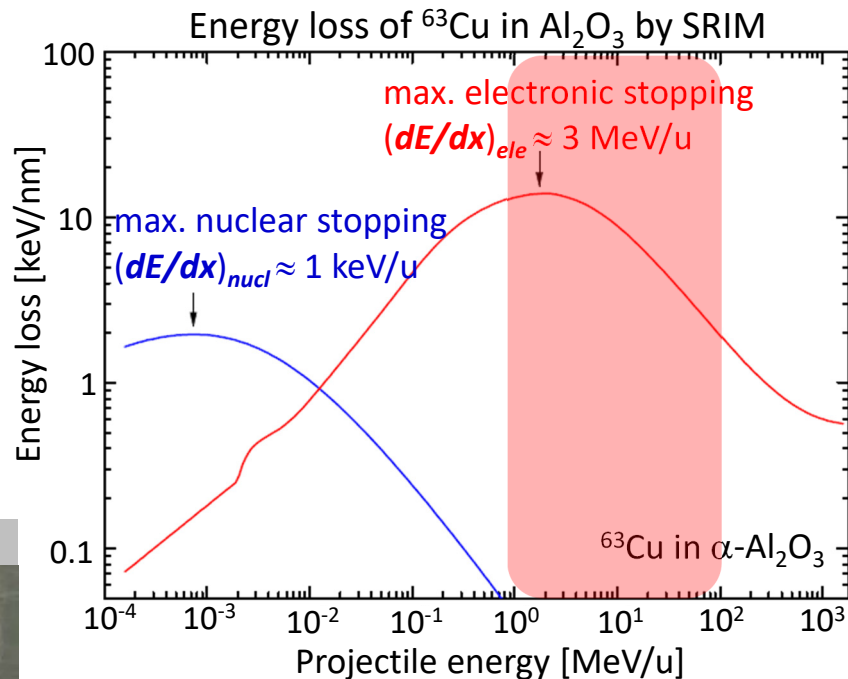
Energy loss in material

$$-\left(\frac{dE}{dx}\right) = 2\pi N_A r_e^2 m_e c^2 \rho \cdot \frac{Z}{A} \cdot \frac{z^2}{\beta^2} \left[\ln\left(\frac{2m_e \beta^2 \vartheta^2 W_{max}}{I^2}\right) - 2\beta^2 \right]$$

1 MeV/u < E_{kin} < 100 MeV/u

large dE/dx \Rightarrow large damage

Ion	Energy [MeV/u]	Range R [μm]	dE/dx [keV/nm]	Damage σ_d [10^{-14}cm^2]
^{14}N	3,6	26	1,5	0,03
^{132}Xe	4,8	27	28,5	20
^{197}Au	5,9	37	38,5	38
^{209}Bi	4,8	31	41,4	48



Energy loss in material

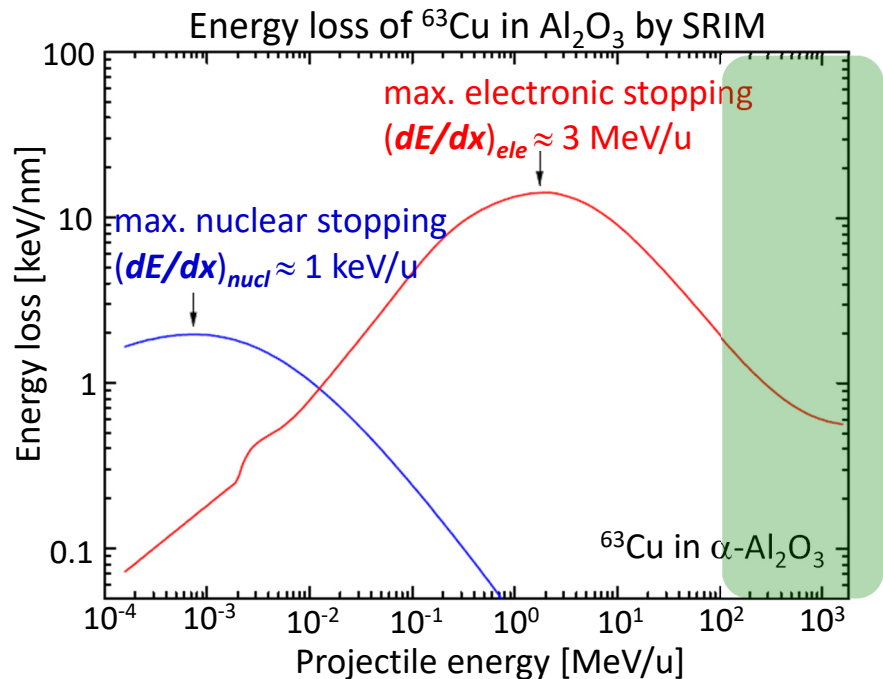
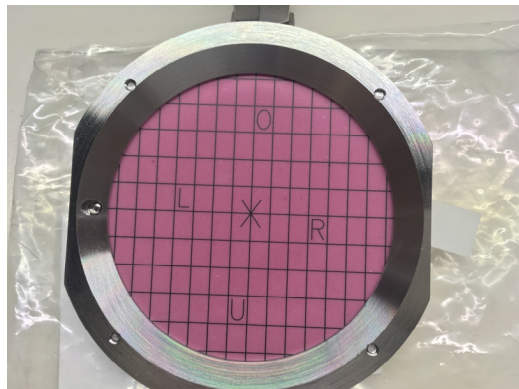
$$-\left(\frac{dE}{dx}\right) = 2\pi N_A r_e^2 m_e c^2 \rho \cdot \frac{Z}{A} \cdot \frac{z^2}{\beta^2} \left[\ln\left(\frac{2m_e\beta^2\vartheta^2 W_{max}}{I^2}\right) - 2\beta^2 \right]$$

$E_{kin} > 100 \text{ MeV/u}$

low $dE/dx \Rightarrow$ low damage

Ion	Nucl. Z	Energy [MeV/u]	dE/dx [keV/nm]
^{59}Ni	28	300	0.9
^{238}U	92		10

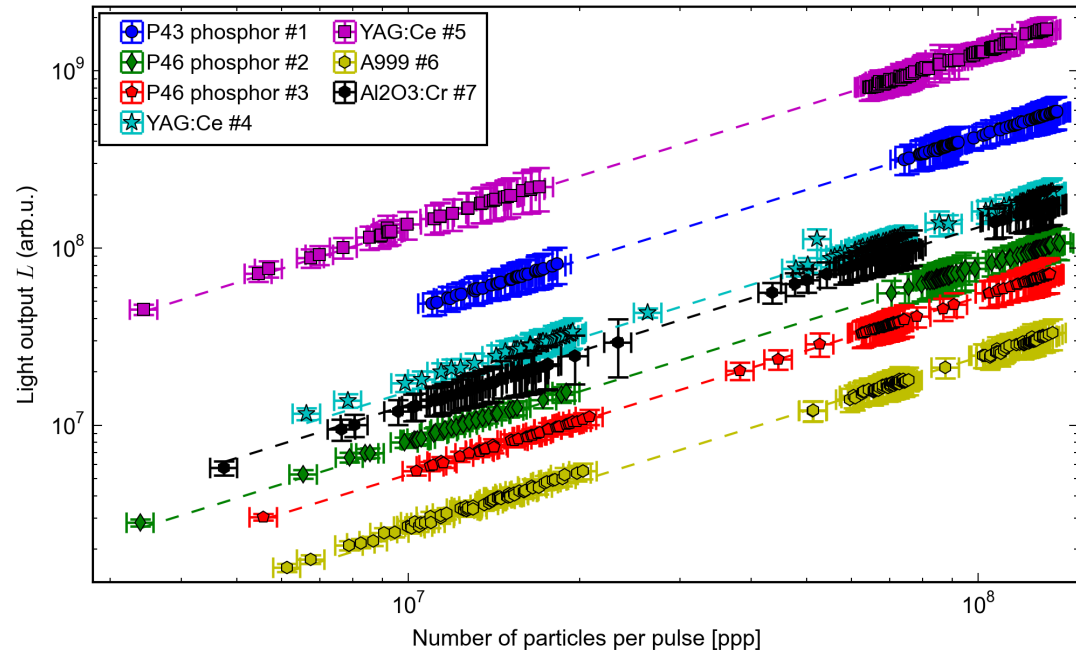
range $R \gg d_{target} = 0.25 - 1 \text{ mm}$



Screens for ion beams

Light yield L of different screens

	material	thickness (mm)
#1	P43	0.05
#2	P46	0.05
#3	P46	0.1
#4	YAG:Ce	0.25
#5	YAG:Ce	1
#6	Al_2O_3	1
#7	$\text{Al}_2\text{O}_3:\text{Cr}$	1



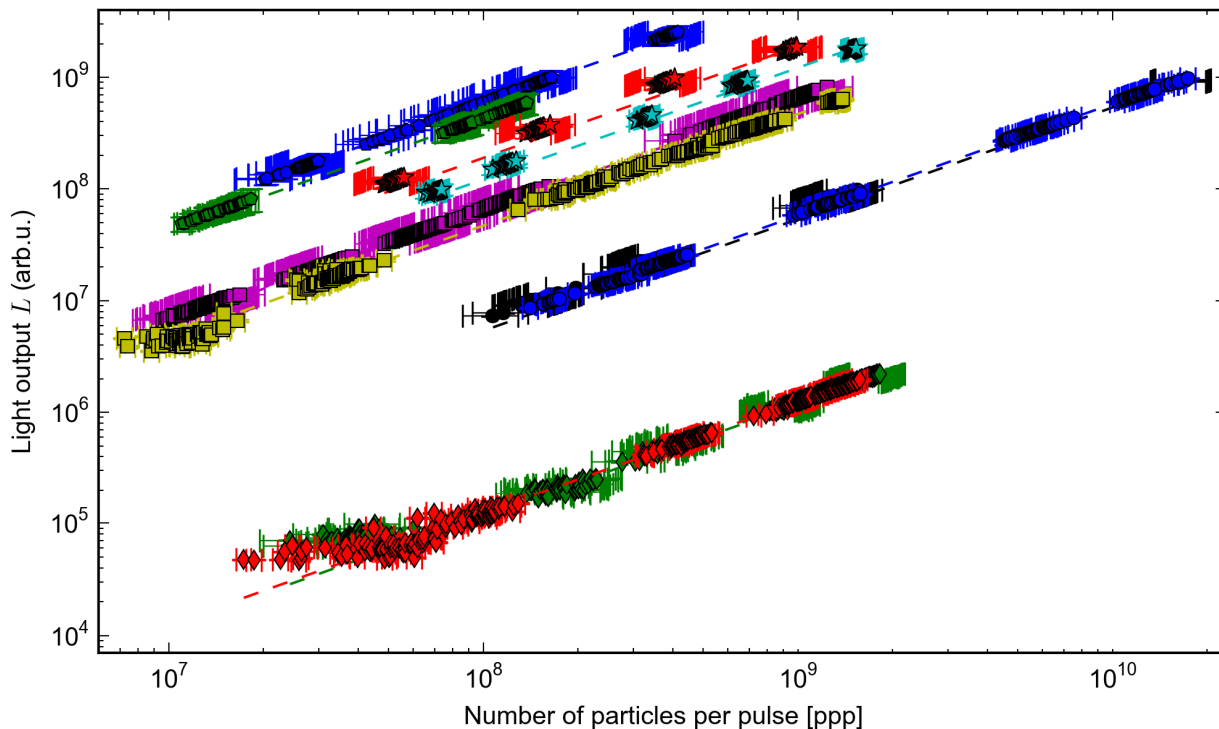
Beam parameters: Uranium at 300 MeV/u, 10^6 – 10^9 particles per pulse (ppp), 1 μs pulse length

- ❖ “linear” behaviour in light yield
- ❖ light yield depends on material and it thickness
- ❖ YAG:Ce #5: max. L observed (10 times more than YAG:Ce #4)
- ❖ Al_2O_3 : Cr doping results in five times more L per ion as for Al_2O_3
- ❖ P43 is the most efficient from all the phosphors

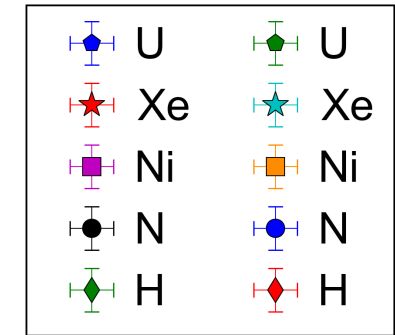
A. Lieberwirth et al., NIMB, Volume 356 (2015)

Screens for ion beams

Light yield L of P43 phosphor screen for different ion species fast and slow extracted



slow (1s): fast (1μs):

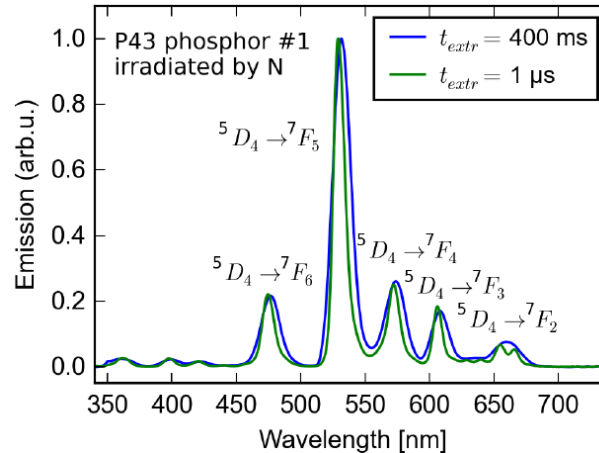
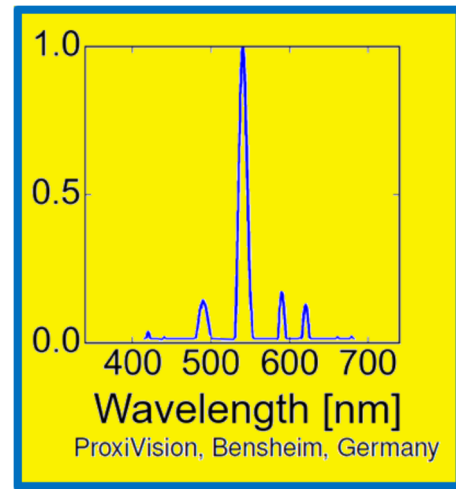


Beam parameters: heavy ions at 300 MeV/u

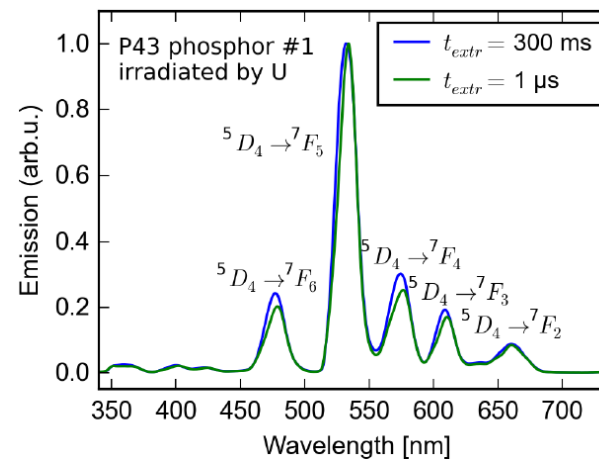
- ❖ protons induce the lowest light output
- ❖ light output increase with atomic number
- ❖ similar behavior for others scintillator materials

Screens for ion beams

Emission Spectrum of P43 phosphor screen for different ion species fast and slow extracted



fast/slow extraction N-beam
10⁹ ppp



fast/slow extraction U-beam
10⁹ ppp

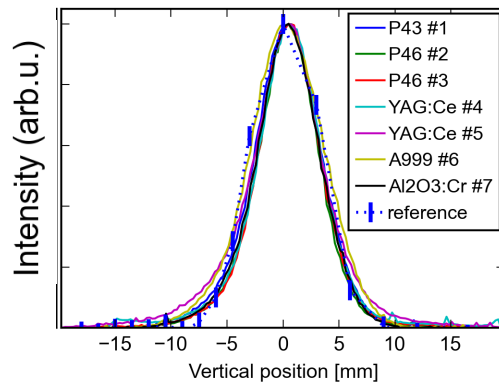
Beam parameters: heavy ions at 300 MeV/u

- ❖ good agreement with literature values for all ion species

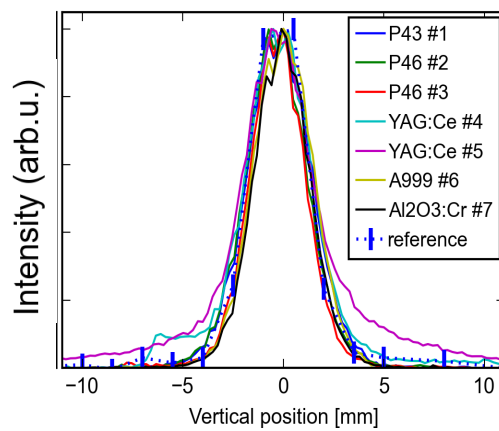
A. Lieberwirth et al., NIMB, Volume 356 (2015)

Screens for ion beams

Beam profile reading for different screens and different ion species



fast extraction N-beam 10^9 ppp



fast extraction Xe-beam 10^9 ppp

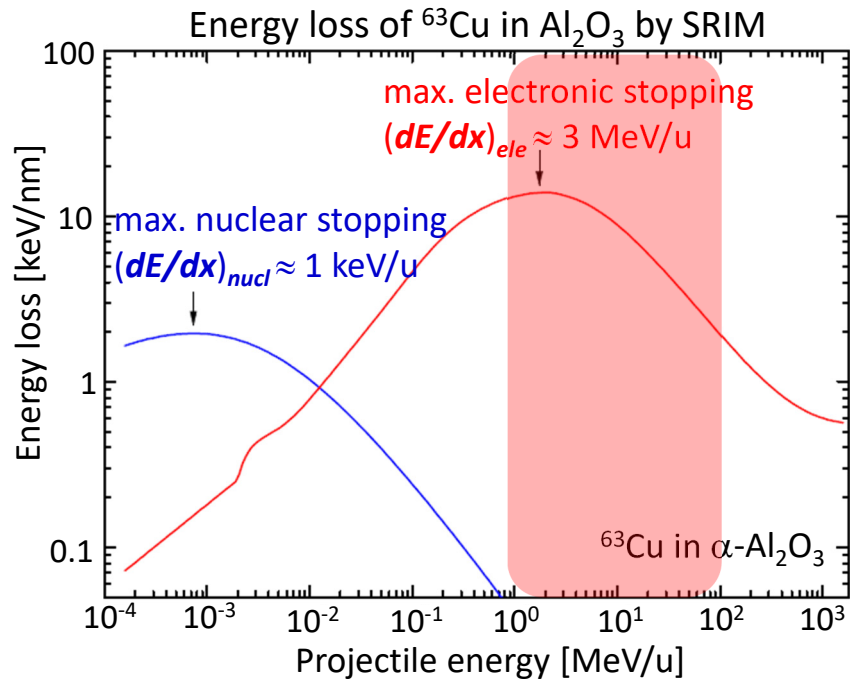
Beam parameters: heavy ions at 300 MeV/u

- ❖ good agreement with reference method (SEM-Grid) for all scintillator materials and ion species

Energy loss in material

$$-\left(\frac{dE}{dx}\right) = 2\pi N_A r_e^2 m_e c^2 \rho \cdot \frac{Z}{A} \cdot \frac{z^2}{\beta^2} \left[\ln\left(\frac{2m_e \beta^2 \vartheta^2 W_{max}}{I^2}\right) - 2\beta^2 \right]$$

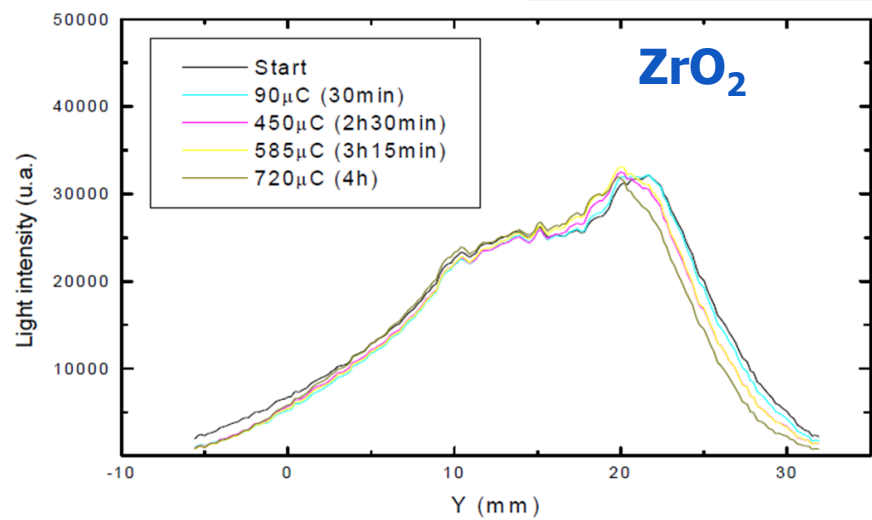
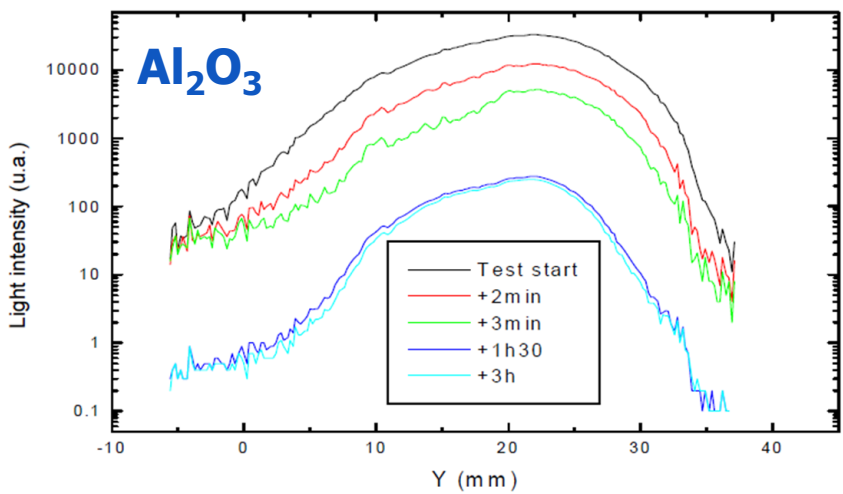
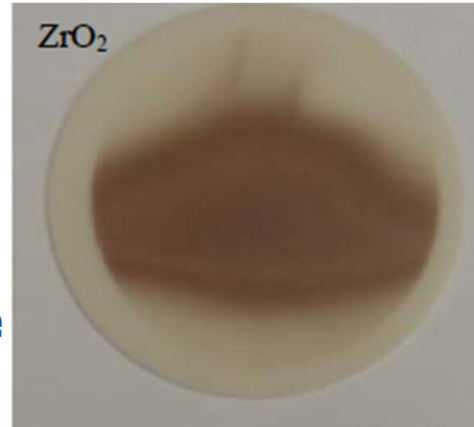
1 MeV/u < E_{kin} < 100 MeV/u
large $dE/dx \Rightarrow$ large damage



Screens for ion beams

Different materials showed different behavior during irradiation

- ❖ standard used Chromox was fading with time
- ❖ Al_2O_3 light yield decreased with time
- ❖ ZrO_2 very stable behavior although coloration of surface



Beam parameters: Pb^{54+} , 4.2MeV/u, 100 μA , 60 μs

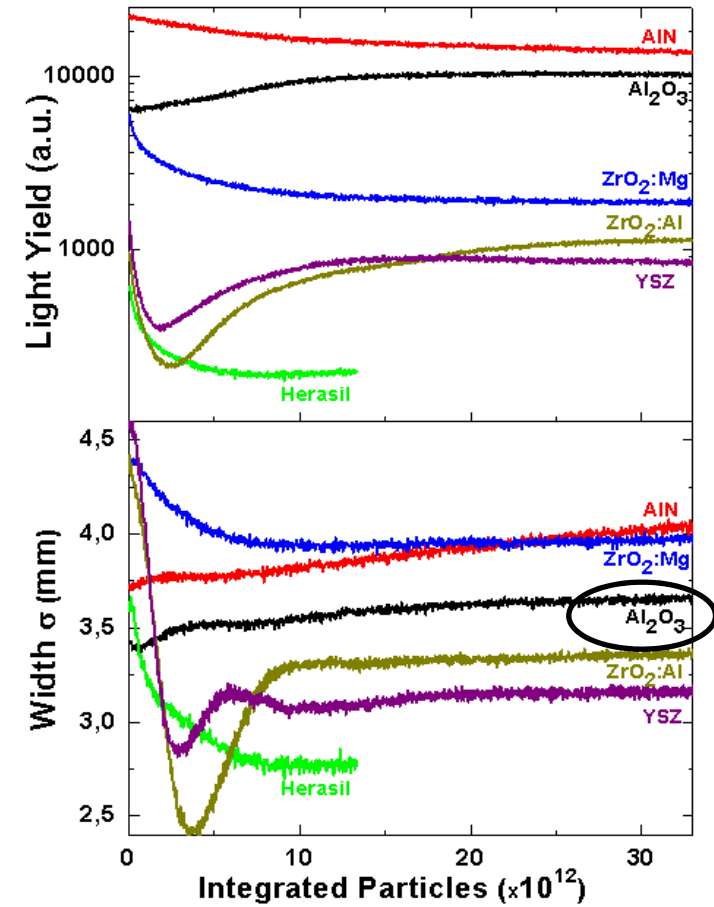
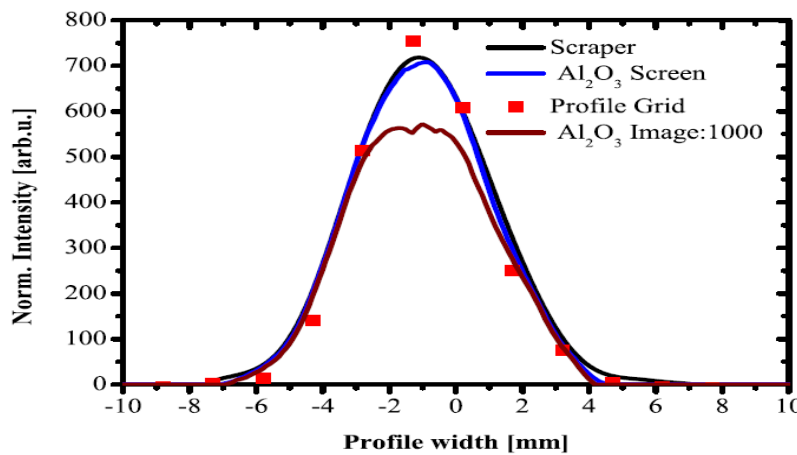
C. Bal, CERN, DIPAC2005

E. Bravin, Scintillating Screen Workshop Darmstadt 2011

Screens for ion beams

Different materials showed different behavior during irradiation

- ❖ light output and profile width depend on material
- ❖ different dynamical behavior
- ❖ change in the beam width and shape
- ❖ possible reasons: material modification and thermal quenching



Beam parameters: Ar¹⁰⁺, 11.4 MeV/u,
 $3.3 \cdot 10^{10}$ ppp in 0.2 ms, 260 µA, 1000 pulses

Screens for ion beams

Empirical Birks model for radiation damage in intrinsic scintillator: scintillation caused by imperfection in lattice

Light yield $S(\Phi)$ as function of fluence Φ

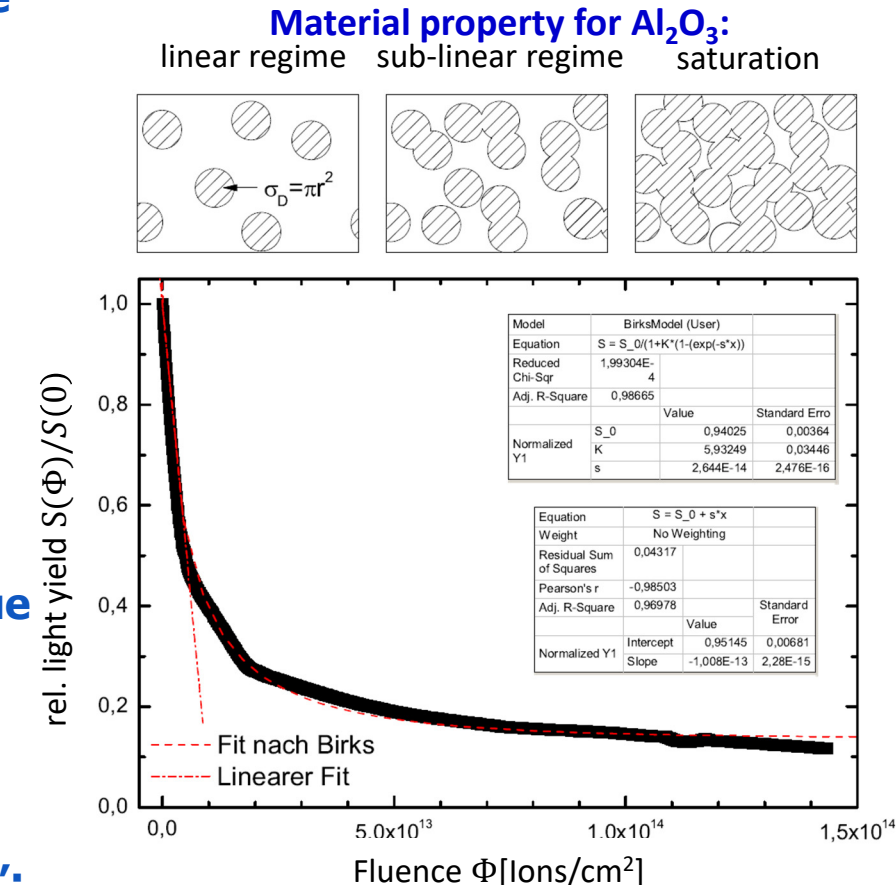
$$S(\Phi) = S(0) \cdot \frac{1}{1+K \cdot [1-\exp(-\sigma_D \Phi)]}$$

σ_D : damage cross section of a single ion

K: quenching factor

Description:

1. Radiation leads to damages of the scintillator in the ion channel, e.g. displacements \Rightarrow lower luminescence due to quenching
2. Partly destroyed material
3. Finally saturation of 'destroyed material': probability for 'landing' in a vacancy increases



S. Lederer et al., NIM B 359, 2015

P. Forck, ADA-ARIES Workshop, Krakow 2019

Screens for ion beams

**Empirical Birks model for radiation damage in intrinsic scintillator:
scintillation caused by imperfection in lattice**

Light yield $S(\Phi)$ as function of fluence Φ

$$S(\Phi) = S(0) \cdot \frac{1}{1+K \cdot [1-\exp(-\sigma_D \Phi)]}$$

σ_D : damage cross section of a single ion

K : quenching factor

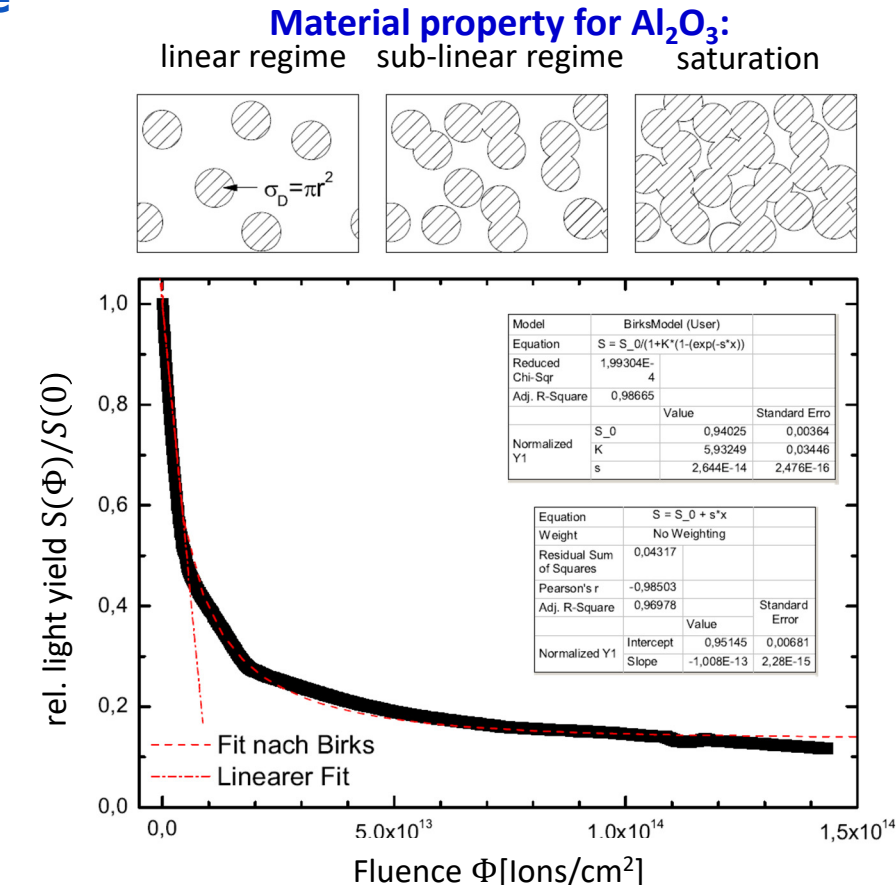
Findings:

Initial: Large decrease in light yield

$$S(\Phi) = S(0) \cdot \frac{1}{1+K \cdot \sigma_D \Phi}$$

Final: Lower, but constant light yield

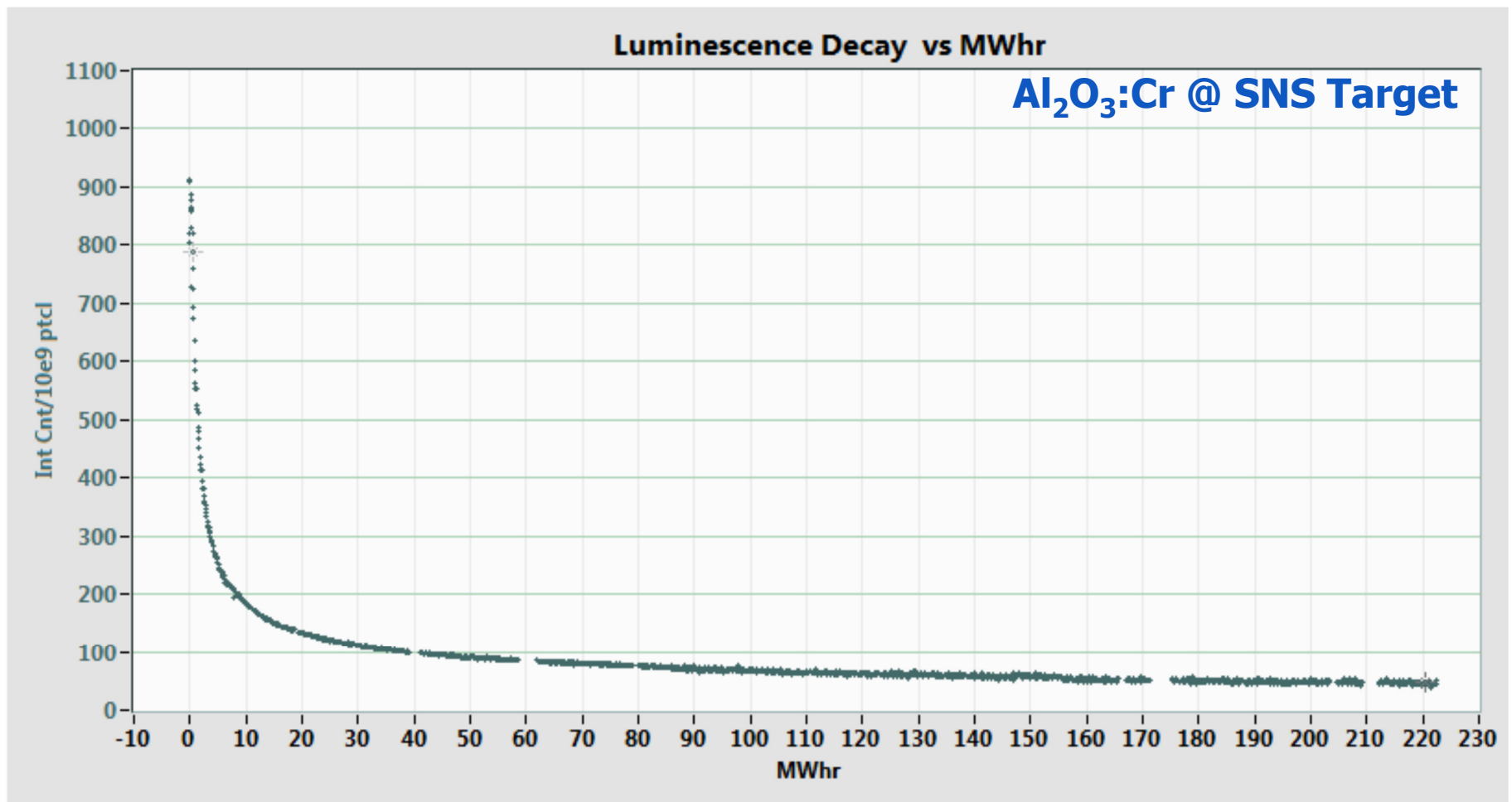
$$S(\Phi) = S(0) \cdot \frac{1}{1+K}$$



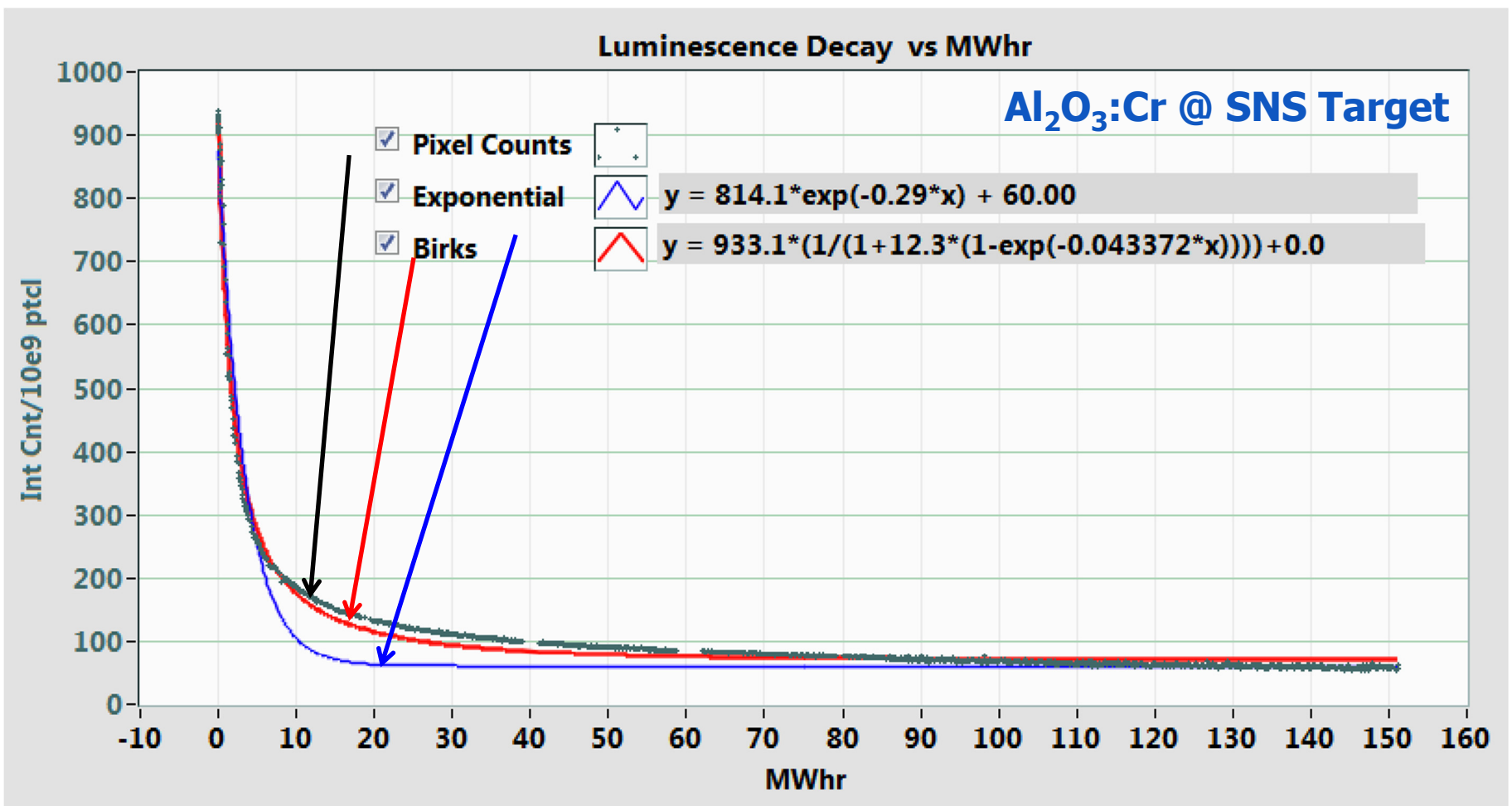
S. Lederer et al., NIM B 359, 2015

P. Forck, ADA-ARIES Workshop, Krakow 2019

Screens for ion beams

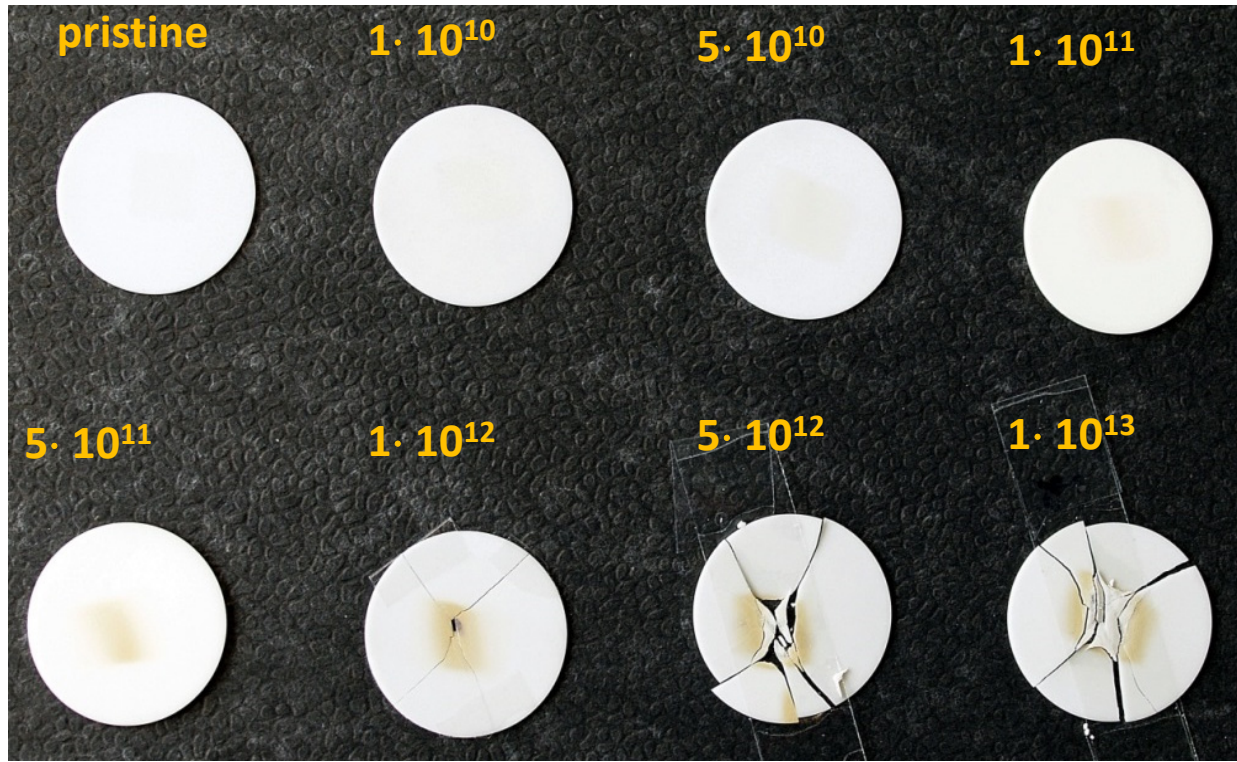


Screens for ion beams



Material modifications during the irradiation

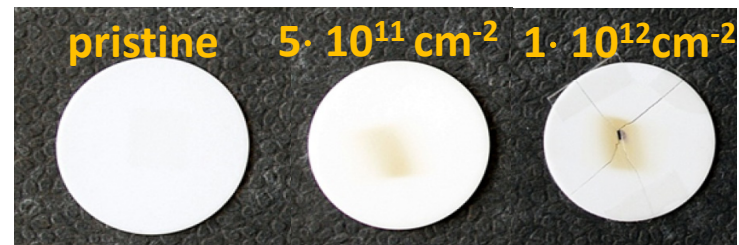
- ❖ coloring of the material



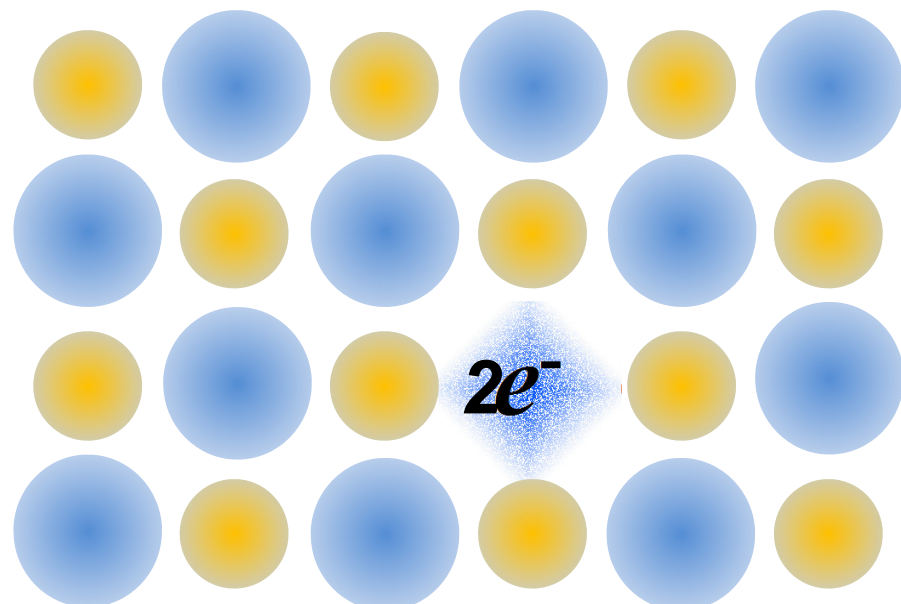
Screens for ion beams

Material modifications during the irradiation

- ❖ coloring of the material
- ❖ color center (F-center) at anion vacancy



Color Center	# anion vacancies	# trapped electrons	Emission λ [nm]
F	1	2	413



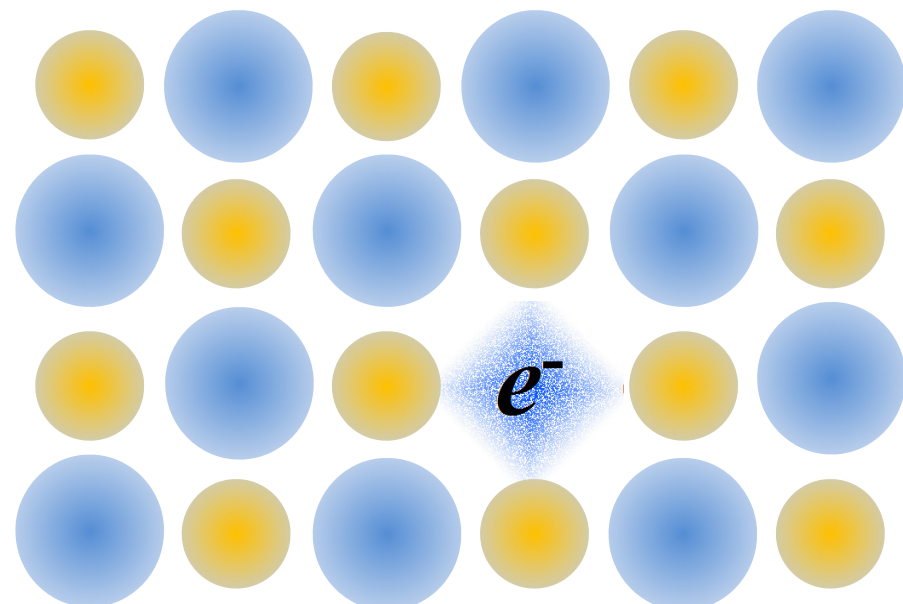
Screens for ion beams

Material modifications during the irradiation

- ❖ coloring of the material
- ❖ color center (F-center) at anion vacancy



Color Center	# anion vacancies	# trapped electrons	Emission λ [nm]
F	1	2	413
F^+	1	1	326



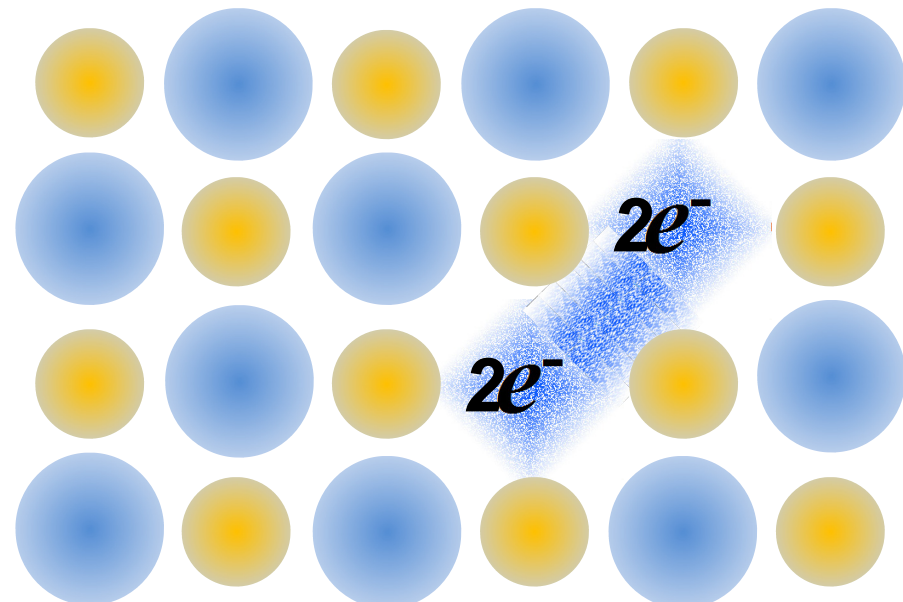
Screens for ion beams

Material modifications during the irradiation

- ❖ coloring of the material
- ❖ color center (F-center) at anion vacancy



Color Center	# anion vacancies	# trapped electrons	Emission λ [nm]
F	1	2	413
F^+	1	1	326
F_2	2	4	322



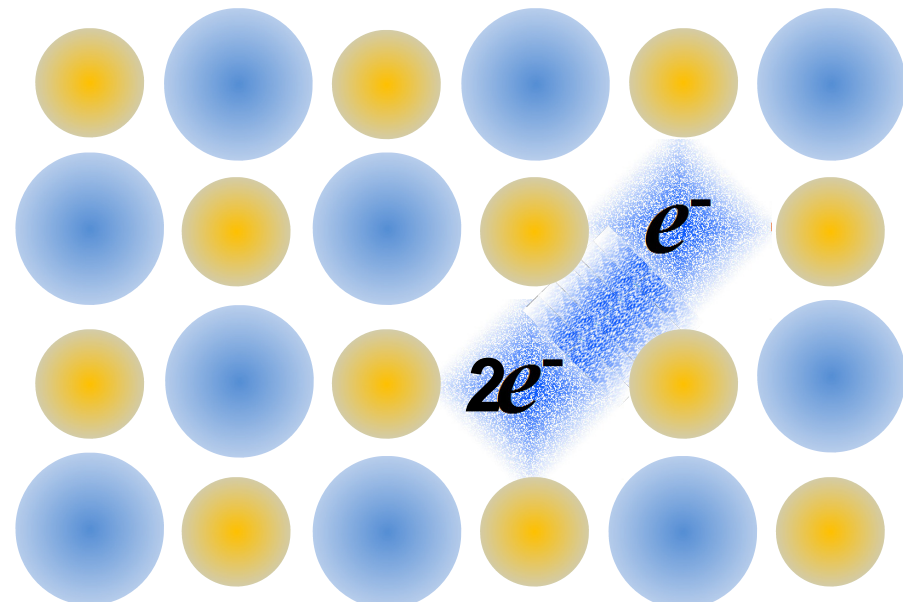
Screens for ion beams

Material modifications during the irradiation

- ❖ coloring of the material
- ❖ color center (F-center) at anion vacancy



Color Center	# anion vacancies	# trapped electrons	Emission λ [nm]
F	1	2	413
F^+	1	1	326
F_2	2	4	322
F_2^+	2	3	380



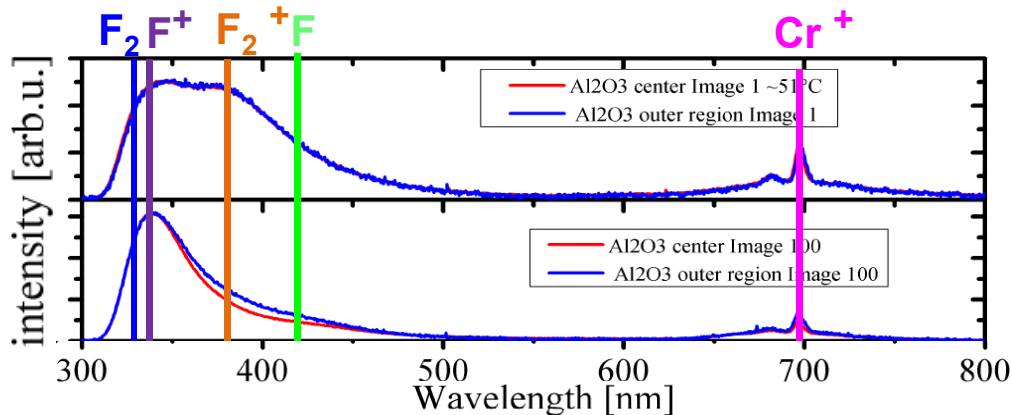
Screens for ion beams

Wavelength spectra and image reproduction for intrinsic Al₂O₃

❖ Light emission originated from vacancies in lattice

❖ Spectrum influence by :

- material modification by ions
- temperature

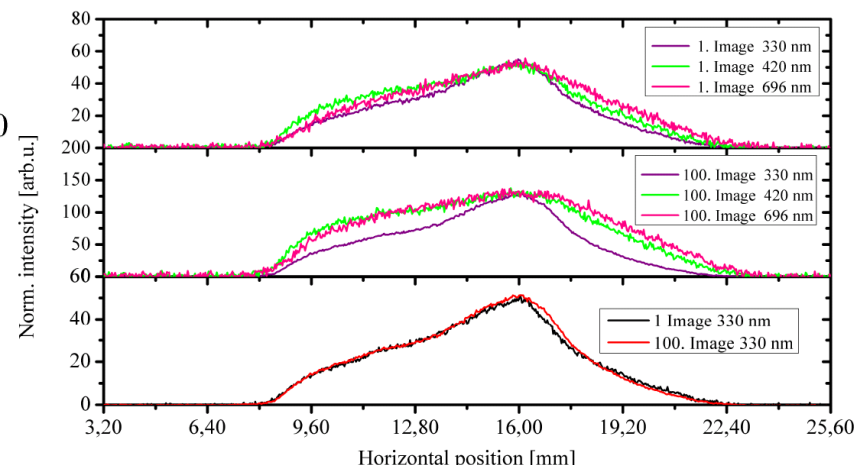


some transitions are less sensitive
to ion irradiation

Goal: Find right wavelength interval!

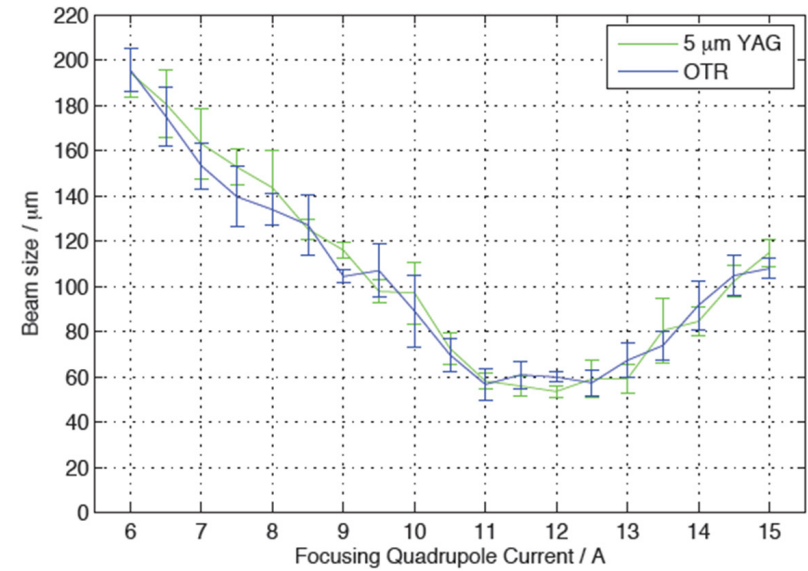
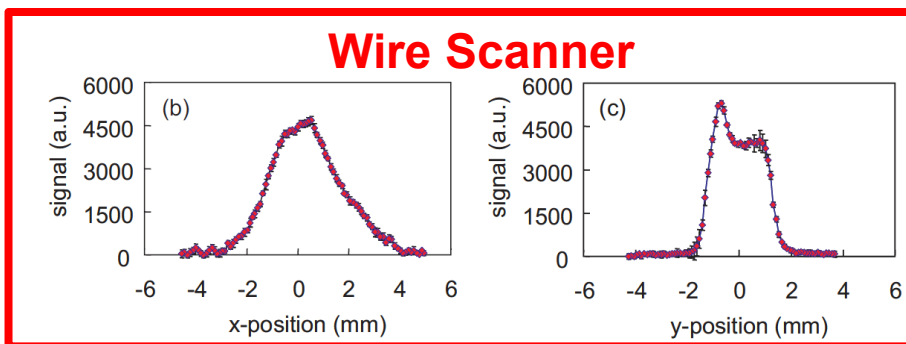
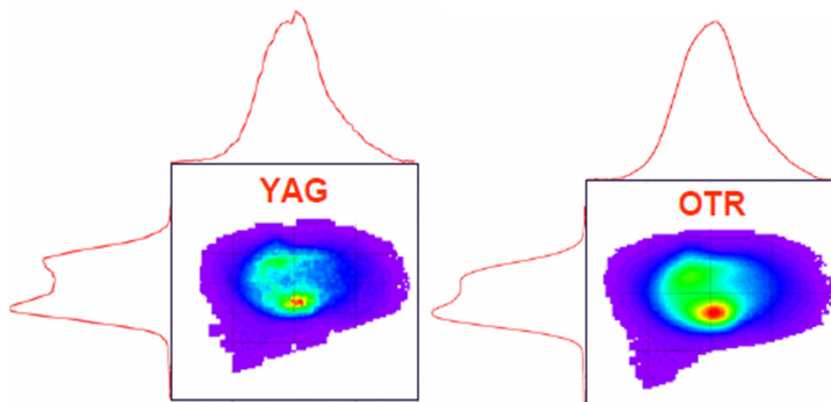
Beam parameters: Ca¹⁰⁺, 4.8 MeV/u,
5·10¹⁰ ppp in 3.3 ms, 30 µA, 100 pulses

Color Center	# anion vacancies	# trapped electrons	Emission λ [nm]
F	1	2	413
F ⁺	1	1	326
F ₂	2	4	322
F ₂ ⁺	2	3	380



E. Gütlich et al., DIPAC'11, SCINT'11: IEEE Nucl. Sc. 59 (2012)

Screens for electron beams

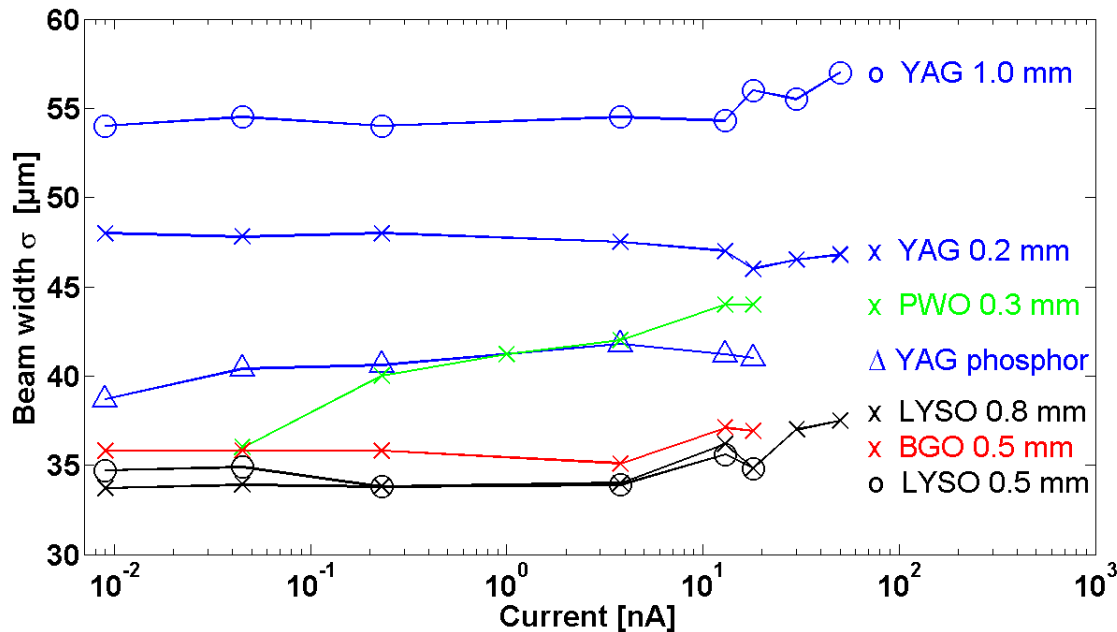


Beam parameters: electrons at 130 MeV, 200 pC

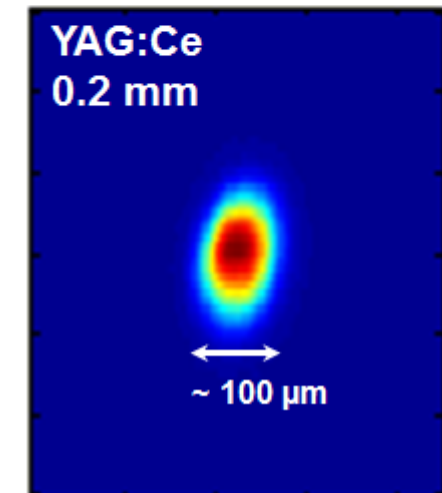
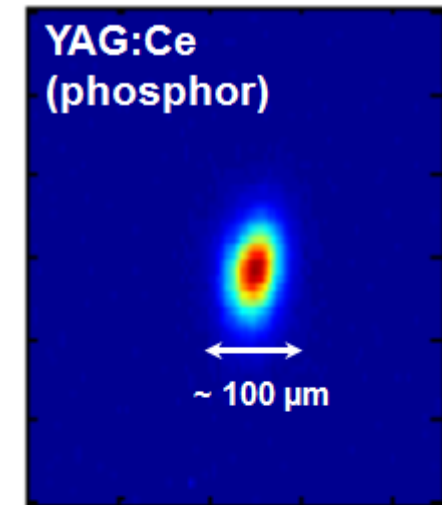
- ❖ OTR/YAG show good agreement down to 60 μm rms

- ❖ YAG screen shows detailed structure of beam during one bunch
- ❖ good comparison to OTR and wire scanner

Screens for electron beams



Beam parameters: electrons at 855 MeV, 0.01 – 50 nA



- ❖ different image reproduction, but reproducible behavior
- ❖ beam profile readings depend on material and its thickness
- ❖ best resolution is achieved with the LYSO and BGO screens

Screens for electron beams



- ❖ beam profile readings depend on material and its thickness

material	thickness (mm)	beam width (μm)
<i>OTR (for comparison)</i>		25
CRY019	0.3	25.5
LYSO	0.3	25.8
BGO	0.3	28.6
CRY018	0.3	28.7
LuAG:Ce	0.3	31.5
YAG:Ce	0.3	34.1

G. Kube et al., IPAC 2012

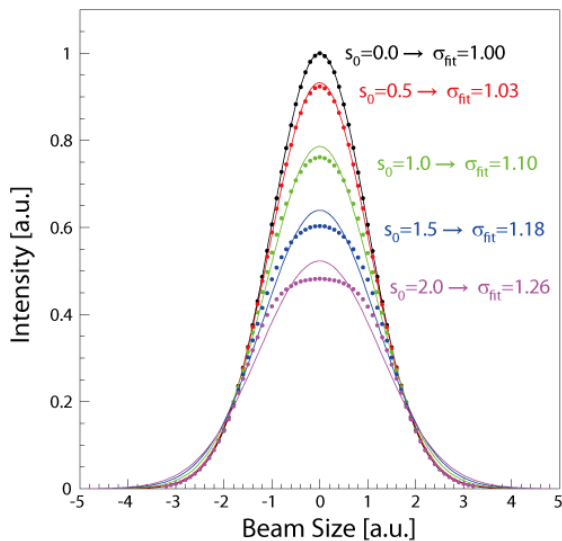
material	thickness (mm)	beam width (μm)	light yield relative to OTR
<i>OTR (for comparison)</i>		15.8	1
YAG:Ce	0.1	16.4	252
CRY019	0.1	23.4	102
Diamond	0.1	106.6	1.9
$\text{Al}_2\text{O}_3:\text{Cr}$	1	252.2	432

R. Ischebeck et al., Phys. Rev. ST Accel. Beams 18 (2015)

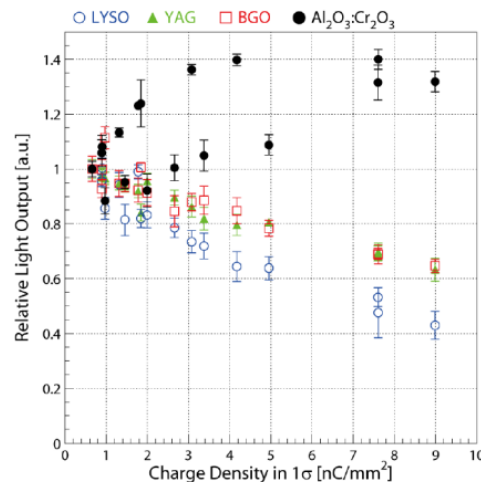
Screens for electron beams

Scintillator non-linearities

overestimation of the beam size due to saturation

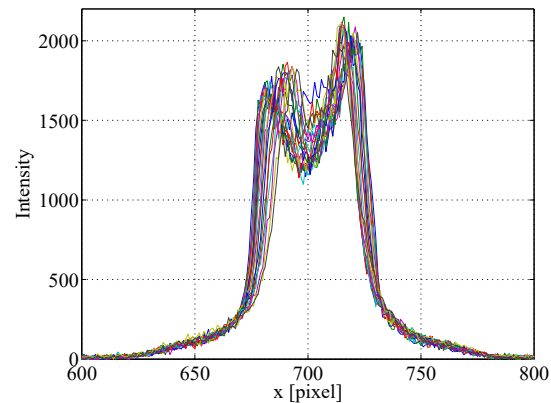


F. Miyahara et al., IPAC'17

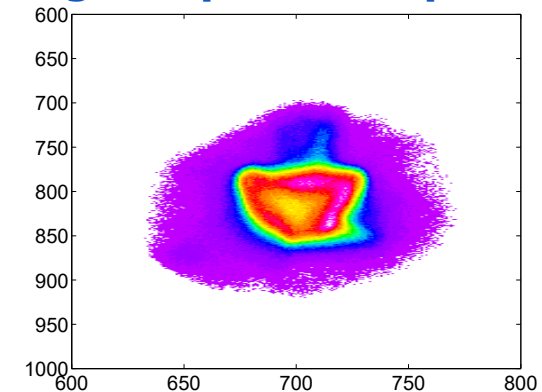


Electron beam@ KEK linac, charge density of 0.5-9 nC/mm²

"smoke-ring" shaped beam profiles

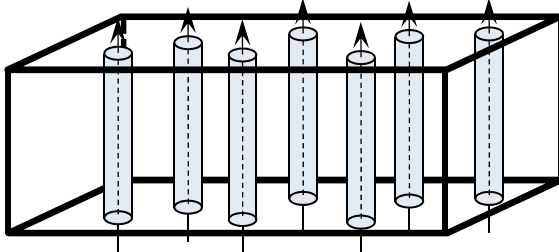


G. Kube et al., IBIC 2018

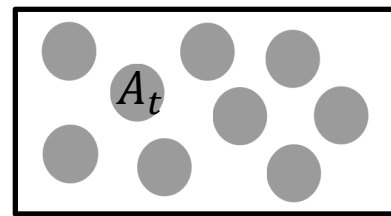


Scintillator non-linearities

- ❖ Energy loss in LYSO:Ce for ultra relativistic electron energies (@ Fermi Plateau)
 $\Delta E \approx 266\text{keV}$ in $200\mu\text{m}$ thick scintillator
- ❖ electron passage modeled as straight tube of ionization with radius R_δ
 - ionization track radius for LYSO:Ce $\sim 3.8\text{nm}$
- ❖ low charge density beam



2D representation
→

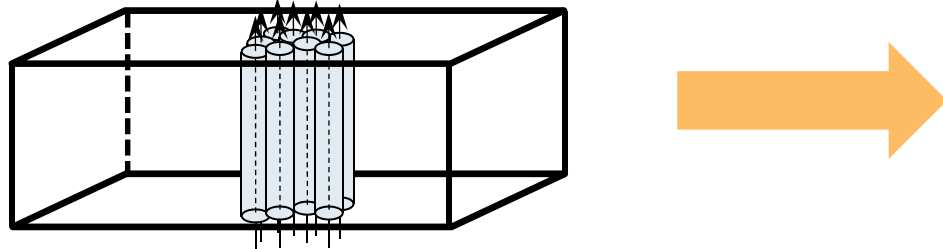


$$A_t = \pi R_\delta^2$$

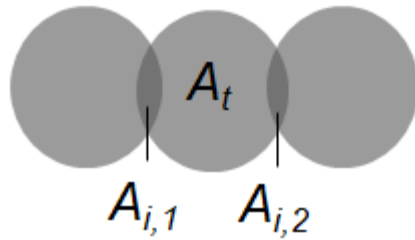
Screens for electron beams

Scintillator non-linearities

- ❖ high charge density beam

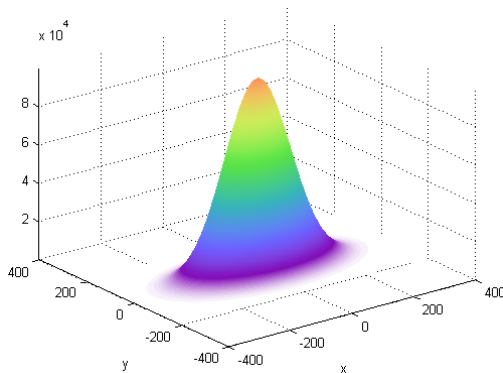


- ❖ measure for ionization track density n_t
 - ❖ area of the track A_t + area of intersections A_i



Scintillator non-linearities - quenching model for beam profiles

- ❖ gaussian beam profile transform into 2D surface density profile



- ❖ derive mean distance between ionization tracks
- ❖ calculate measure for ionization track density
- ❖ weight factor for each point of beam profile
 - ❖ Birks-type weight factor for scintillator non-linearity

$$w = \frac{1}{1 + \alpha \frac{dE}{dx}} \quad \text{with} \quad \frac{dE}{dx} \propto (n_t)^3$$

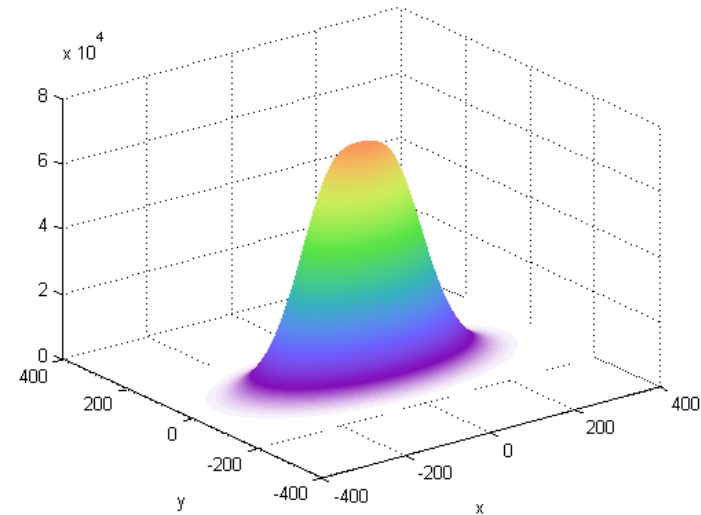
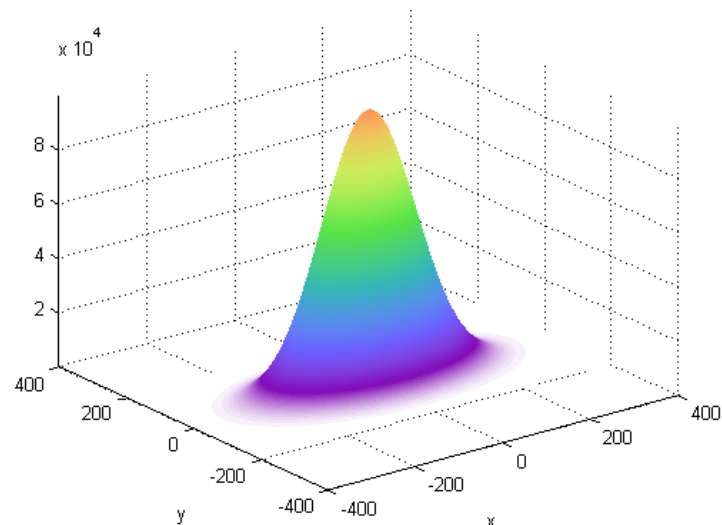
α : free adjustable parameter
(quenching strength)

G. Kube et al., IBIC 2018

Screens for electron beams

Scintillator non-linearities - quenching model for beam profiles

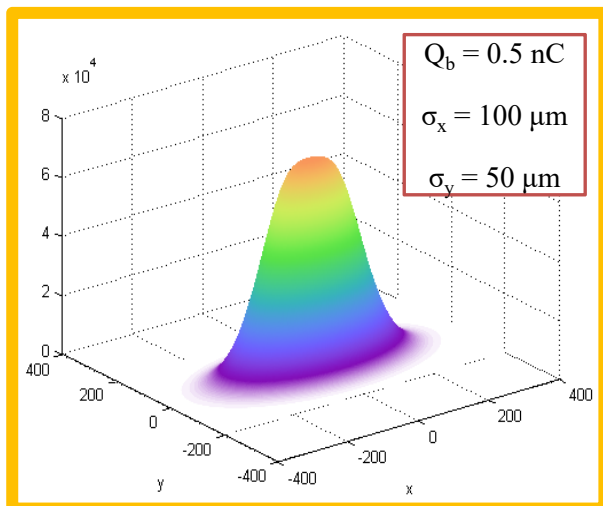
- ❖ distorted beam profile ($\alpha = 6.4 \cdot 10^{-5}$)



Screens for electron beams

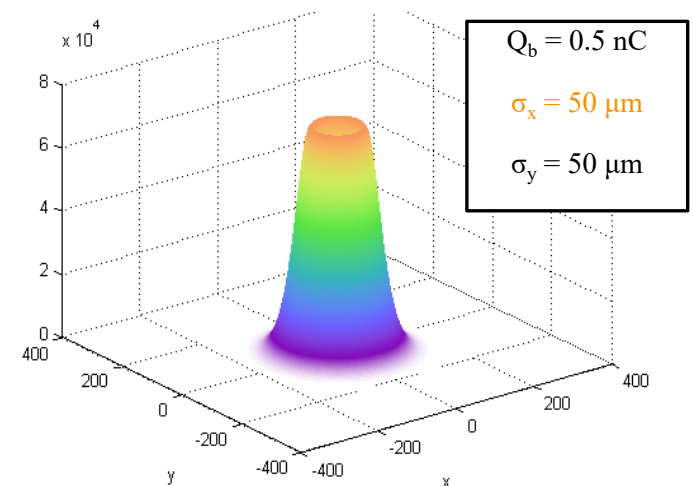
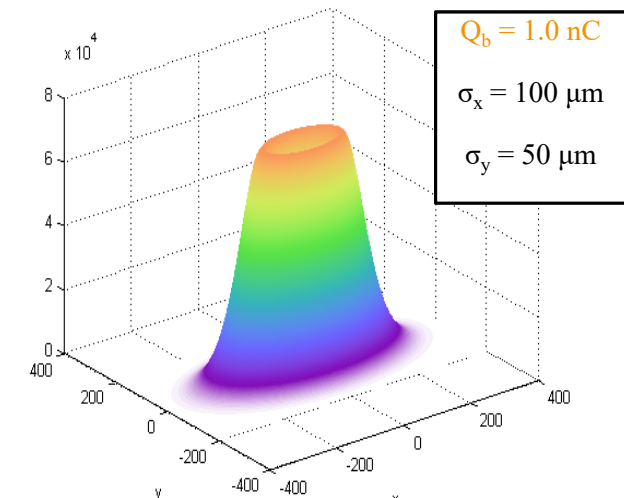
Scintillator non-linearity - quenching model for beam profiles

❖ distorted beam profile



increased beam current

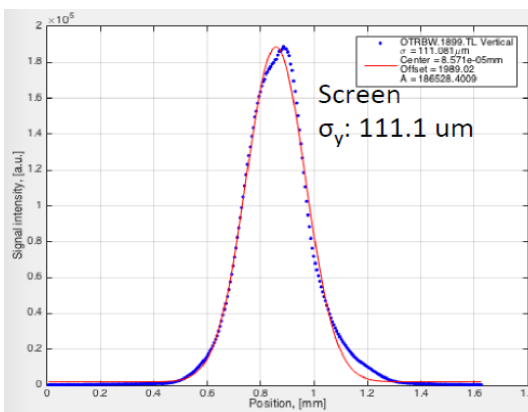
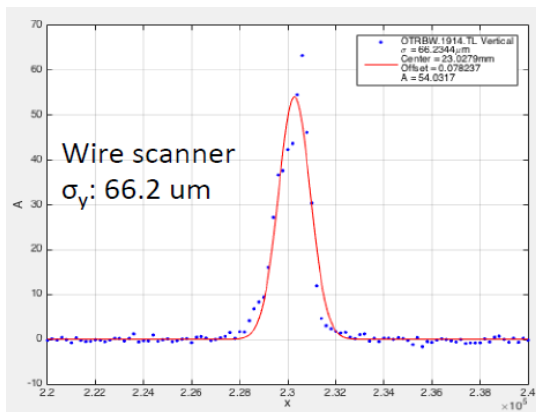
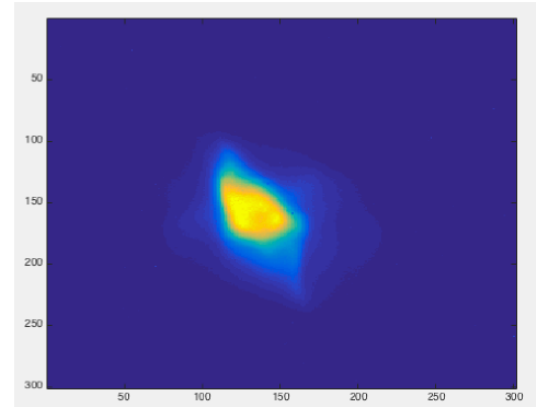
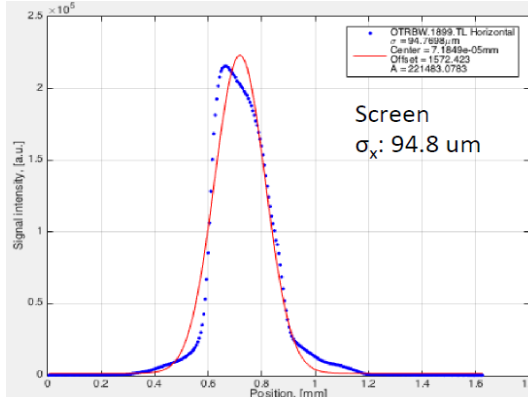
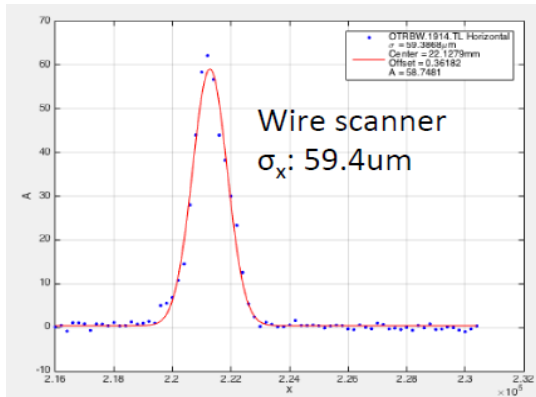
reduced beam size



Screens for electron beams

Scintillator non-linearity - quenching model for beam profiles

❖ comparison screen- wire scanner



- ❖ Model calculation
 - wire scanner beam size as input
 - calculated beam size

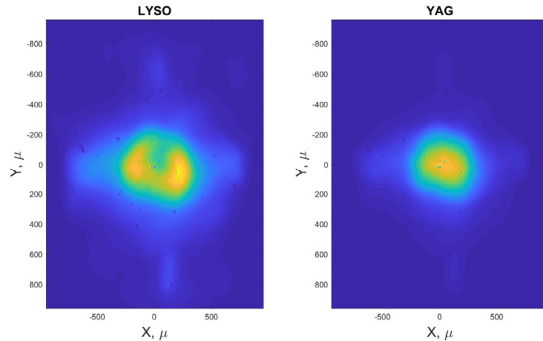
$\sigma_x = 97 \mu\text{m}, \sigma_y = 108 \mu\text{m}$

XFEL beam parameters: electrons, 500 pC bunch charge

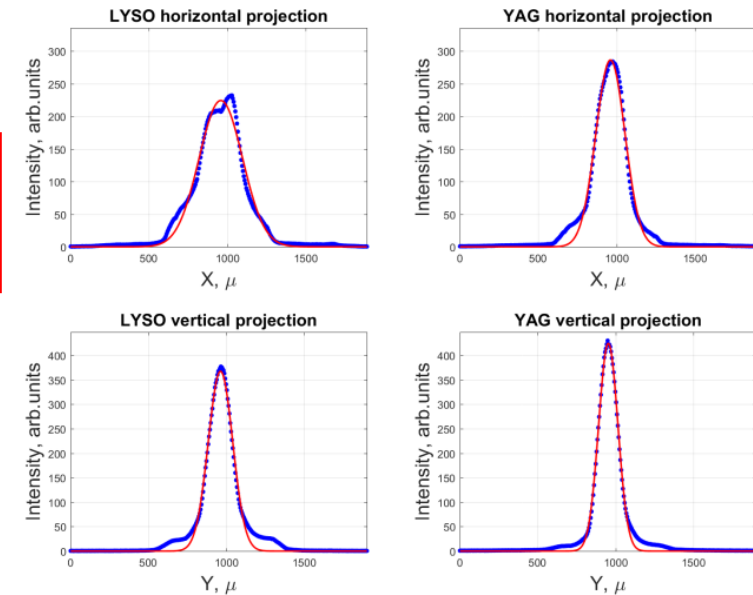
Screens for electron beams

Scintillator non-linearity – LYSO:Ce/YAG:Ce comparison (first experiments)

- ❖ “smoke-ring” shaped beam profile and profile widening only for LYSO:Ce

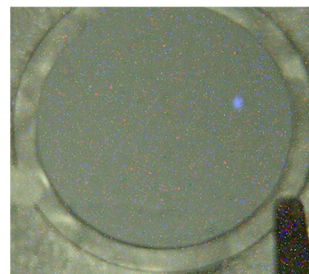


XFEL beam parameters:
electrons at 14 GeV, 1nC
bunch charge



YAG:Ce high mobility of excitation carriers
reduced quenching probability

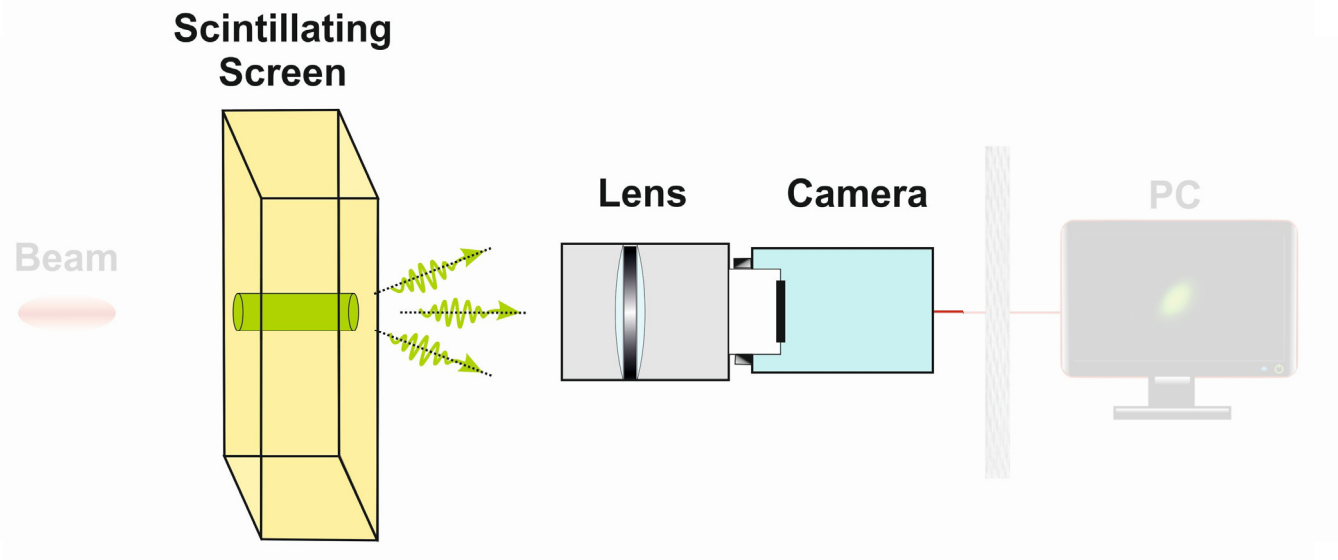
Boron Nitride Nano Tube
Screens new material
proposed by K. Jordan
(JLab). Measured at
11 GeV electrons



G. Kube et al., ARIES-ADA Workshop Krakow 2019

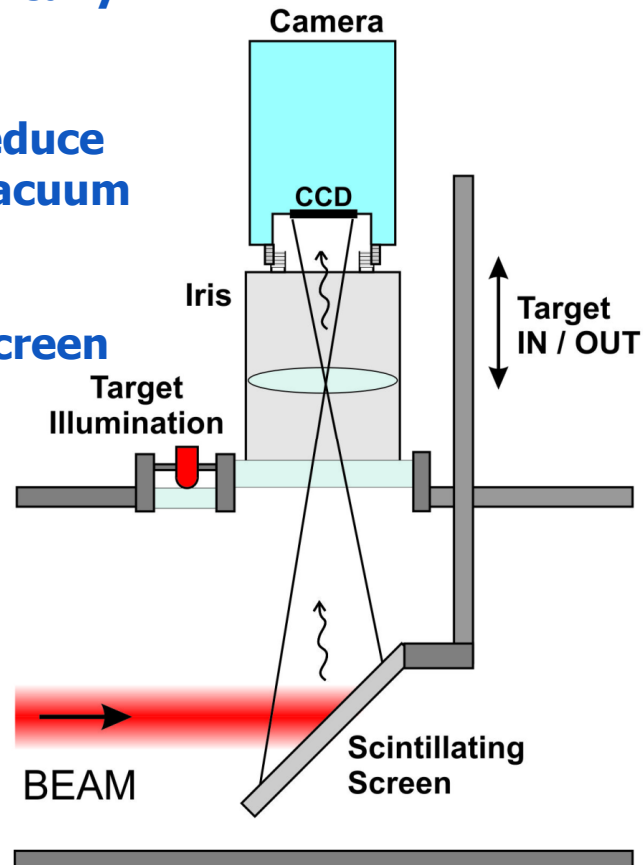
Optical setup

Aim: to capture a sharply focused image of the scintillation plane



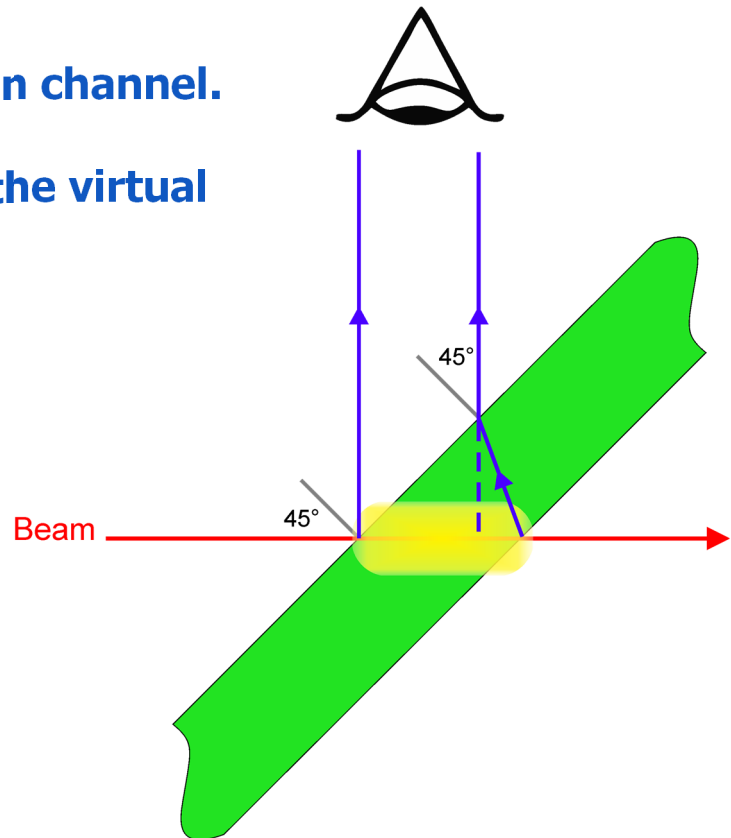
Scintillator-camera typical setup

- ❖ Particle beam impinges on flat scintillator screen, typically tilted at 45 degrees.
- ❖ Camera is housed and positioned far from beam to reduce radiation, and observes the tilted screen through a vacuum window.
- ❖ A lens (system) is included to form an image of the screen on the camera sensor.
- ❖ Include light source to illuminate target.



Light generation and refraction at scintillator

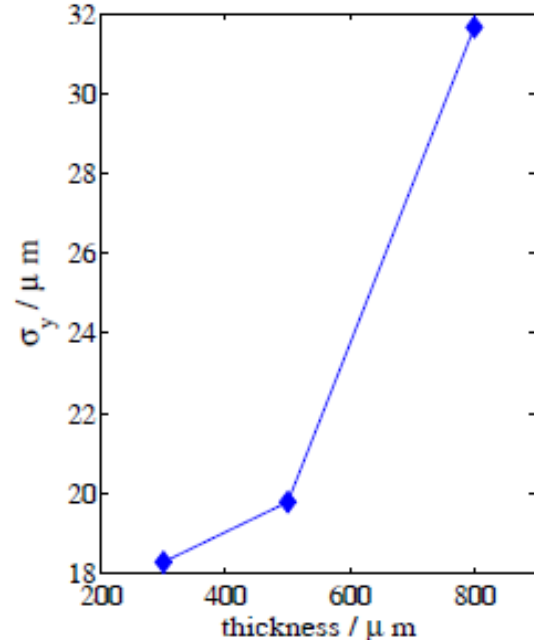
- ❖ Each particle creates an ionization channel.
- ❖ Light is emitted isotropically along the ionization channel.
- ❖ Refraction of this light at the boundary affects the virtual image size and achievable resolution.
- ❖ Scintillator thickness is an issue.



Light generation and refraction at scintillator

- ❖ Choice of scintillator thickness is a trade-off:
 - Choice depends on particle energy and beam intensity.
 - Thicker screen provides more photons.
 - Thinner screen gives better resolution.
 - Stability of screen mount, thermal effects.

Available types	Diameter	Thickness
Large imaging screens	up to 105 mm	down to 200 µm
Standard screens	typically up to 50 mm	typically 100-1000 µm
Very thin free-standing screens	up to 50 mm up to 10 mm	down to 50 µm down to 20 µm
Very thin screens with ring support: ➢ aluminium ➢ stainless steel ➢ ceramics (alumina)	up to 10 mm up to 50 mm	down to 20 µm down to 50 µm
Ultra-thin screens on substrate (down to 170µm): ➢ fiber optics ➢ glass, quartz glass ➢ YAG, sapphire	up to 40 mm up to 30 mm	10 µm 5 µm



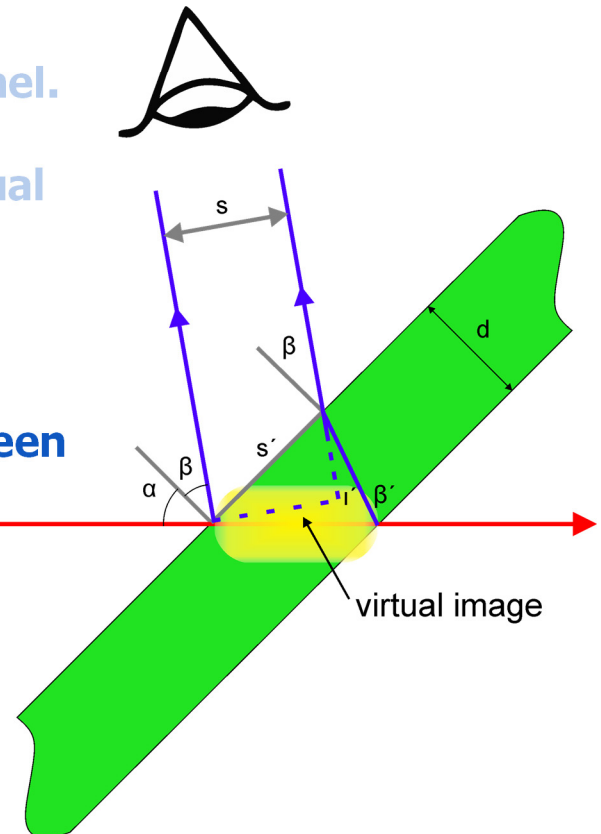
G. Kube et al., Proceedings of IPAC2012

J. Parizek, ADA-ARIES Workshop, Krakow 2019

Light generation and refraction at scintillator

- ❖ Each particle creates an ionization channel.
- ❖ Light is emitted isotropically along the ionization channel.
- ❖ Refraction of this light at the boundary affects the virtual image size and achievable resolution.
- ❖ Scintillator thickness is an issue
- ❖ **Incident beam hits scintillating screen at angle α**
- ❖ **Optical system positioned at angle β to scintillating screen**

$$s = d \cos \beta \cdot \sqrt{\frac{1}{1 - \frac{\sin^2 \beta}{n^2}} + \frac{1}{\cos^2 \alpha} - 2 \frac{\cos \left[\arcsin \left(\frac{\sin \beta}{n} \right) + \alpha \right]}{\sqrt{1 - \frac{\sin^2 \beta}{n^2}} \cos \alpha}}$$



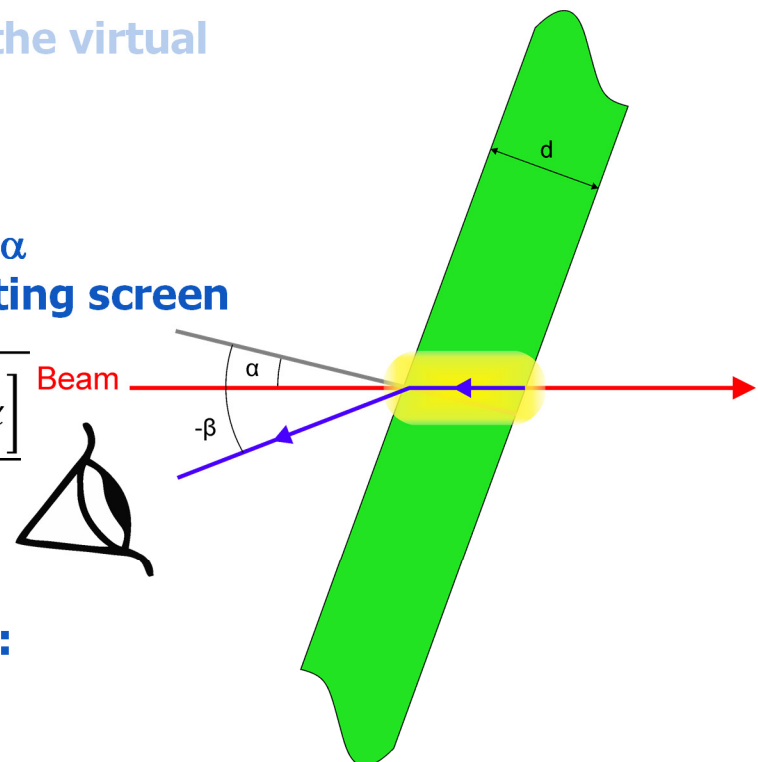
R. Ischebeck et al., Phys. Rev. ST Accel. Beams 18 (2015)

S. Gibson, ADA-ARIES Workshop, Krakow 2019

Light generation and refraction at scintillator

- ❖ Each particle creates an ionization channel.
- ❖ Light is emitted isotropically along the ionization channel.
- ❖ Refraction of this light at the boundary affects the virtual image size and achievable resolution.
- ❖ Scintillator thickness is an issue
- ❖ Incident beam hits scintillating screen at angle α
- ❖ Optical system positioned at angle β to scintillating screen

$$s = d \cos \beta \cdot \sqrt{\frac{1}{1 - \frac{\sin^2 \beta}{n^2}} + \frac{1}{\cos^2 \alpha} - 2 \frac{\cos \left[\arcsin \left(\frac{\sin \beta}{n} \right) + \alpha \right]}{\sqrt{1 - \frac{\sin^2 \beta}{n^2}} \cos \alpha}}$$



- ❖ Apparent size is zero ($s=0$) when viewing angle:

$$\beta_{ideal} = -\arcsin(n \sin \alpha)$$

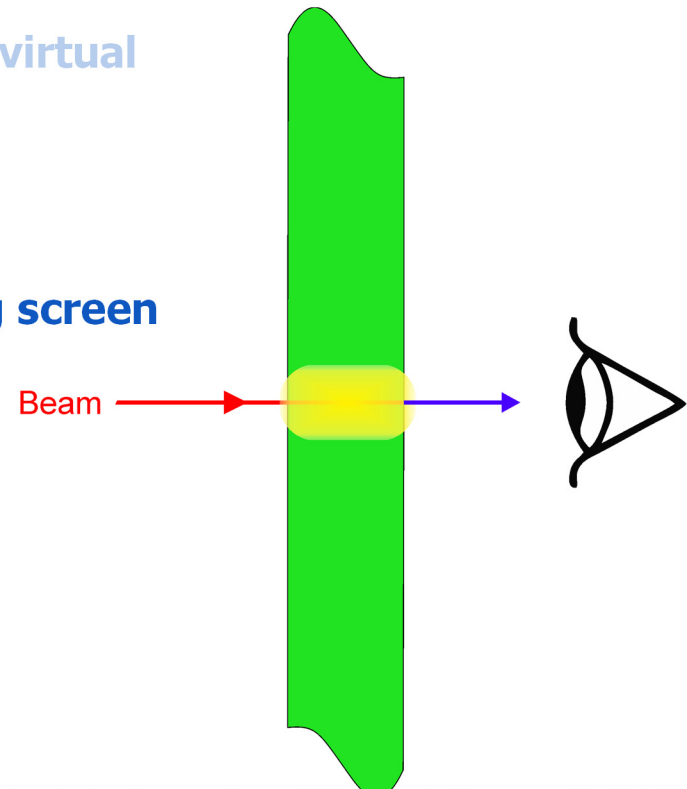
R. Ischebeck et al., Phys. Rev. ST Accel. Beams 18 (2015)

S. Gibson, ADA-ARIES Workshop, Krakow 2019

Light generation and refraction at scintillator

- ❖ Each particle creates an ionization channel.
- ❖ Light is emitted isotropically along the ionization channel.
- ❖ Refraction of this light at the boundary affects the virtual image size and achievable resolution.
- ❖ Scintillator thickness is an issue
- ❖ Incident beam hits scintillating screen at angle α
- ❖ Optical system positioned at angle β to scintillating screen

$$s = d \cos \beta \cdot \sqrt{\frac{1}{1 - \frac{\sin^2 \beta}{n^2}} + \frac{1}{\cos^2 \alpha} - 2 \frac{\cos \left[\arcsin \left(\frac{\sin \beta}{n} \right) + \alpha \right]}{\sqrt{1 - \frac{\sin^2 \beta}{n^2}} \cos \alpha}}$$



- ❖ Apparent size is zero ($s=0$) when viewing angle:

$$\beta_{ideal} = -\arcsin(n \sin \alpha)$$

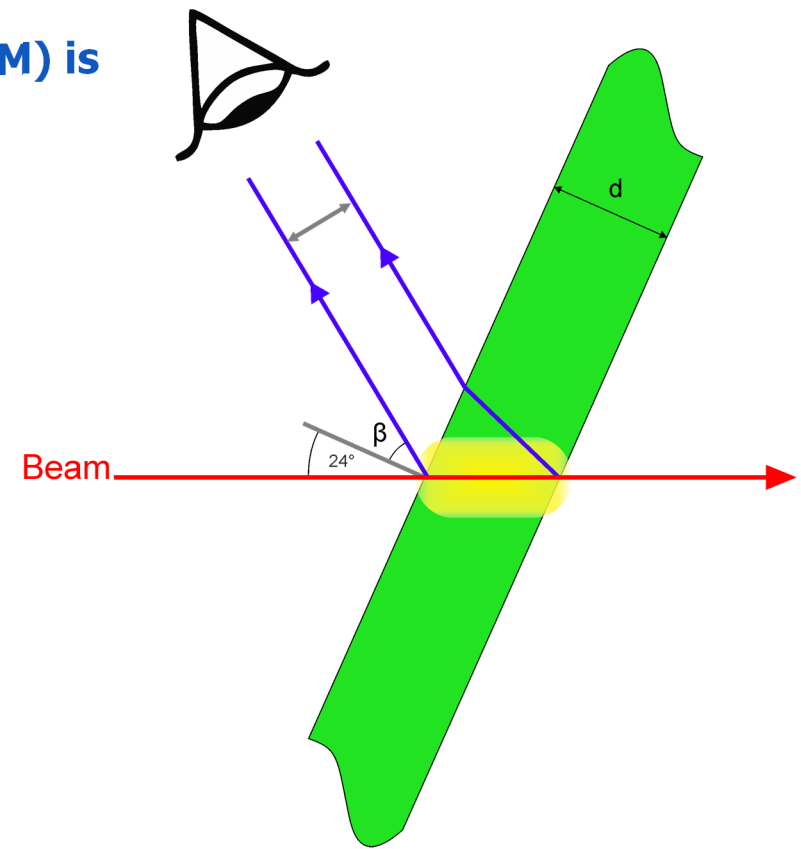
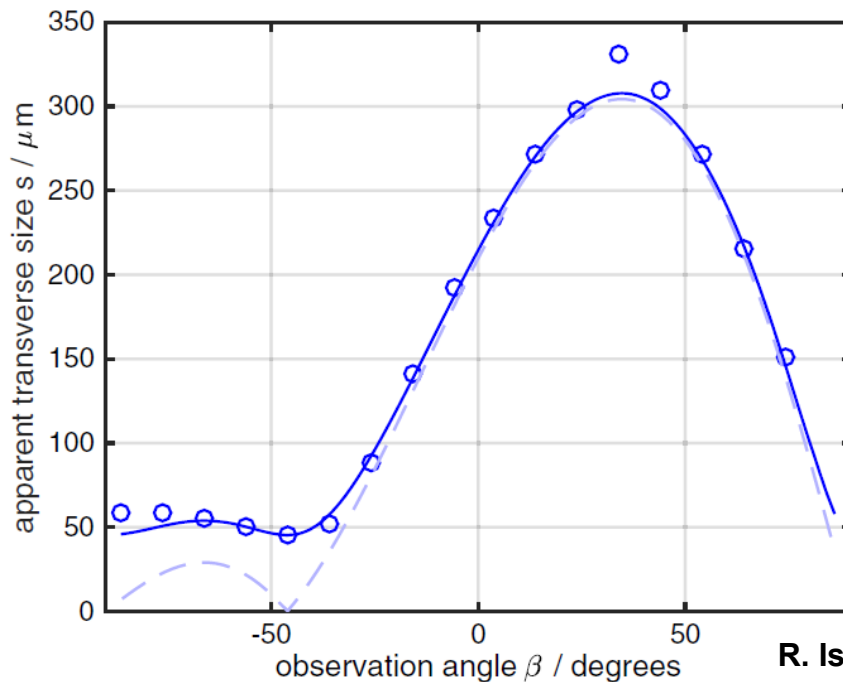
R. Ischebeck et al., Phys. Rev. ST Accel. Beams 18 (2015)

S. Gibson, ADA-ARIES Workshop, Krakow 2019

Optical Setup

Experimental verification of angle dependency

- ❖ primary beam “simulated” by diode laser ($\lambda=410\text{nm}$)
- ❖ primary beam with $45\mu\text{m}$ transverse size (FWHM) is intercepted by YAG:Ce screen ($d=500\mu\text{m}$)
- ❖ primary beam has an incidence angle of 24°

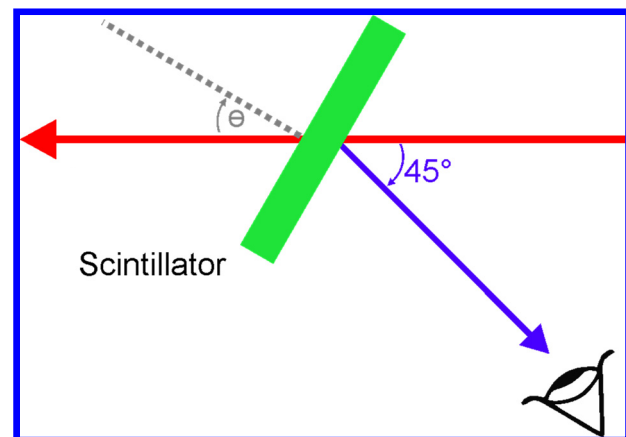
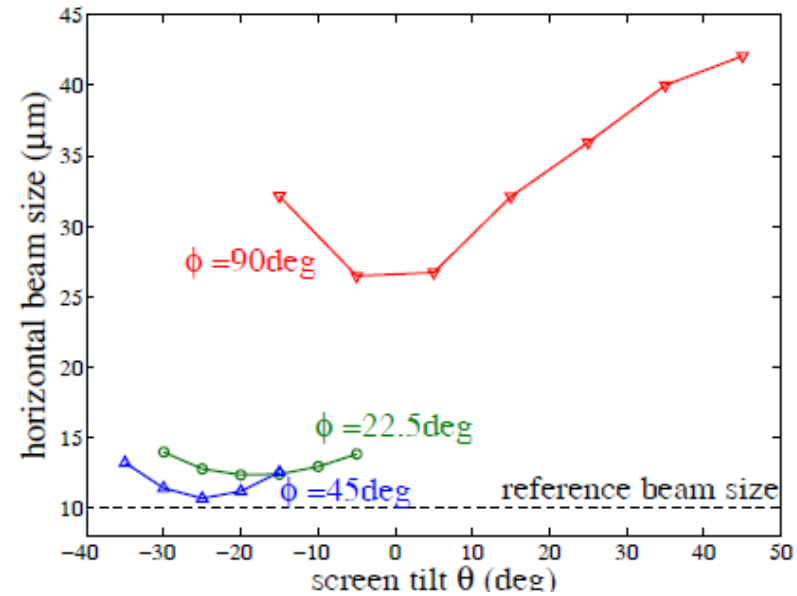
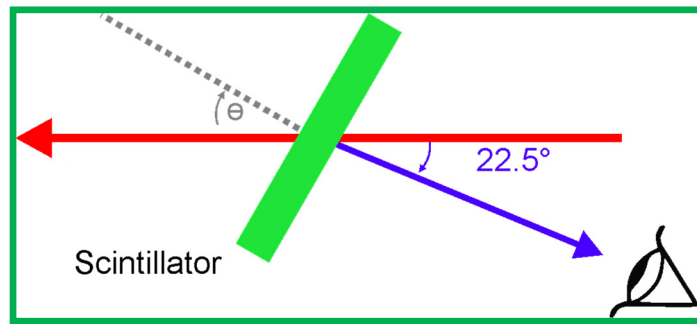
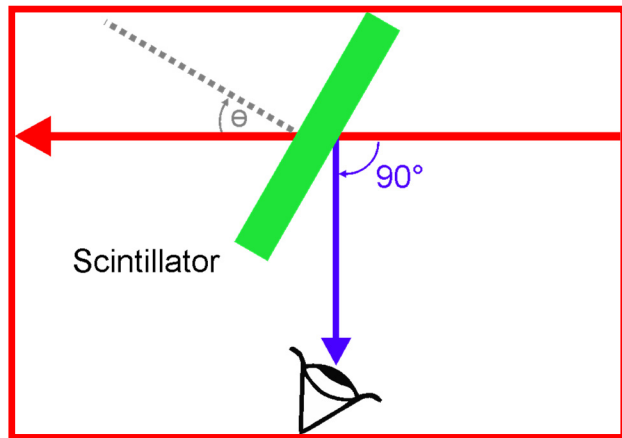


R. Ischebeck et al., Phys. Rev. ST Accel. Beams 18 (2015)

Optical Setup

Verification of angle dependency

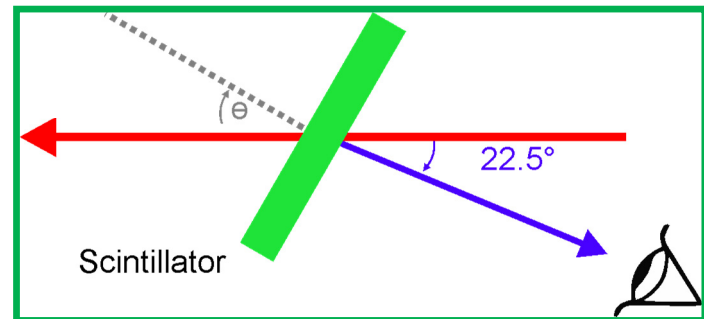
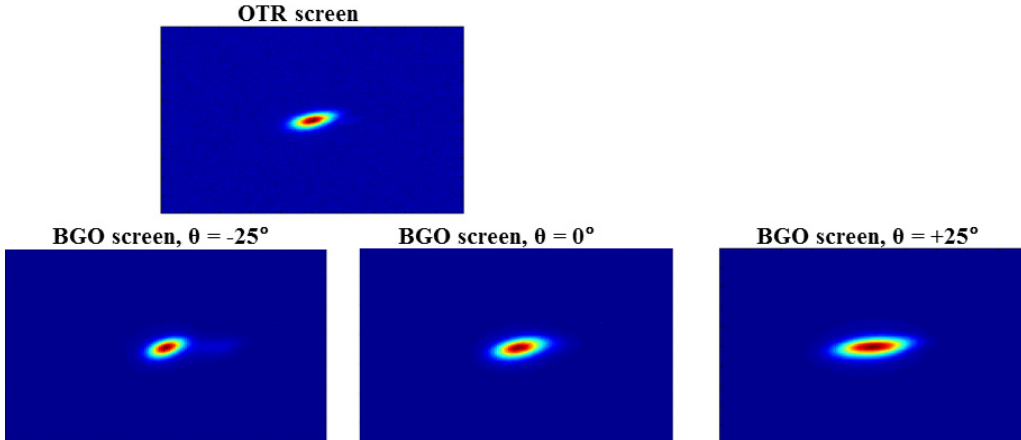
- ❖ reference beam with $10\mu\text{m}$ transverse size is intercepted by BGO screen ($d=300\mu\text{m}$)



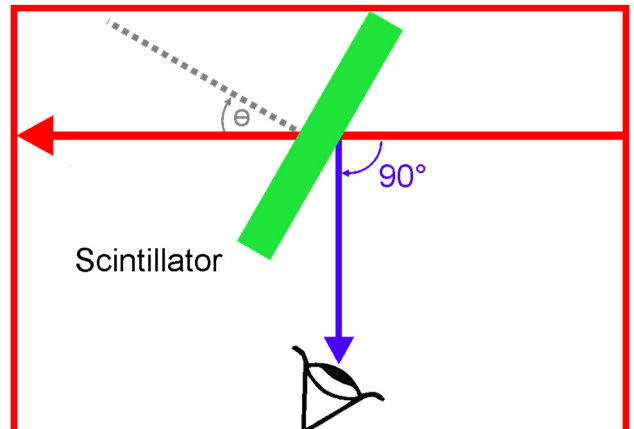
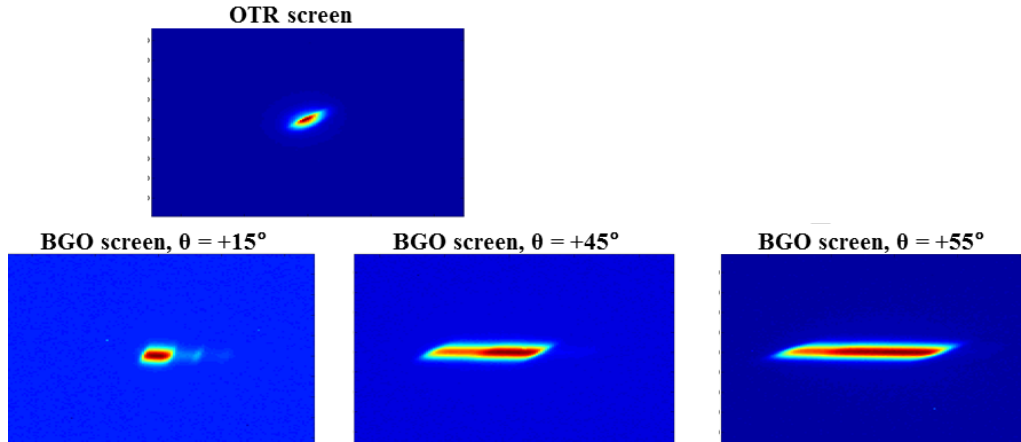
Optical Setup

Verification of angle dependency

- ❖ scintillation light generated by 855 MeV electron beam

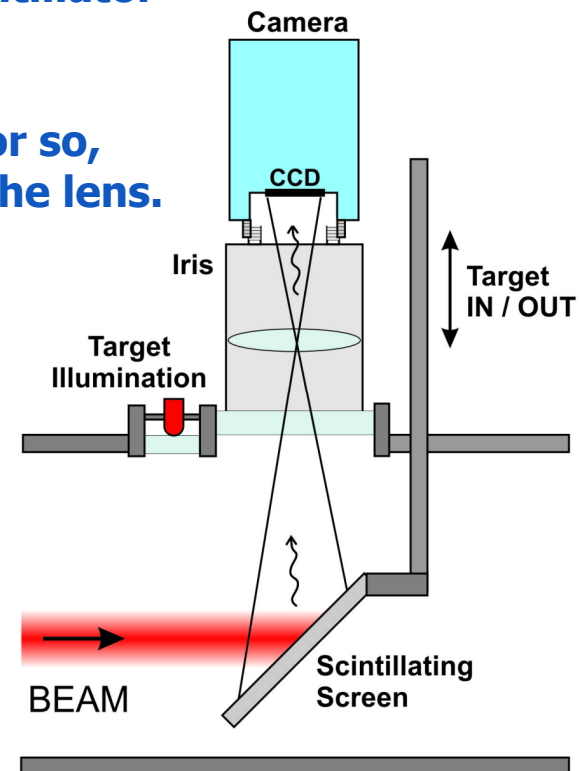


G. Kube et al., Proceedings of IPAC2012



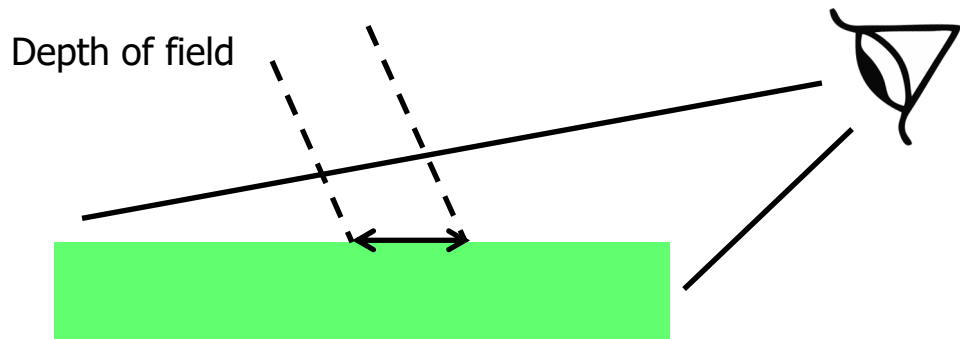
Depth of field

- ❖ In the typical setup, the camera-lens must focus on a scintillator plane surface that is at an oblique angle...
- ❖ This works for very small electron beams of only few μm or so, when the distribution is well within the depth-of-field of the lens.



Depth of field

- ❖ For larger beams only part of the scintillator plane will be in focus:

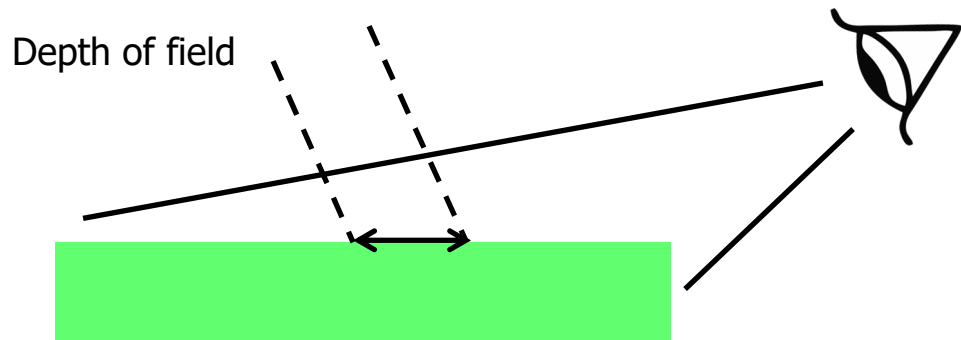


DEPTH OF FIELD
DEPTH OF FIELD

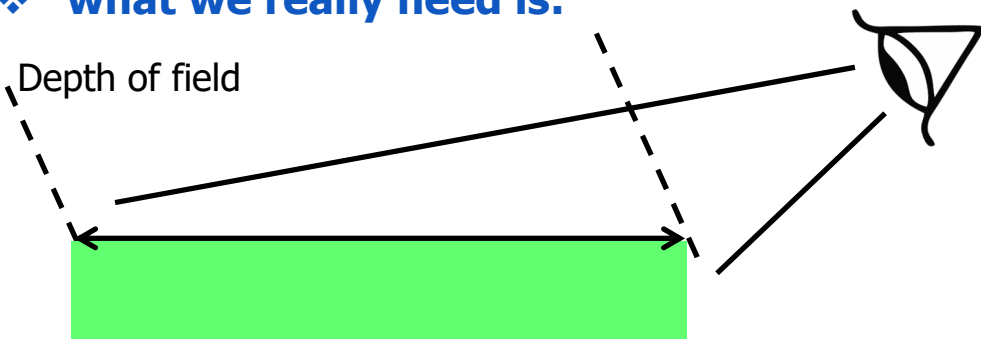
© Cambridge in colour

Depth of field

- ❖ For larger beams only part of the scintillator plane will be in focus:



- ❖ what we really need is:



Optical Setup

Depth of field

- ❖ This is a solved problem in photography and is the basis of the “view camera”



S. Gibson, ADA-ARIES Workshop

Optical Setup

Depth of field

- ❖ This is a solved problem in photography and is the basis of the “view camera”
- ❖ View cameras can move the lens in x & y tilt, and z translation; and are still made today



S. Gibson, ADA-ARIES Workshop



© Danny Burk Photography

Optical Setup

Depth of field

- ❖ This is a solved problem in photography and is the basis of the “view camera”
- ❖ View cameras can move the lens in x & y tilt, and z translation; and are still made today
- ❖ Captain Theodor Scheimpflug was an Austrian Army & Navel officer who used aerial photography to make accurate maps with undistorted images from balloon-suspended cameras (not pointing straight down).

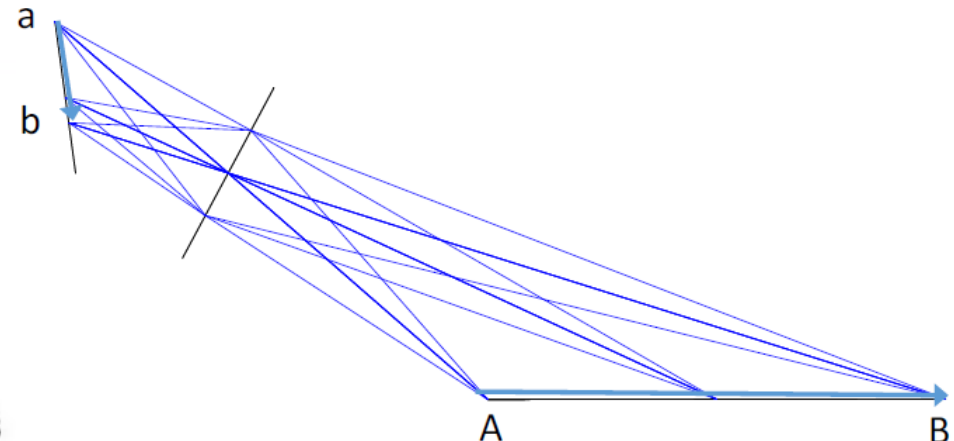
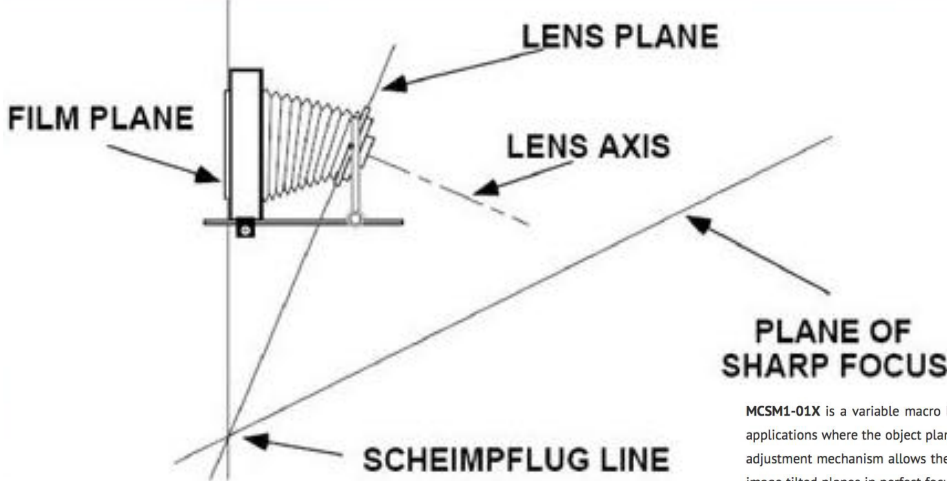


© Wikipedia

Optical Setup

The Scheimpflug principle

- ❖ His principle states that if subject plane, lens plane and image plane intersect in a single line as shown, then the subject plane is completely in sharp focus.



MCSM1-01X is a variable macro lens expressly designed for 3D measurement and imaging applications where the object plane is not perpendicular to the optical axis. A precise built-in adjustment mechanism allows the lens to accurately meet the Scheimpflug condition and to image tilted planes in perfect focus. This lens offers a wide range of magnifications and view angles. It can be interface with any structured light source to build up extremely accurate 3D imaging systems. Image sharpness is maintained even when the lens is tilted by a wide angle, since the Scheimpflug adjustment tilts around the horizontal axis of the detector plane. The tiltable mount is compatible with any C-mount camera.

KEY ADVANTAGES

Precision Scheimpflug mount

Image focus is retained across any tilted plane.

Compatible with any C-mount cameras

The back focal length meets the C-mount standard.

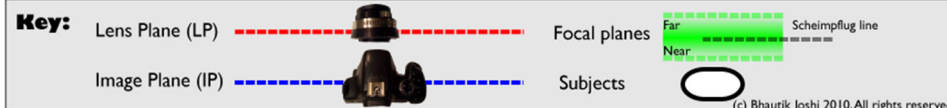
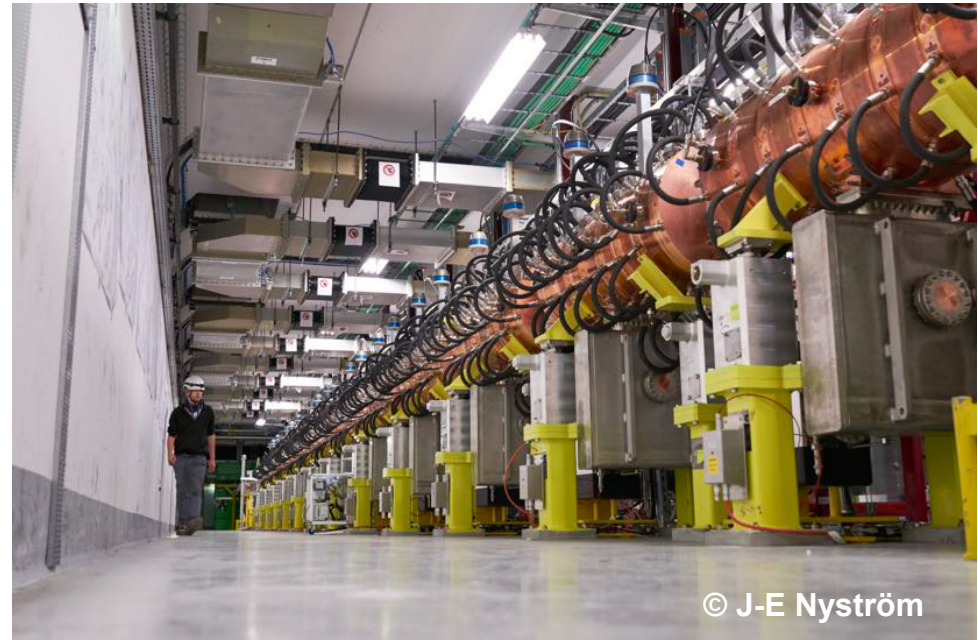
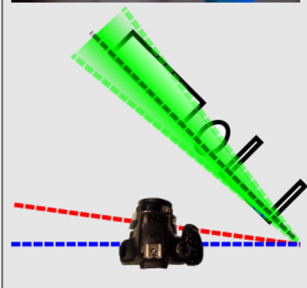
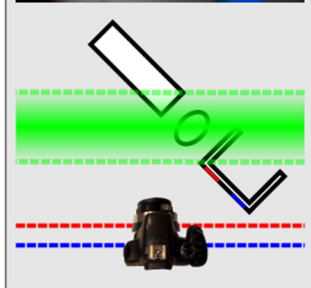
Application flexibility

Supports a wide range of magnification factors and viewing angles.

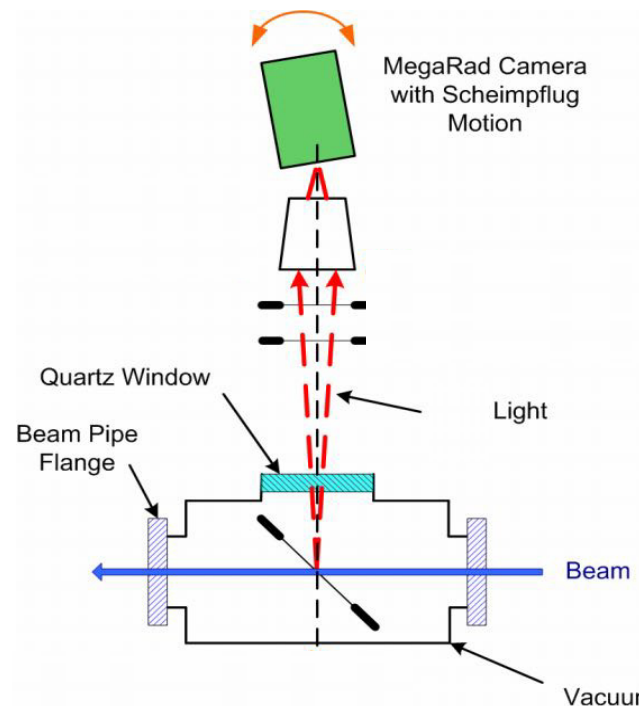


©Stemmer Imaging

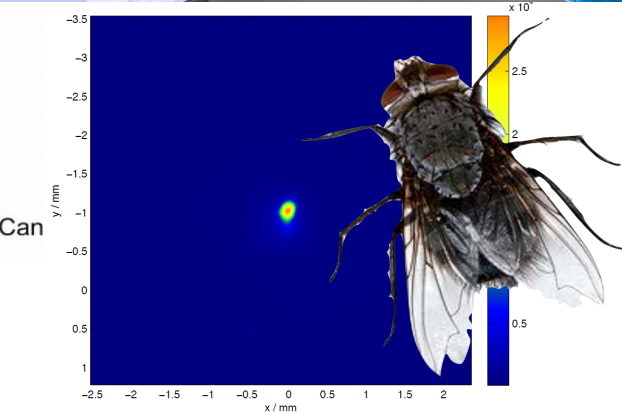
Optical Setup



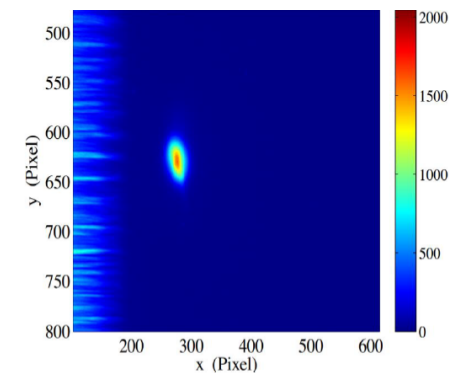
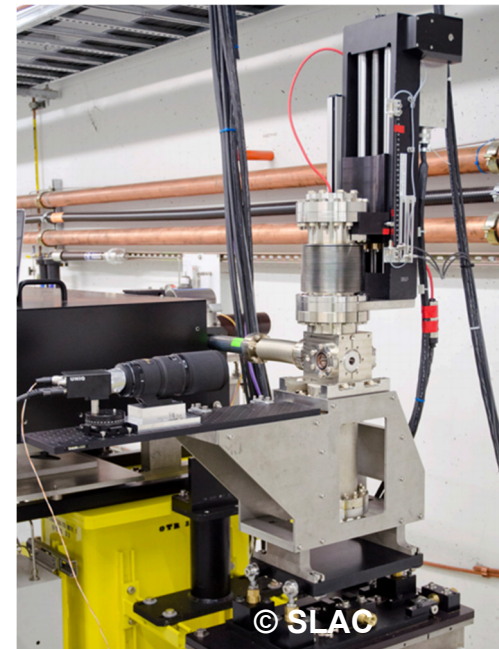
Optical Setup



V. Scarpine, PAC2005



R. Ischebeck, ADA-ARIES Workshop

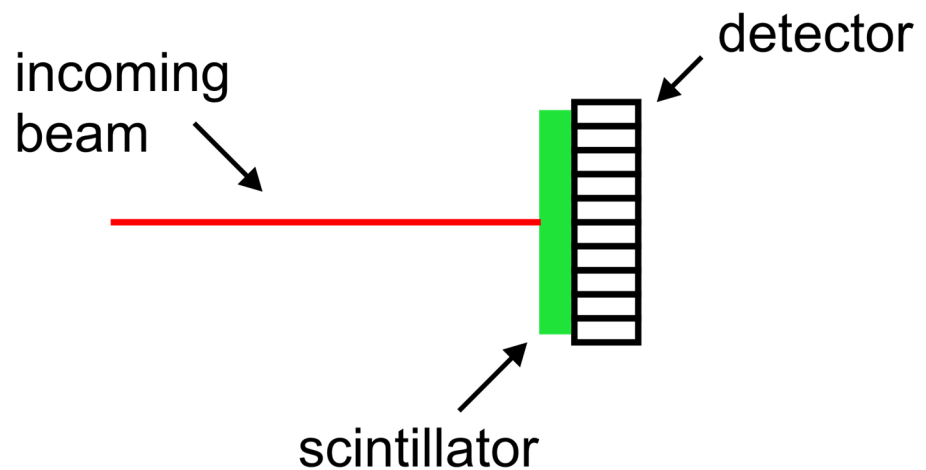


P. Krejcik, ADA-ARIES Workshop

Optical Setup

Common scintillator layouts

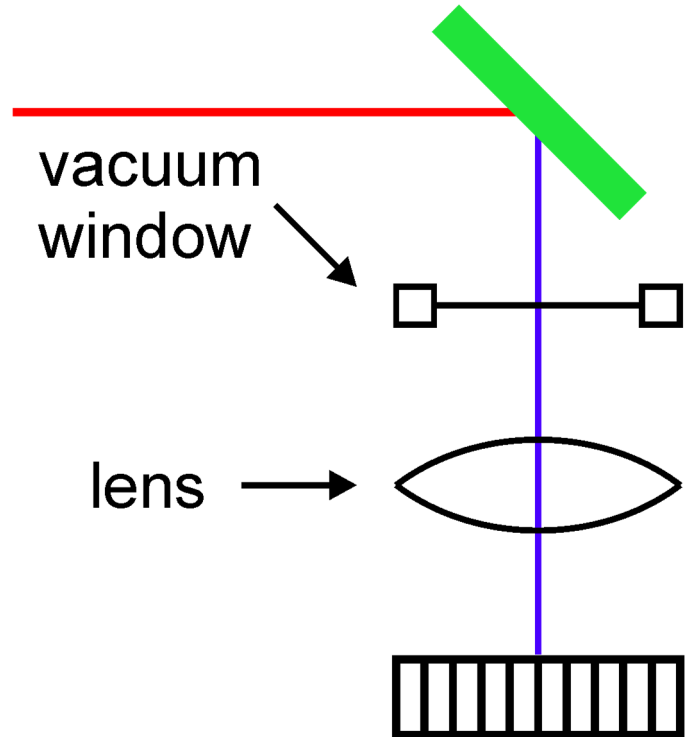
- ❖ direct detection of the light



Optical Setup

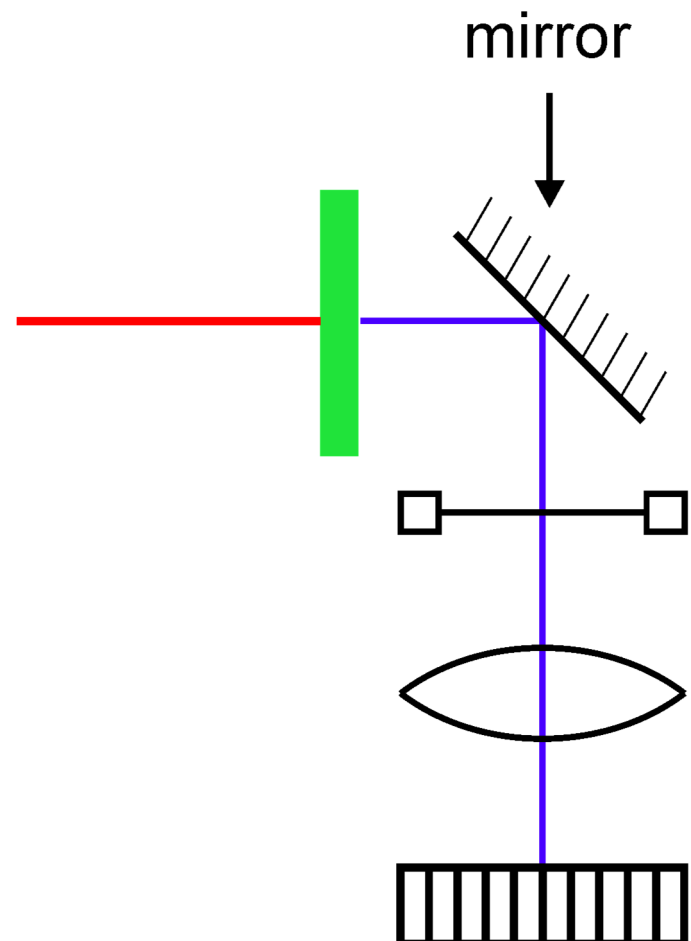
Common scintillator layouts

- ❖ direct detection of the light
- ❖ imaging the light through a vacuum window



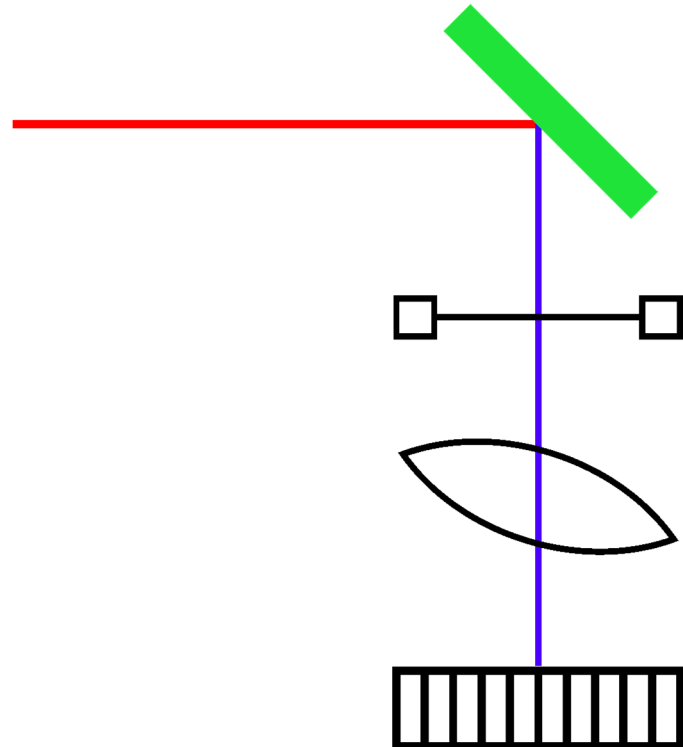
Common scintillator layouts

- ❖ direct detection of the light
- ❖ imaging the light through a vacuum window
- ❖ using an additional in-vacuum mirror



Common scintillator layouts

- ❖ direct detection of the light
- ❖ imaging the light through a vacuum window
- ❖ using an additional in-vacuum mirror
- ❖ observing the Scheimpflug imaging geometry



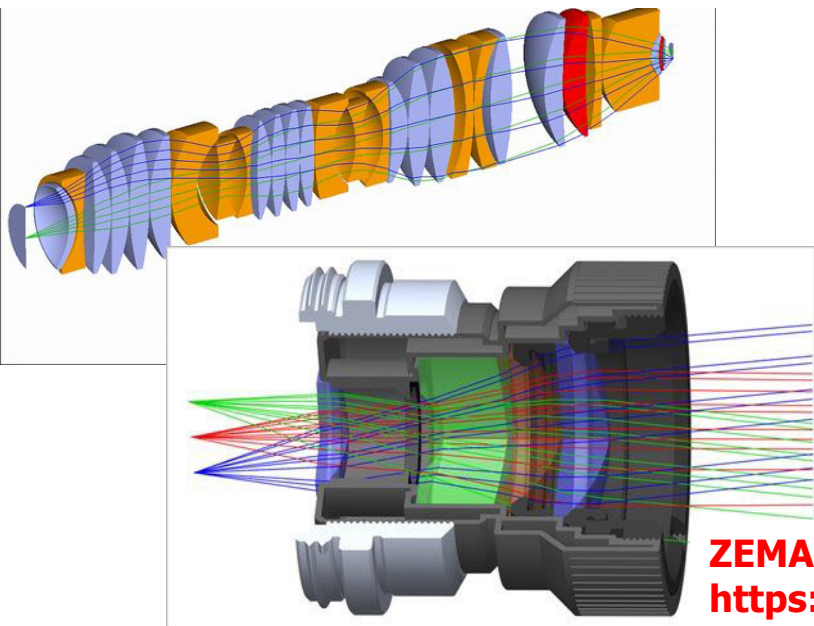
Optical Setup

Optical design with ray tracing software

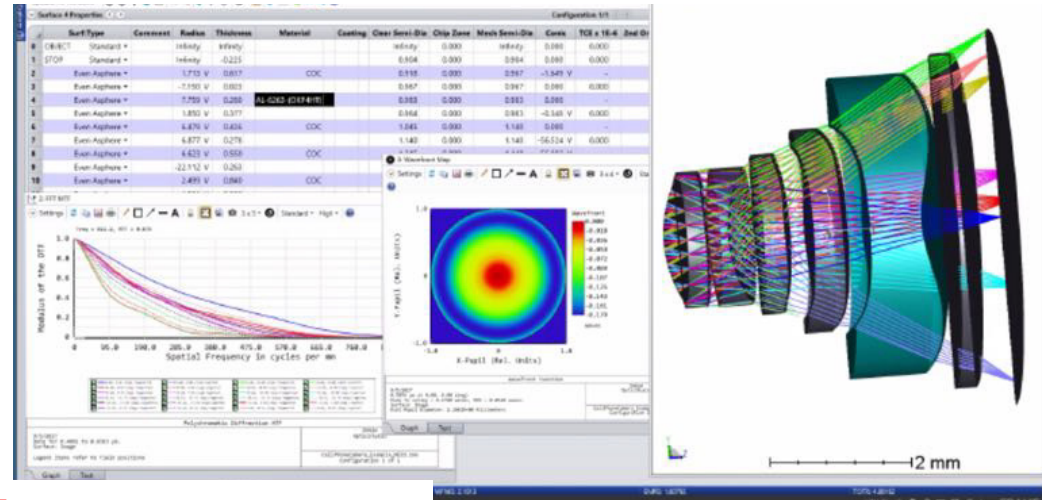
- ❖ Ray tracing divides the real light field into discrete monochromatic rays that are propagated through the system. Can input real light distribution.
- ❖ Several professional software suites available.

**OSLO: Optics Software for layout
and Optimization**

<https://www.lambdares.com/oslo/>



WinLens3D - lens design & optimization software
http://www.opticalsoftware.net/index.php/how_to/lens_design_software/winlens3d/



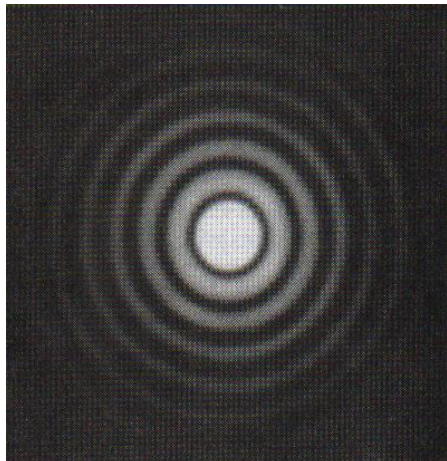
ZEMAX
<https://www.zemax.com/>

Screen Resolution and PSF

- ❖ In addition to observation geometry, the resolution at the image plane can be influenced by **diffraction** at any restrictive apertures, around obstructions (dust), or **aberrations** due to lens imperfections or refractive index variations in the optical system.

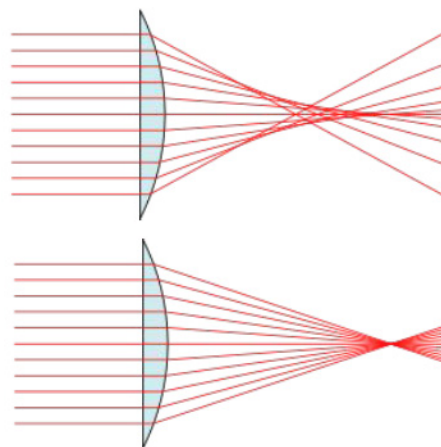
Diffraction in 2D

on circular aperture



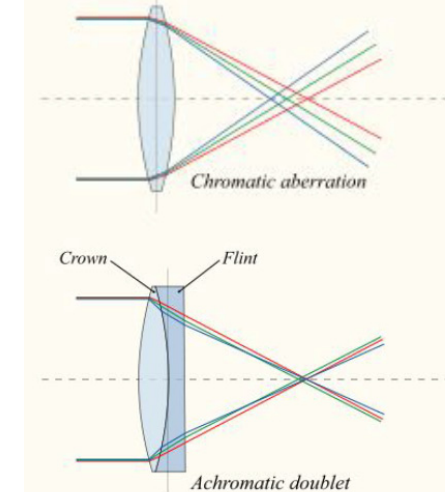
Spherical aberration

off axis rays focus as different distances.
can be corrected with Schmitt plate.



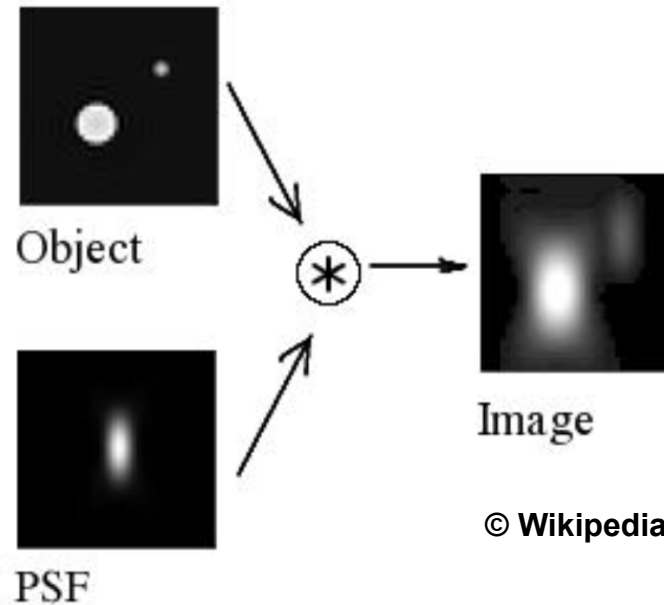
Chromatic aberration

colours refract by different angles due to dispersion.
Correct with achromatic doublet.



Screen Resolution and PSF

- ❖ An important parameter to determine is the Point Spread Function (PSF): the optical response of the system to a single point of light at the object plane.
- ❖ Measurement and/or calculation of the PSF allows a deconvolution of the image to enhance the resolution.



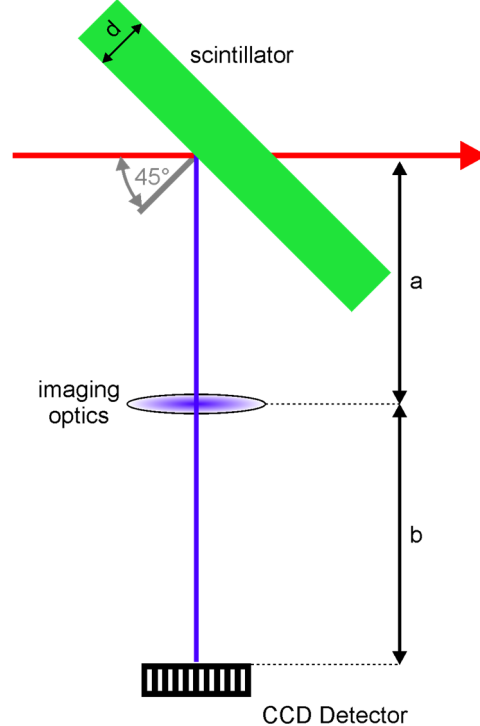
© Wikipedia

- ❖ In the case of a beam profile measurement, one charged particle gives a single point of light in the object plane

Optical Setup

Exploring the resolution limits

- ❖ micrometer beam size experiments

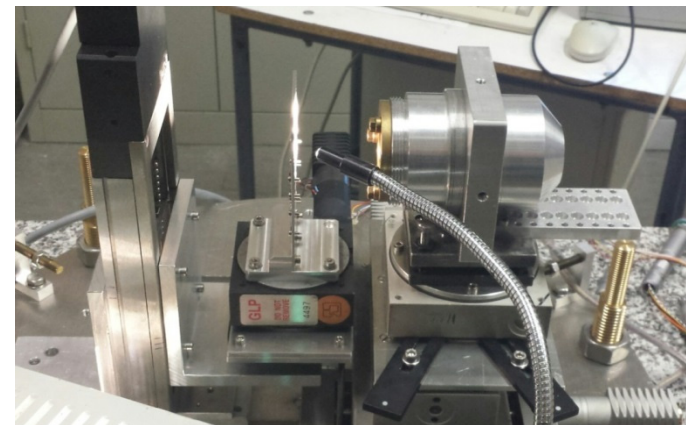


$a = 27.54 \text{ mm}$

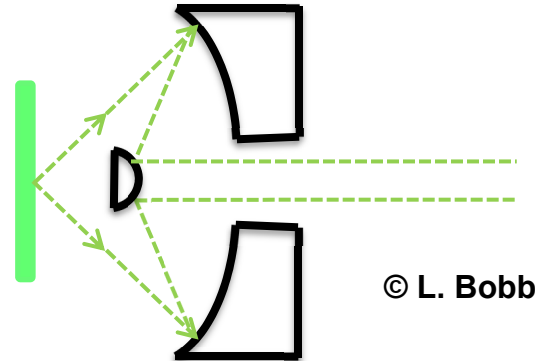
$b = 1155.46 \text{ mm}$

Magnification = 41.95

Beam parameters: electrons at 855 MeV



Schwarzschild Objective



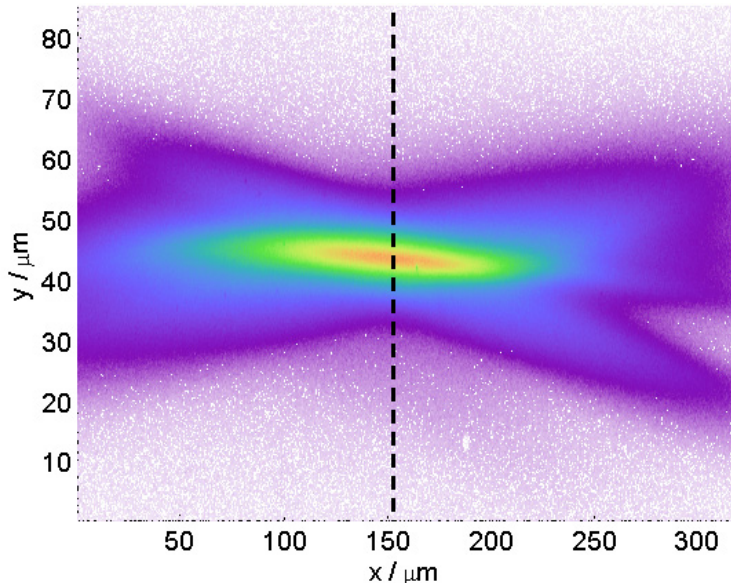
**2 concentric spherical mirrors
corrected for spherical aberrations**

$f = 26.90 \text{ mm}$

NA = 0.19 (nominal)

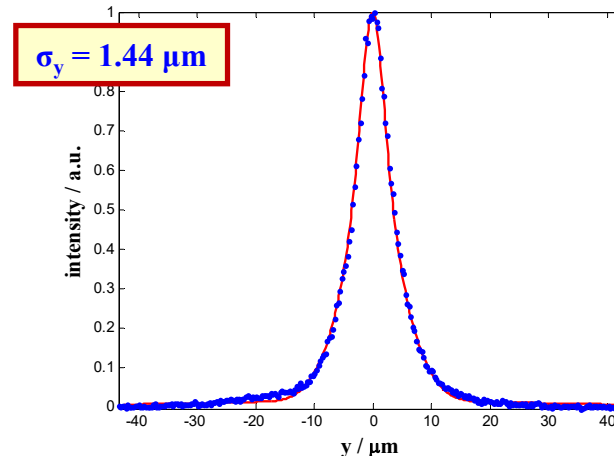
Exploring the resolution limits

❖ measured beam image



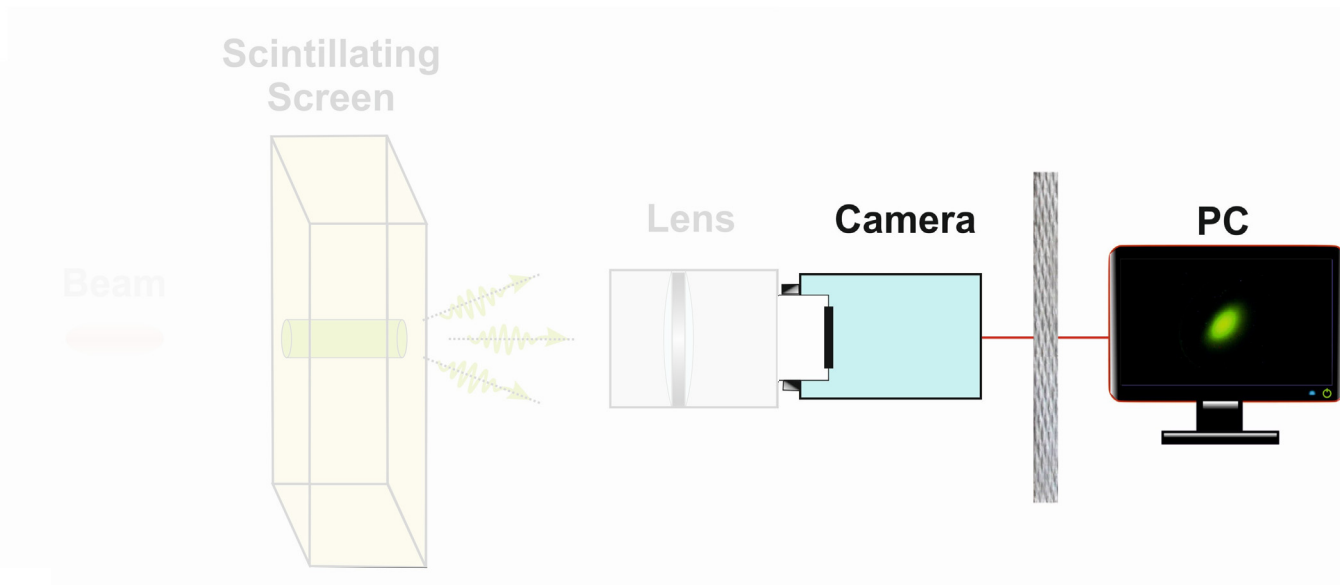
❖ analysis: Zemax model

- ❖ light emission from single electron
- ❖ single particle resolution function (SPF): 2D intensity distribution characterizing scintillator influence
- ❖ SPF convolution with 2D gaussian beam profile
- ❖ vertical cut and comparison



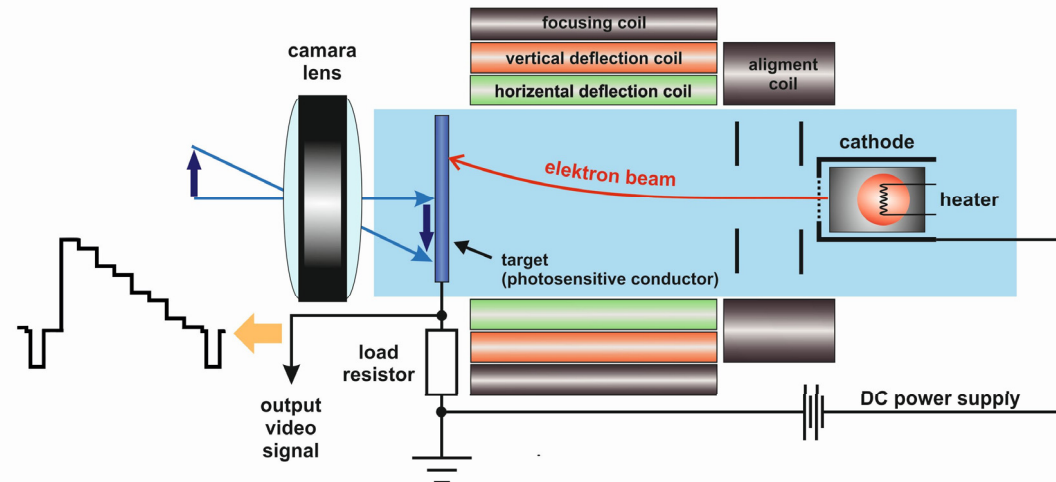
- ❖ horizontal beam profile
 - affected by 90° observation geometry
- ❖ vertical beam profile
 - affected by depth-of-focus
- ❖ restriction: analysis only along vertical cut

Image sensors and post processing



Analogue video cameras e.g. Vidicon

- ❖ charge-density pattern is formed by the imaged scene radiation on a photo-conductive surface which is then scanned by a beam of low-velocity electrons
- ❖ Analogue video signal
- ❖ Frame grabber for digitizing, storage and post-processing needed
- ❖ Radiation hard
- ❖ Out of production



Digital video cameras e.g. CCD, CMOS, CID, ...

- ❖ each pixel converts the incoming photons into electrical information
- ❖ digital output
- ❖ high dynamic range (up to 12 bit, standard)
- ❖ sufficient high resolution (1000x1000 pixel)
- ❖ remote operating and post-processing by software
- ❖ low to moderate radiation hardness
- ❖ CMOS chip development and price driven by consumer market



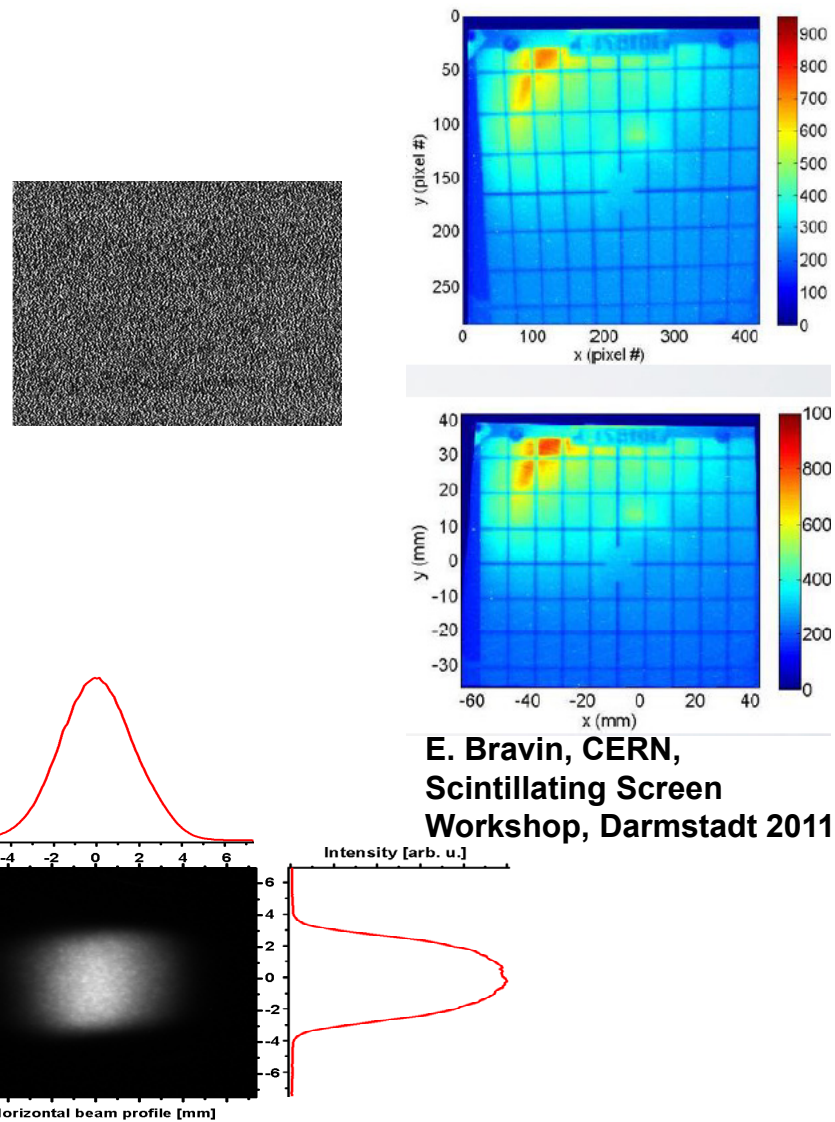
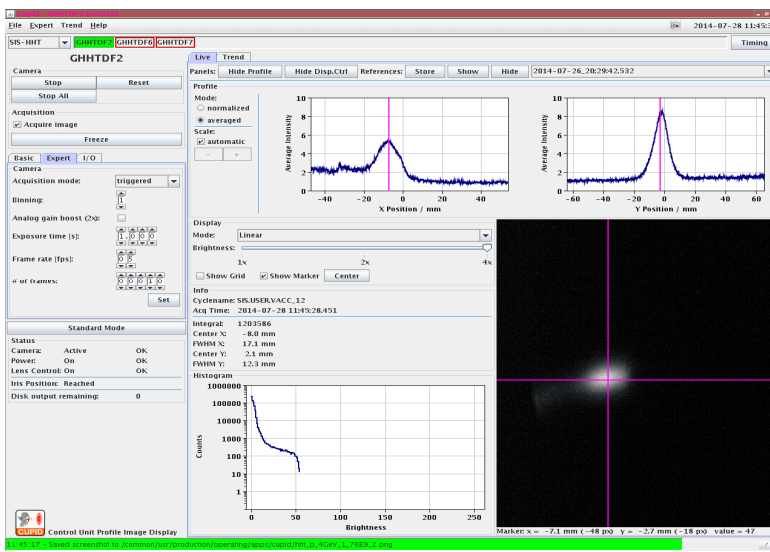
Post Processing- Analysis tools



❖ camera provider offer tools

❖ usually we need to do:
background subtraction
geometrical corrections
projection and/or fitting

❖ most of the time we use in-house
developed tools (JAVA, C/C++ etc.)



E. Bravin, CERN,
Scintillating Screen
Workshop, Darmstadt 2011

- ❖ **Scintillator screens are a good choice for precise beam profile measurements in ion and electron machines**
- ❖ **Resolution of the screen system can be improved by:**
 - proper choice of screen material
 - understanding the screen response
 - thickness of the screen
 - observation geometry
 - screen tilt
 - focal plane
- ❖ **Radiation damages have to be taken into account, in particular for low energy ion beams**
- ❖ **Camera technology and post-processing give a lot of possibilities in the imaging world**

Acknowledgment



ARIES-ADA Topical Workshop 

Scintillation Screens and Optical Technology for transverse Profile Measurements

Krakow, Poland, April 1 to 3, 2019

INDICO-site: <https://indico.cern.ch/event/765975/>

Workshop Summary

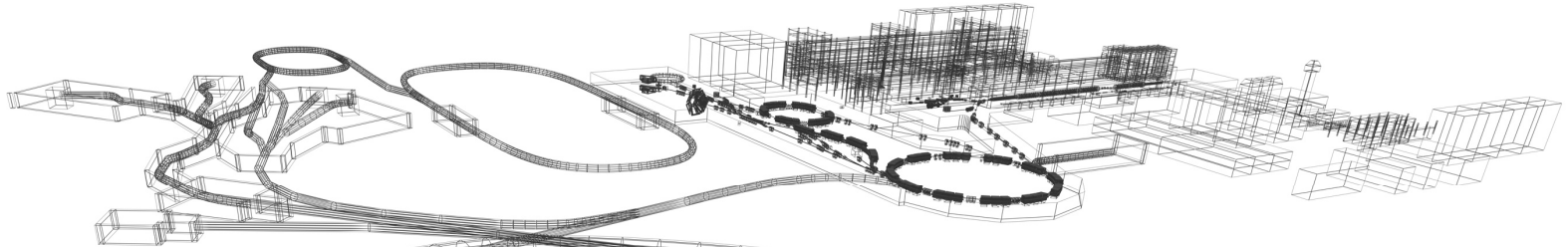
A group photograph of approximately 40 workshop participants, mostly men, standing in two rows against a white wall. Some individuals are wearing lanyards with name tags.

Organized by:     

Sponsored by:        

This project has received funding from the European Union's Horizon 2020 programme under Grant Agreement No 730871

Special thanks to:
P. Forck
K. Höhne
R. Ischebeck
G. Kube
H. Rödl
C. Schmidt



The End!

Thank you
for your
attention!

Bandwidth of applications



huge application range for inorganic scintillators

	Ions	Electrons	PANDA 'standard' usage
application	transversal beam profile measurement → primary beam hits the scintillator		particle tracking calorimetry
particle energy	1 keV -100 GeV/u	100 keV -10 GeV	up to 10 GeV
spot size	1 mm - cm	1 µm - mm	1 cm – 100 cm
counts per pulse	10^4 - 10^{13}	10^7 - 10^{10}	< 10^8
dose rate	very high	high	low
energy deposition	very large	medium	low
saturation effects	expected	possible/high	none
material modification	expected	possible	low

Examples for dose rates on scintillator screen:

GSI UNILAC: standard high current operation: dose rate $\sim 10^6$ Gy/pulse

PANDA: standard operation: dose rate ~ 27 mGy/h